Study on Phenological, Morphological and Hydrological Changes of Mangrove Forest along the Southwest Coast of Bangladesh

July 2014

ANWAR MD. SHIBLY

Study on Phenological, Morphological and Hydrological Changes of Mangrove Forest along the Southwest Coast of Bangladesh

Graduate School of Systems and Information Engineering

University of Tsukuba

July 2014

ANWAR MD. SHIBLY

ACKNOWLEDGEMENTS

It would never have been able to write my doctoral dissertation without the help, guidance, advice and encouragement from supervisor, friends, lab mates and support from my family and wife.

I would like to express my deepest gratitude to my advisor, Professor, Dr. Satoshi Takewaka, for his excellent guidance, caring, patience, and providing me with an excellent atmosphere for doing doctoral study in the Department of Engineering Mechanics and Energy of the University of Tsukuba. The good advices, suggestions and directions from him, have been invaluable on both an academic and a personal level, for which I am extremely grateful. I also express my deep sense for his personal care and most importantly, his friendship during my stay in Japan life is a memorable one.

I would like to say thank to the member of my dissertation committee, Professor Harumichi Kyotoh, Associate Professor Yuko Hatano, Associate Professor Naoki Shirakawa and Dr. Masatoshi Denda for their valuable assistances and suggestions that they have given during the refereeing phase of this thesis.

I am very much grateful to Professor Md. Mafizur Rahman, supervisor during my Master's program in BUET, Bangladesh, for his assistance and help at the very beginning of Ph.D. study. Without his unexplainable effort, I could not able to start my Ph.D. study here in Japan. I have no word to say him thanks, because his blessing for me is much higher than my thanks.

I am very much thankful to the Ministry of Education, Culture, Sports, Science and Technology (MEXT) for providing Monbukagakusho Scholarship that made my study possible at the Department of Engineering Mechanics and Energy of the University of Tsukuba.

Special and sincere thanks should go to my friends in Bangladesh, Md. Anwarul Abedin, Md. Samir Uddin and Md. Atiqul Islam for their kind and tremendous effort to collect the hydrological and metrological data from Bangladesh.

Sincere thanks to my present and former laboratory members for their prompt and generous assistance in my every stages during staying in Japan. I am grateful for the help and friendship received from my Japanese and other countries colleagues and friends during the course of the study. I would like to express my sincere gratitude and appreciation to Dr. Elsayed Mohamed Galal Elghandour for his valuable and constructive suggestions and assistances to improve my thesis writing.

I would also like to express my thanks to my parents. They were always supporting me and encouraging me with their best wishes. Finally, I would like to thank my wife, Farjana Umme. She was always there cheering me up and stood by me through the good times and bad.

TABLE OF CONTENTS

ABSTRACT

Drastic changes in river discharge and salinity levels are threatening the phenology and morphology of the coastal mangrove of Sundarbans along the southwest coast of Bangladesh. The study have used AVHRR GIMMS (1985-2006) and MODIS (2005-2010) satellite Normalized Difference Vegetation Index (NDVI) data to identify the temporal variation of the phenology of the mangroves. Linear interpolation and Fourier-based adjustment were applied to remove noise from the NDVI time series. Then linear regression analysis on a single area (8 km × 8 km) and a composite of 36-Areas for three NDVI statistics, the annual minimum, annual average, and annual maximum, were performed over the time periods 1985-1990, 1990-2000, 2000-2006 and 2005-2010 to identify possible functional changes in NDVI time series around the Sundarbans. Furthermore, to characterize the local morphological behavior of the southwestern coast, seven non-overlapping segments along the coast designated as A through G were studied. Segments A-D are covered with mangrove forest, segments E and F have a small mangrove forest area at their tip, and G is a flat sandy beach. Fourteen LANDSAT images spanning the period 1989-2010 are analyzed to estimate the spatiotemporal rate of shoreline changes over the three time periods 1989-2000, 2000-2006, and 2006-2010. Beside the satellite data, hydrological, metrological and wave hindcast data also have been taken into consideration to identify the possible relation of these factors with the phonological and morphological changes along Sundarbans. In addition, a field survey was conducted in March, 2013 to understand the present conditions of salinity, soil characteristics, forest etc.

Annual variations of NDVI of 36-Areas are categorized into three types. Type-1 is found mainly at high saline zone, southwest corner of Sundarbans, while moderate saline zone (central part) and fresh water zone (north to northeast corner) is dominated by Type-2 and Type-3 respectively. A decreasing trend in the annual minimum NDVI was observed in

most of the areas of the Sundarbans for the period 1990-2000, especially in the areas which are categorized into Type-2 and Type-3. On the other hand, mangroves of high saline zones, categorized as Type-1, still had increasing trends in the annual minimum NDVI for this period. During the years 2000-2006, the trends of the three NDVI statistics became significantly positive at all over 36-Areas, indicating an improvement of the mangrove phenology. Some positive trends are found at the southwest and east corner of Sundarbans in the present period of 2005-2010, whereas most of area is facing decreasing trends in annual minimum NDVI. Decreasing trend also was dominating in other NDVI variables at all 36-Areas. The coast underwent rapid erosion from 1989-2000 and 2006-2010. However, the rate substantially declined between 2000 and 2006, when accretion was dominant.

The advent of the upstream Farakka barrage caused a significant reduction in the Ganges-Gorai river discharge and increased the salinity in and around the Sundarbans. This study suggests that this may be responsible for the degradation of mangrove phenology and accelerated erosion in the earlier and recent periods. In the interim, 2000-2006, improved river discharge and salinity levels due to the Ganges water sharing agreement (1996) and dredging of the Gorai river bed (1998-1999) enhanced the mangrove phenology and helped the coast to gain land.

Shorelines of segments covered with mangroves (segment, A-D) changed more rapidly than flat sandy beaches (segment, G), contradicting the general consensus that mangrove stabilizes the land. Low river discharge and concomitant higher salinity level within mangrove covered segments may have adversely affected, with some delay, the growth of the mangrove forests and accelerated the rate of erosion through slaking and dispersion. On the other hand, sandy beach is little affected by slaking and dispersion induced by adverse saline conditions anyway in contrast to the clayey soil of the segments covered with mangroves, which may be one of possible reason for the lower erosion rate of sandy

segment G. Further, southwestern side of southerly facing shoreline of every segment was facing continuous erosion over all time periods, which may due to prevailing waves from south-south-west and consequent sediment transport from west to east.

LIST OF FIGURES

LIST OF TABLES

LIST OF ABBREVIATIONS

ASTER	Advanced Spaceborne Thermal Emission and Reflection Radiometer
AVHRR	Advanced Very High Resolution Radiometer
BIWTA	Bangladesh Inland Water Transport Authority
BMD	Bangladesh Metrological Department
BWDB	Bangladesh Water Development Board
EC	Electrical Conductivity
ECMWF	European Centre for Medium-Range Weather Forecasts
ESP	Exchangeable Sodium Percentage
ETM	Enhance Thematic Mapper
E-W	East-West
GBM	Ganges- Brahmaputra- Meghna
GIMMS	Global Inventory Modeling and Mapping Studies
GRRP	Gorai River Restoration Project
GWSA	Ganges Water Sharing Agreement
MK Test	Mann-Kendall Test
MODIS	Moderate Resolution Imaging Spectroradiometer
NDVI	Normalized Difference Vegetation Index
NOAA	National Oceanic and Atmospheric Administration
ORNL DAAC	Oak Ridge National Laboratory Distributed Active Archive Center
N-S	North-South
PPT	Parts Per Thousand
TM	Thematic Mapper
W-E	West-East

CHAPTER ONE

INTRODUCTION

1.1 General

Mangroves forests are found in the intertidal zone in the tropical and subtropical regions of the world (e.g. Bangladesh, India, and Kenya). The area where mangrove occurs includes estuaries and marine shorelines. This ecosystem acts as buffer zone between the land and sea which protects the coast against cyclones and reduce erosion due to wind, waves, water currents and protect coral reefs, sea-grass bed and shipping lanes against siltation. Mangrove forests is a host of a number animal species, mammals, reptiles, amphibians and birds-offer nutrients to the marine food web and provide spawning grounds to a variety of fish and shellfish, including several commercial species. It provides a large variety of wood and non-wood forest product and also known to absorb pollutants. Among other services the forests control the water flow and maintain the water quality (Islam and Gnauck, 2009) makes breeding, feeding and nursery grounds for many estuarine and marine organisms (Giri et al., 2007). Their unique root systems create a great deal of physical roughness, thus capturing and storing vast quantities of sediment from upland and oceanic origin. Thus the distribution of mangrove forest can be used as an indicator of coastal changes (Blasco et al., 1996).

The socio-economic and environmental significance of mangroves is being increasingly recognized, but the extent and diversity of this forest are still decreasing globally at a rapid rate and much of the remaining forests are in degrade condition. Anthropogenic activities and their consequences, including climate change and natural threats, are negatively impacting mangrove biodiversity and ecosystem services. There has been considerable recent interest in the probable response of mangrove phenology and morphology to natural (Woodroffe, 1990) and other man made causes, both in terms of the mangroves themselves

and their losses due to shore erosion. To mitigate these losses, a better understanding of how coastal mangrove ecosystems interact with the environment and how they respond to anthropogenic impacts is required. The understanding of mangrove forest dynamics can lead to conservation and management directives, such as the establishment, protection and management of re-afforestation plots in the framework of regeneration or restoration projects including projects related to minimize the possible anthropogenic effect on mangrove forest.

Satellite imagery has been used to monitor and assess vast coastal areas such as mangroves (Ramachandran et al., 1998). To be effective, protection and restoration of mangroves require information on the exact distribution of these ecosystems and the extent to which they have been changed. This can be problematic as mangroves tend to be found in remote, relatively inaccessible areas, and degradation in these ecosystems tends to be sporadic (Islam et al., 1997, and Lucas et al., 2009). Satellite remote sensing provides supplementary information quickly and efficiently to gather information on inaccessible areas and offers many advantage including synoptic coverage, availability of low-cost or free satellite data availability of historical satellite data, and repeated coverage. In addition, recent advances in the hardware and software used for processing a large volume of satellite data has helped increase the usefulness of remotely sensed data. Moreover, it is extremely difficult to get into vast swamps of mangrove forests, and conducting field inventory is time consuming and costly. With the difficulty of conventional monitoring techniques in mangrove environments, the data obtained from satellite remote sensing is an efficient tool that has been adopted increasingly, particularly when analyzing vegetation history and coast dynamics (Giri et al., 2007).

The “Normalized Difference Vegetation Index” (NDVI), the most commonly used satellite product, has being satisfactorily related to functional characteristics of vegetation, particularly with the fraction of photosynthetically active radiation intercepted by vegetation,

and consequently with primary productivity (Seller et al., 1992, and Paruelo et al., 1997). Long term series (~20 years) of NDVI data, generated from coarse spatial resolution sensors, are valuable tools for the detection of both temporally discrete changes, like forest clearing, as well as gradual changes such as long term change of vegetation activity (Heumann et al., 2007, and Hansen et al., 2004). On the other hand, multispectral remote sensing satellites provide digital imagery in various spectral bands, including the near infrared where the land-water interface is well defined. Owing to this characteristic of infrared bands in satellite imageries can be used successfully to extract shoreline positions with sufficient accuracies. The shoreline, which is defined as the position of the land-water interface at one instant in time (Gens, 2010), is a highly dynamic feature and is an indicator for coastal morphological changes (erosion and accretion).

This study makes use of such capabilities of remote sensing data to assess the long term change of mangroves phenology and coast dynamics in the Sundarbans mangrove forest in Bangladesh. A number of studies conducted in the Sundarbans have begun to develop and apply remote-sensing techniques mainly for mapping and change detection purposes (Islam et al., 1997, Dwivedi et al., 1999, Blasco et al., 2001, and Michael and Peterson, 2006). These studies were conducted either in Bangladeshi or Indian parts of the Sundarbans at different times.

1.2 Background and Review of Literature

Bangladesh is a small, densely populated country (over 140 million in 2011) bordered on the west, north, and east by India and on the south along a 710-km-long coastline by the Bay of Bengal. The country is a low-lying delta, formed at the confluence of the Ganges, Brahmaputra, and Meghna Rivers (GBM) and their tributaries, as high volume of discharge of these river system traditionally carried extremely large sediment loads (~10^9

ton/yr from different parts of Himalayas and up stream of Bengal delta (Goodbred and Kuehl, 2000). About 90% of the country is less than ten meter above mean sea level, making it one of the most vulnerable countries in the world to natural catastrophes every year (Karim and Mimura, 2008).

The coastal zone of Bangladesh, important for its natural resources and ecosystems, covers 19 out of the country's 64 districts and contains 28% of the country's population. The Sundarbans, the world's largest stretch of mangrove forest, is on the southwest coast of Bangladesh (Iftekhar and Saenger 2008). The Sundarbans is located in the lower basin of the

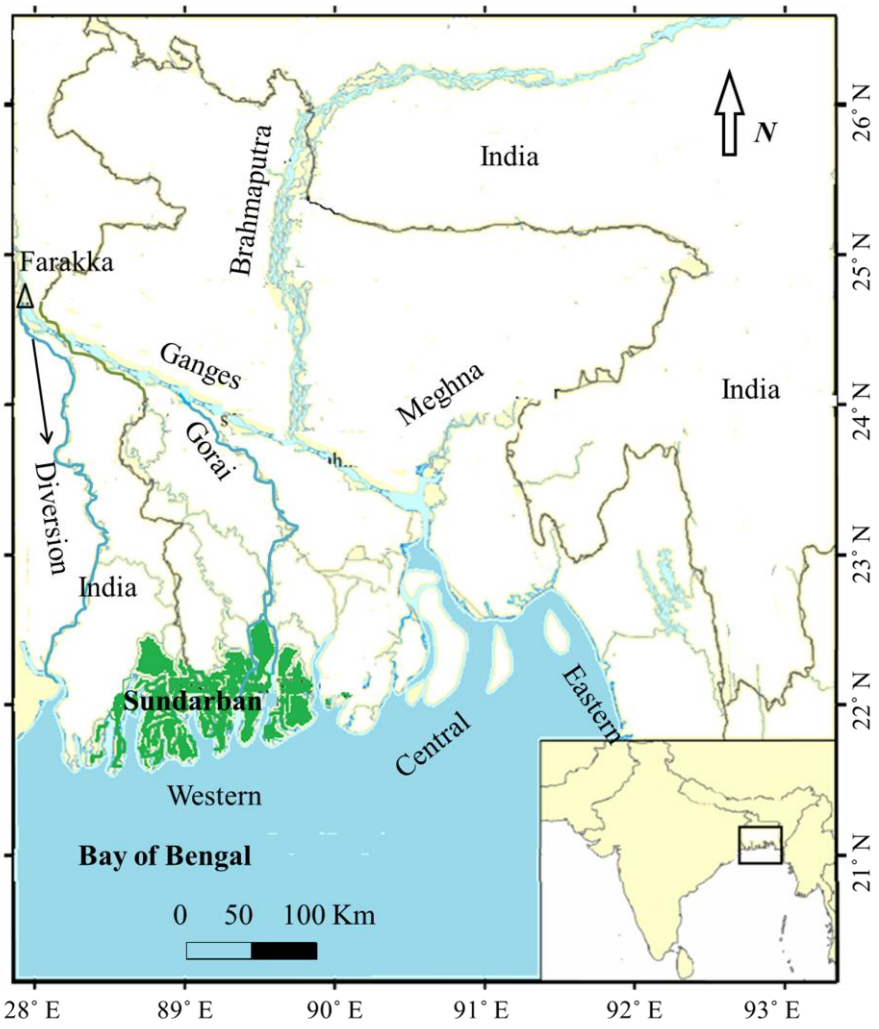

Figure 1.1 Bangladesh's main river systems and location of Sundarbans and ∆ Farakka Barrage.

Ganges River, and a large number of channels and creeks flow into larger river networks. Its hydrology is dominated by the flow of freshwater from the Ganges, which exhibits very high seasonal variation. The Gorai River (Fig. 1.1) is the major distributary of the Ganges River and an important provider of freshwater to the channels and creeks of the Sundarbans. The river system has mitigated surge amplification (Sinha et al., 1985), salinity intrusion, and the backwater effect (Ali, 1999) and increased sediment accretion.

The disappearance of some distributaries and diversion of river water has diminished the flushing of freshwater along the southwest coast and consequently affected the biodiversity of the Sundarbans (Brij and Chauhan, 2006). The Ganges River system has undergone some drastic changes since India completed a barrage on the Ganges River in 1975 at Farakka, 16.5 km from the border of Bangladesh (Fig. 1.1). The consequent changes in sediment and discharge processes of the rivers and increase in salinity levels has severely affected the phenology and morphology of Sundarbans. There have been several studies carried out which describe the undesirable effects of this diversion on agriculture, forestry, industry, and drinking water in the southwest region of Bangladesh (Mirza 1998, Islam and Gnauck, 2009).

Michael and Peterson (2006) quantified changes in the Sundarbans, using LANDSAT satellite imagery from 1989 and 2000, and identified areas of deforestation. The study suggested that higher water and soil salinities due to low river discharge, shrimp farming, and other human influences are partly responsible for the degradation of the Sundarbans. Of these factors, increases in salinity and decreases in river discharge are more pronounced in the post-Farakka period (Mirza, 1998).

Using LANDSAT images from 1973, 1979, 1989, 2000, and 2010 to monitor the dynamics of the coastline of the Sundarbans, Rahman et al., (2011) found an average erosion rate of 7.2 km^2/yr from 1973 to 2010. Accretion showed a rate of 10 km^2/yr between 1973

and 1989, but substantially declined to ~4 km^2/yr between 1989 and 2010. Accretion rate has declined in the recent years but erosion rate has remained relatively high. This would be an evidence of low sediment supply from the upstream river at this period.

Sarwar and Woodroffe (2013) reported a systematic assessment of rates of shoreline changes over 20 years periods along whole Bangladesh coast from 1989-2009, using six LANDSAT images for each year of 1989 and 2009.

These erosion rates are significantly higher than previously stated by Allision (1998), who used digitized survey maps from 1792, 1840, 1904, and 1908 and a LANDSAT image from 1984 to estimate a net erosion rate of about 1.9 km^2/yr for the Sundarbans delta. On the contrary, Giri et al. (2007), using LANDSAT images from 1973, 1979, 1989, and 2000, reported that the forested area had not changed significantly throughout the 25 years of their study period. However, they claimed that 38 km^2 of land along the major river channels and extreme southern edge of the Sundarbans were eroded during that same period. All of these studies reported that the rate of accretion has been declining and erosion has been increasing in the all successive year along the Sundarbans coast. This may due to the fact that decreased Ganges River discharge and sediment deprived in the Sundarbans due to the advent of the Farakka Barrage and other anthropogenic disturbances in upland.

Due to the 30-year treaty between India and Bangladesh on sharing the Ganges waters (signed on 12 December 1996) and the pilot dredging project for the Gorai River (Fig. 1.1) in 1998 and 1999, a significant increase in freshwater flow has been achieved with a corresponding decrease in salinity in and around the Sundarbans (Wahid et al., 2007). We hypothesized that there has been some transitional variation of the mangrove phenology and coastal morphology due to this increased river discharge. The previous studies tried to estimate the mangrove vegetation (Michael and Peterson, 2006) and coastal dynamics (Allision, 1998, Giri et al., 2007, and Rahman et al., 2011) along the Sundarbans using

satellite images with ten-year or more gaps between images. None of the studies to date have clarified coastal dynamics and variation of the mangrove phenology using images with shorter one-year or fewer gaps or described the influence of variations in river discharge and salinity on the coast dynamics and phenology.

1.3 Objectives of the Study

In accordance with the background described above, the objectives of the study are set as follows:

i) To analyze the changing features from 1985-2010 of the mangrove phenology of the Sundarbans using the Normalized Difference Vegetation Index from satellite database.

ii) To detect the shoreline position using fourteen satellite images for the period 1989-2010 to understand the morphological behavior of the southwest coast of Bangladesh, focusing on the mangrove forests, and

iii) To identify the relation of phenological and morphological changes to the variations of river discharge and salinity.

1.4 Organization of the Study

The rest of the thesis is organized as follows. Chapter 2 describes brief information about the south-western coast of Bangladesh and segmentation of study area to observe the local phonological and morphological changes. Chapter 2 also describes the river system, hydrological and salinity regimes of the study area. In addition, mangroves distribution of Sundarbans depending on the salinity variation also is included.

Chapter 3 presents data sets used in this study. This study used AVHRR (Advanced Very High Resolution Radiometer) GIMMS (Global Inventory Modeling and Mapping Studies) (1985-2006), and MODIS (2005-2010) satellite NDVI data set to identify the

temporal variation of the phenology of the mangroves. Furthermore, the study used fourteen LANDSAT images spanning the period 1989-2010 to estimate the spatiotemporal rate of shoreline changes over the different time periods. Chapter 3 also explains the satellite data processing techniques to smooth the NDVI data receiving from AVHRR GIMMS and MODIS data set and to detect the shoreline positions form LANDSAT images. To identify possible influencing factors on phenological and morphological changes, hydrological, metrological and wave hindcast data are also included in this chapter. A statistical method named Sequential Mann-Kendall (MK) test is applied to detect the potential turning points of trends in the time series of NDVI variables.

Chapter 4 presents seasonal and time series of NDVI variation, corrected with the procedures described in chapter 3. Linear trends analysis results of NDVI variables over different time periods are shown in this chapter. In addition, detected shoreline positions and rate of accretion and erosion over different time period is presented. Long term variations of river discharge and salinity around Sundarbans are presented and finally a cross correlation between NDVI variables, river discharge and salinity is performed in this chapter.

Chapter 5 discusses the impact of river discharge and salinity on the long term variation of vegetation phenology of Sundarbans and explains the role of river discharge and salinity on shore stability. Finally, this chapter describes the other possible factors which may have affected the Sundarbans phenology and morphology.

Chapter 6 summarizes the study and illustrates the issues to be considered for future research.

CHAPTER TWO

STUDY AREA: SOUTH-WESTERN COAST OF BANGLADESH

2.1 General

The southern coastal area of Bangladesh can be divided into three distinct regions, the eastern, the central, and the western regions (Fig. 2.1), based on geomorphological features.

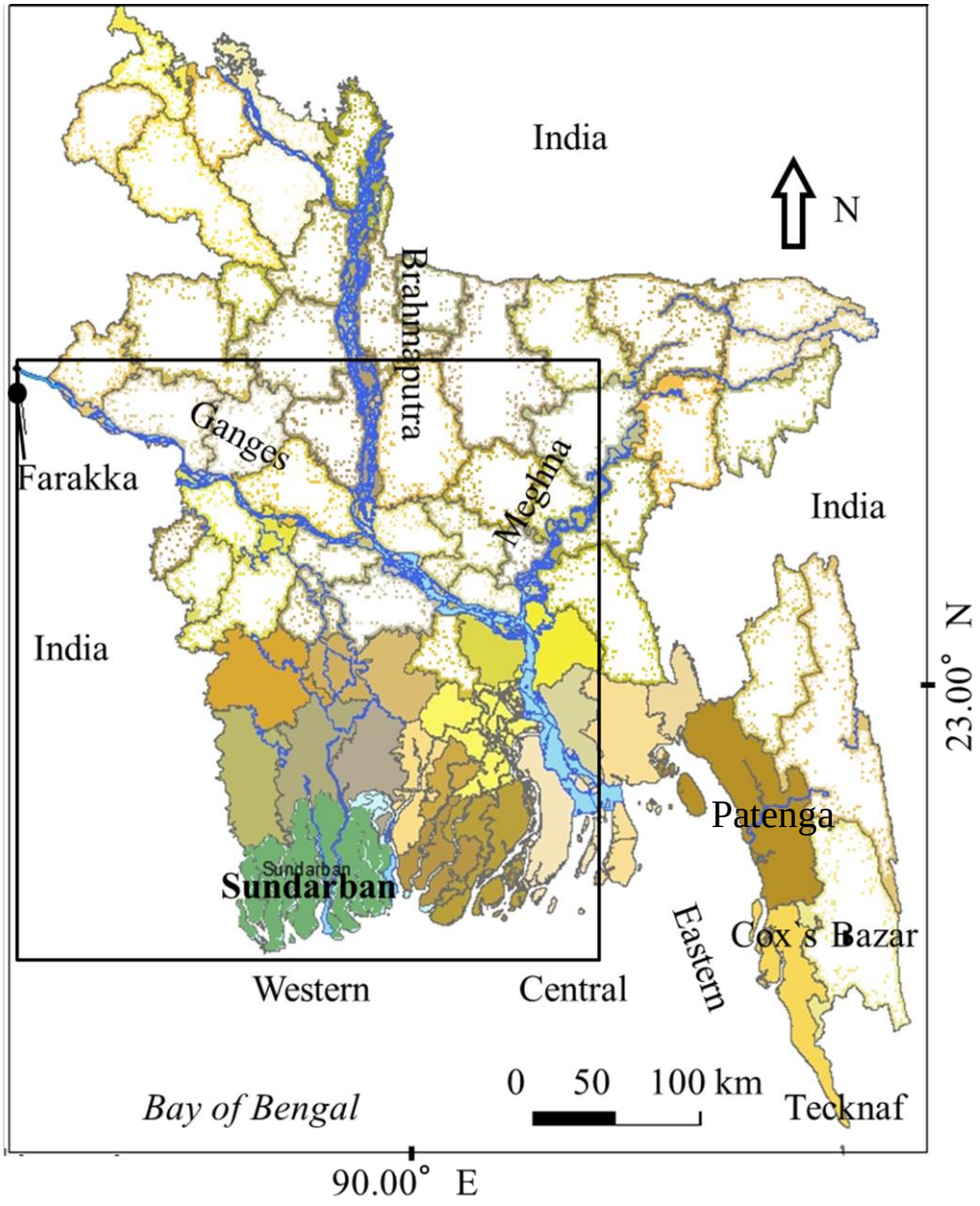

Figure 2.1 Bangladesh map showing three coastal regions. Solid box--blow up in Fig 2.2.

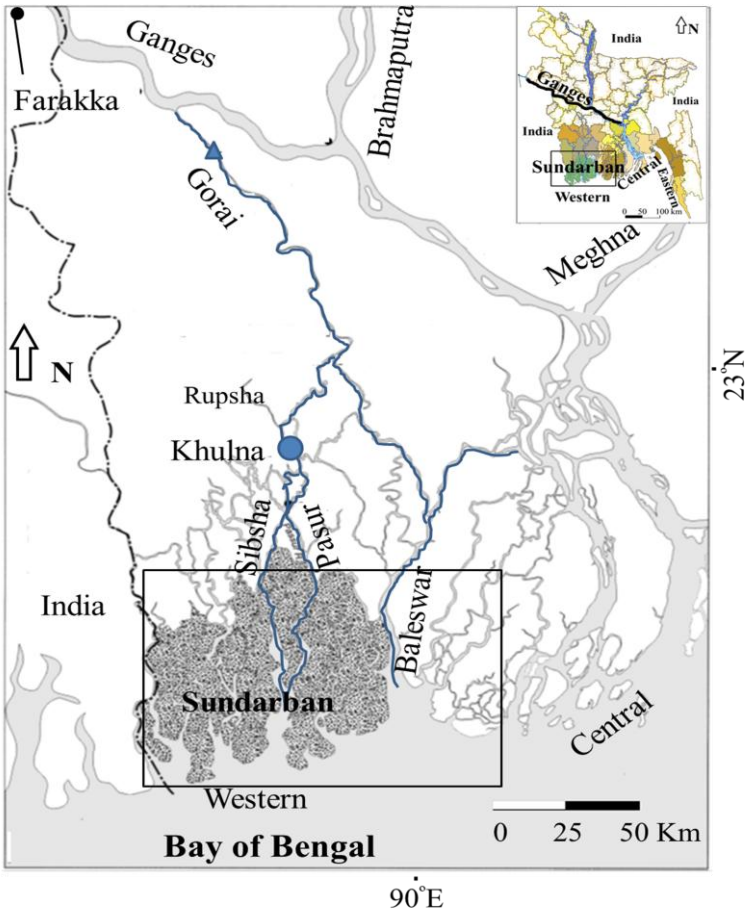

Figure 2.2 Bangladesh's main river systems and the study area. ● Farakka Barrage, ∆ Gorai Railway Bridge, ○ Khulna Station, Box--study area (blowup in Fig. 2.3).

Eastern coastal zone are dominated by submerged sands and mudflats (Islam, 2003) and has a long sandy beach of 145 km extending from Cox's Bazar to Tecknaf. Two of the country's most important sandy beaches from tourists perspective, namely Patenga and Cox's Bazar are located in this coastal zone. Fish farming, fishing in the bay, salt production and tourism are main economic activities of the zone. Except the eastern zone, all other parts of the Bangladesh coastal zones are plain land with extensive river networks and accreted land.

The central zone receives a large volume of discharge from the Ganges-Bhrahmputra-Meghna (GBM) River system, and the land is formed from silty deposition. Because of the sediment supply and strong river current, the morphology of the

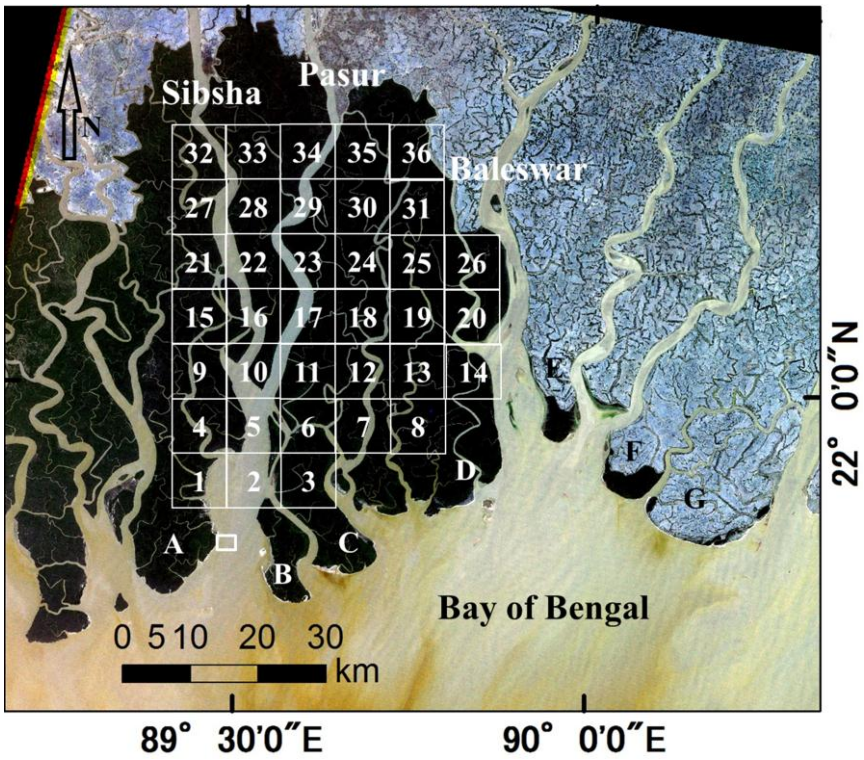

Figure 2.3 Western coast of Bangladesh and segments A-G. Base image: LANDSAT 4; bands 1, 2, and 3; 1989/01/12. □ Tide station (Hiron Point). Solid boxes (Areas 1-36): NDVI analysis location.

zone is very dynamic and erosion and accretion rates in the area are very high. Numerous islands are located in the area. Many islands have been formed in last few years in the area by the process of land accretion. At the same time many have been eroded or disappeared. The Baleswar River is falling into Bay of Bengal at western side of the central region which is feeded by the both Gorai River and GBM River system.

This study focuses on the western coast of Bangladesh (solid box Fig. 2.2). Figure 2.3 presents a closer view of the study area, with the dark portions representing the mangrove forests and the bright portions, the agricultural lands or bare lands without mangrove forests. The western coast, known as the Ganges tidal plain, comprises a semi-active delta and is covered with a mangrove forest popularly known as the Sundarbans (the Beautiful Forest), named after the Sundari trees found in abundance there.

The land of Sundarbans is very low and flat and dominated by silty loam or alluvium

(Islam, 2003). The elevation of much of the area ranges between 0.9 to 2.1 m above mean sea level (Iftekhar and Islam, 2004). The area has a large number of fluvial and tidal landscapes created by the continuous deposition of sediment by the GBM River system. Radiocarbon and clay mineral evidence suggests that the lower delta plan of Sundarbans were originally formed by the sediment deposited by Ganges River (Alison and Kepple, 2001).

At the beginning of the colonial era (1757-1947) in India, the Sundarbans mangrove forest occupied approximately twice its current extent (Islam et al., 1997). Currently, Sundarbans covers 10000 km^2 in the south-western part of Bangladesh coast and south-eastern part of West Bengal of India. A total area of 62% lies in the Bangladesh part, while the remaining 38% is in India. This study concentrates on the Bangladesh portion Sundarbans. The Bangladesh portion's Sundarbans (present study area) locates between latitudes 21.516° N and 22.5° N and longitudes 89.3° E and 90.3° E (Katebi, 2001).

The Sundarbans offers coastal protection to millions of people in Bangladesh. The forests lie in a zone of cyclonic storms and tidal bores that originate in the Bay of Bengal and periodically devastate coastal areas. The mangroves provide feeding and breeding grounds for fish and shrimp species, enriching the area's biodiversity.

In addition to role of mangrove forest in environmental issues, already reported in section 1.1, the Sundarbans plays an important role in the economy of the southwestern region of Bangladesh as well as in the national economy. Approximately 600,000 people are dependent on the Sundarbans for their livelihoods (Michael and Peterson, 2006). The forest provides raw materials for wood based industries (e.g. newsprint paper mill, match factory, hardboard, boat building, furniture making). Furthermore, traditional forest produce timber, fuel wood, pulpwood etc., large scale harvest of non-wood forest products such as thatching materials, honey, bees-wax, fish, and crustacean and mollusc resources of the forest takes place regularly. Last but not the least, the Sundarbans provides a wonderful aesthetic

attraction for local and foreign tourists.

For its outstanding natural value, the World Heritage Committee of UNESCO inscribed the Sundarbans of Bangladesh in the World Heritage list by their 21st session in 1997 and accordingly the Government of the People's Republic of Bangladesh declared the Sundarbans as World Heritage site in December 1997 (Nuruzzaman et. al, 1999).

2.2 Hydrology and Salinity Regimes of Sundarbans

The Sundarbans ecosystem receives a large amount of freshwater and alluvium from river tributaries flowing from the north, and saltwater twice daily through tides. The Gorai River (Fig. 2.2) supplies Ganges River water to the Sundarbans mangrove wetlands through the Pasur and Sibsha Rivers (Figs. 2.2 & 2.3), which eventually reach the Bay of Bengal. These two rivers play an influential role in the Sundarbans's ecosystems. The Baleswer River (Figs. 2.2 & 2.3) flows through the eastern side of the Sundarbans and empties into the Bay of Bengal. It is connected to the Gorai River as well as to the Ganges-Brahmaputra- Meghna (GBM) River System; therefore, the Baleswar River receives more freshwater than the Sibsha and Pasur Rivers. The drainage pattern has shifted eastward along with the west-to-east tilt of the Sundarbans, resulting in a substantial reduction in freshwater flow into the western side of the Sundarbans. The freshwater flows down the rivers with the tidal ingress creating a gradient of salinity that varies both spatially and temporally near the mouths of the rivers; in general, the salinity is higher nearer the coast and lowers further inland and natural west-to-east salinity gradient across the delta. The combined flow through GBM is much higher than the Ganges flow, also resulting in a decrease in salinity from west to east along the coast.

Bangladesh has received a low quantity of water discharge since the construction of the Farakka Barrage on the Ganges River in India. The purpose of the barrage was to divert

river water downstream in India for irrigation and navigation purposes in the dry season (Mirza, 1998). Under a temporary agreement signed in April 1975, Bangladesh consented to a ‘‘test operation’’ of the Farakka Barrage for 41 days. After expiry of the temporary agreement, India unilaterally withdrew water from June 1975 to November 1977. A five-year agreement on the sharing of the Ganges waters was signed in November 1977. The agreement expired in 1982, but was renewed twice with some modifications up to 1987 (Mirza, 1998). There was no water-sharing agreement between India and Bangladesh for the Ganges flow during the period of 1988-1996. Since the end of the 1980s, this has caused a significant reduction in the flow of water through the Gorai River and increased salinity dramatically in the Sundarbans, especially in the dry season (Islam and Gnauck, 2008, and Nazim and Anisul, 2010). The possible impact of the this reduction of Ganges discharge, huge amounts of sediment settled on the bed of the Gorai River, further blocking the flow of water (Mondal, 2013). This may also have led to a reduction in the sediment concentration along the Sibsha and Pasur Rivers and halted the transport of sediment to the sea. This shortage of freshwater in the Ganges-Gorai basin is the primary cause of the reduction in the flow of freshwater into the mangrove delta and consequent increased salinity levels. In addition to Gorai River, some narrow rivers or canals which were fed by Ganges River water, eventually reaches in southwestern reason, has dried up completely or disappeared.

The Ganges Water Sharing Agreement (GWSA, 1996) between India and Bangladesh became effective for the southwest part of Bangladesh when Bangladesh Government executed the Gorai River Restoration Project (GRRP, 1998-1999), a dredging project for the riverbed of the Gorai River instituted to restore the regional ecological balance by restoring the volume of water flow in the dry season. A 20-km dredging of the Gorai River bed took place in a downstream direction from the fork of the Gorai branch and the Ganges. The dredging removed about 18.5 million m^3 of sediment from the river (Groot and Groen,

2001). The aim of the project was preventing environmental deterioration in southwestern region of Bangladesh, especially around mangrove forests in Sunderbands. It was expectedly achieved by (1) increasing the dry-season inflow volume from Ganges River to Gorai River and maintaining the water volume by dredging at the inflow point, (2) improving the system to effectively utilize the inflowing freshwater, and (3) increasing the organizational power, based on sustainability, to manage and maintain the restored water systems. As a result of the GWSA, 1996, and GRRP, 1998-1999, the Gorai River dry season flow increased, which decreased soil- and water-salinity levels of the Sundarbans (Nazim and Anisul, 2010) for a certain period of time.

The relative influence of freshwater and saltwater on the mangrove ecosystem is seasonal; the peak freshwater flow is during the monsoon (June to September), and the peak saline water influence is during the dry season (December to June). In the dry season, the rivers of the Sundarbans are fed by the Ganges, whereas in the wet season, the rivers are fed solely by local rainfall (IWM, 2003). The annual average local rainfall is between 1640-2000 mm and decreases as one proceeds from the lower to the upper areas of the Ganges basin. The rainfall is strongly seasonal with 85% falling in the wet season. Thus water flow in the dry season in the lower Ganges basin become a matter of great concern because reduction of the river flow in the dry summer months promotes inland penetration of high salinity levels thereby degrading the unique habitat of the Sundarbans (Smith et al., 2009).

2.3 Distribution of Mangroves of the Sundarbans

The Sundarbans freshwater swamp forest is a moist, tropical broadleaf forest ecoregion of Bangladesh contiguous with the brackish Sundarbans mangrove forests. Three principal mangrove species have been recognized in broad correlation with varying degrees of water salinity, freshwater flushing and physiography. The dominant mangrove species in

the Sundarbans are the Sundari (*Heriteria fomes*), Gewa (*Excoecaria agallocha*), and Goran (*Ceriops decandra*). These mangrove species are distributed into three distinct zones around the Sundarbans:

Oligohaline zone (relatively freshwater): The freshwater zone at the northeast corner, with soil salinity level less than 5 ppt, is dominated by Sundari (the most valuable timber in the forest accounting for over 60 percent of the total volume of commercial timber) with a sporadic distribution of Gewa.

Mesohaline zone (moderately saline): The moderately saline zone (soil salinity level between 5 and 10 ppt), the central and southeastern part, is dominated by Gewa with a varying assortment of Sundari.

Polyhaline zone (saline): The saltwater zone (salinity level exceeding 10 ppt) at the southern and western portion is abundant with Goran trees.

Elision et al. (2000) described the zonation of the mangrove forest by abundance of mangrove species types. These species need freshwater as well as saline water for their regeneration and growth. The mangrove plants are halophytes, which are well adapted to salt water and fluctuations of tide level. However, the germination of the seeds of some halophytes is dependent on a certain level of salinity, and there is an optimum salinity range for maximum growth of different mangrove species (Ball et al., 1997). The Sundari tree has a strong preference for low salinity; its growth rate significantly decreases with increasing levels of salinity. Khan and Vongvisessomjai (2002) found that the optimum surface water salinity range for Sundari is 10 ppt-15 ppt and that above 15 ppt Sundari growth and regeneration is poor.

As a consequence of reduced fresh water discharge and salinity penetration in the Sundarbans, majority of the mesohaline areas will be transformed into Polyhaline areas, while Oligohaline areas would be reduced to only a small pocket along the lower-Baleswar River in the eastern part of the forest due to the availability of fresh water, receiving from GBM system. If the saline water moves front further inland, Sundari (the pioneer species in the landward Oligohaline zone) could be threatened. As a result, Sundari could be replaced by Gewa (now dominant in moderately saline waters), and Gewa by less valuable Goran (dominant in high saline water). That indicates the chain of economical degradation. Therefore, the total productivity of the forest is decreasing and losing their habitat due to high salinity in soil

2.3 Segmentation of Study Area

We chose 36 areas, 8 km × 8 km each, in the Sundarbans to analyze the phenological variation of its mangroves using NDVI data sets (Fig. 2.3). To further characterize the local morphological behavior of the western coast, seven non-overlapping segments along the coast designated as A through G were studied (Fig. 2.3). Segments A, B, C, and D are located in the western region and are covered with mangroves. Segment A, B, C and west side of segment-D are dominated by the Sibsha and Pasur River. The Baleswer River flows through in between of segment D and E. Segment E, F and G are located near the border of the western and central regions. Segment E and F have small mangrove forest in the front tip and segments G have an attractive sandy beach popularly known as Kuakata. The west side of Kuakata is dominated by Baleswar River and whereas east side is dominated by GBM River system. The eastern side of this segment is receiving more fresh water than the western side.

CHAPTER THREE

DATA AND METHODOLOGY

3.1 General

This chapter describes the different data sets that are used in this research. References on satellite data products, their accuracy, spatial and temporal resolution and applicability, are provided in this chapter which make it more complete documentation. Two kinds of satellite data processing have been carried out: i) analysis of the long-term variation of the Normalized Difference Vegetation Index (NDVI) to monitor the changes of mangrove forests, which was downloaded from the AVHRR (Advanced Very High Resolution Radiometer) GIMMS (Global Inventory Modeling and Mapping Studies) NDVI archive (http://glcf.umd.edu/data /gimms/) and from the MODIS ORNL DAAC (Oak Ridge National Laboratory Distributed Active Archive Center, hhttp://daac.ornl.gov database, and ii) detection of shoreline positions through LANDSAT (http://glovis.usgs.gov/) images to observe shore erosion and accretion. Techniques are shown to derive NDVI estimation and shoreline detection from the satellite product.

Beside the satellite data, hydrological (river discharge, salinity), metrological and wave hindcast data also are analyzed to find out the possible role of these variables on phenological and morphological changes along the Sundarbans. A statistical method named Sequential Mann-Kendall (MK) test is applied to find out the possible trend turning points in the NDVI time series. Finally, trends analysis and statistical cross-correlation techniques are shown in this chapter.

Description on a field survey which was conducted around the Sundarbans to understands the present conditions of water- and soil- salinity, soil characteristics and forest of Sundarbans, are described at the end of this chapter.

3.2 Normalized Difference Vegetation Index

Normalized Difference Vegetation Index (NDVI) is a robust, remote-sensing indicator of healthy, green vegetation, computed as the ratio (NIR-VIS)/ (NIR+VIS), where NIR and VIS are the reflectances in the near infrared and visible wavelengths, respectively. Healthy vegetation absorbs most of the visible light that hits it, and reflects a large portion of the near-infrared light. Unhealthy or sparse vegetation reflects less near-infrared radiation. NDVI value for a given pixel always presented as a number that ranges from minus one (-1) to plus one (+1). No green vegetation gives a value close to zero, while values close to +1 (0.8 - 0.9) indicate the highest possible density of green leaves.

NDVI is therefore a measure of vegetation health and productivity, sensitive to vegetation density and photosynthetic capacity. The idea is that degradation of vegetation phenology, as indicated in a decrease in greenness, is reflected in a decrease in the NDVI. NDVI time series data has been successfully used to characterize the structure, functionality, and dynamics of vegetation, detect long-term vegetation changes, monitor drought and desertification etc. (Slayback et al., 2003).

Since the launch of the National Oceanic and Atmospheric Administration (NOAA) satellites in 1970s, a large amount of invaluable and irreplaceable data sets have been available for global vegetation monitoring (Tucker et al., 2005). The Advanced Very High Resolution Radiometer (AVHRR) sensors onboard the NOAA satellites have provided one of the most extensive time series of remotely sensed data and continue to produce daily information regarding surface and atmospheric conditions (Kidwell et al., 1995).

Recently, the Moderate Resolution Imaging Spectroradiometer (MODIS) sensors onboard Terra and Aqua, designed to succeed the AVHRR instrument, has been of great importance for monitoring ecosystem variability and responses to seasonal and inter-annual environmental changes due to the improvement of both the temporal and spectral resolution

relative to AVHRR. Sensors of these types, such as NOAA-AVHRR and MODIS, are appropriate for obtaining time-series data and provide more opportunities for acquiring cloud-free images by the use of composite images collected within a short period, although they are unable to avoid the influence of frequent heavy cloud cover. Many studies have demonstrated the application of these sensors using NDVI data to obtain large-area land-cover information e.g. vegetation cover (Tucker et al., 2005, and Lunetta et al., 2006).

Sensors of the other type, such as the LANDSAT Thematic Mapper/Enhanced Thematic Mapper (TM/ETM+) onboard LANDSAT, Satellite Pour l'Observation de la Terre (SPOT), the Advanced Space borne Thermal Emission and Reflection Radiometer (ASTER) have a relatively high spatial resolution, but small coverage and long revisit period. These satellites are appropriate for obtaining only detailed local information due to incomplete spatial coverage, infrequent temporal coverage with inevitable cloud contamination and the associated large data volumes or high costs that are not feasible for programs operating at a large geographical scale (Defries et al., 2000). Table A1 shows some low or no-cost satellite sensors and data streams utilized for phenology studies.

As a result of the increasing number satellite systems, the user community now has access to an extensive global record of multi-sensor NDVI composites for land surface phenology studies. Sometimes combination of all available sources is more useful, as each sensor system has a different length of record as well as varied spatial, temporal, and radiometric characteristics (Van Leeuwen et al., 2006). Although the use of multi-sensor data can help to fill gaps in spatial and temporal to observe the long term NDVI variation.

Despite these efforts, the inter-sensor NDVI link issue has remained critical and complicated. The main difficulties in the use of multi-sensor NDVI time series for operational global vegetation studies arise from differences in the following: resolution, orbital overpasses times (Privette et al., 1995), geometric, spectral, and radiometric

calibration errors (Teillet et al., 1997), atmospheric contamination, and directional sampling and scanning systems. Because of these reasons the reflectances and NDVI from different satellite sensors cannot be regarded as directly equivalent.

The study presented in this thesis depends on the time series of AVHRR NDVI composite imagery from July 1981 to December 2006, derived from the National Oceanic and Atmospheric Administration's (NOAA) series of AVHRR instruments, with a spatial resolution of 8 km, by the NASA Global Inventory Monitoring and Modeling Systems (GIMMS) group at the Laboratory for Terrestrial Physics. For the recent (2005-2010) NDVI time series, the study selects the MODIS subset data (MODQ13, 250m spatial resolution) set from 2000 to present, provided by the Oak Ridge National Laboratory Distributed Active Archive Center (ORNL DAAC).

3.2.1 AVHRR GIMMS NDVI Data

The only updated global coverage NOAA-AVHRR data set, covering 25 year period spanning from 1981 to 2006, is the GIMMS 8 km resolution NDVI 15-day composite data set (Tucker et al., 2005). Tucker et al., 2005 described in detail, how the GIMMS data set was developed. Here, I am trying to report some key information about this data set.

The daily daytime AVHRR 4-km global area coverage data have been processed to produce an 8-km resolution NDVI dataset for all continents except Antarctica (Tucker et al., 2005). The data set is derived from imagery obtained from the AVHRR instrument onboard the NOAA satellite series 7, 9, 11, 14, 16 and 17. A number of improvements have been made on the GIMMS NDVI database, with respect to previous NDVI data sets, including corrections for: (1) sensor degradation; (2) inter-sensor differences; (3) solar-illumination angle and sensor-view angle effects due to satellite drift; (4) volcanic stratospheric aerosol corrections for 1982–1984 and 1991–1994; (5) missing data in the Northern Hemisphere

during winter, using interpolation; and (6) short-term atmospheric aerosol effects, atmospheric water-vapor effects, and cloud-cover physics. Finally, a new and updated release of the global coverage GIMMS data (1981–2006) was made available in 2007. Two NDVI compositing intervals have been produced: a bimonthly (15-day-composite) global dataset d (24 data sets in a year, two in a month) and a 10-day composite for Africa-only dataset. This data set is considered to be the most accurate, long term NDVI data record (Fensholt et al., 2006). Recent studies confirmed its suitability for long-term vegetation studies by comparing these data to new, improved coarse-resolution remotely sensed data from SPOT vegetation instrument and MODIS instruments (Fensholt et al., 2006).

From the whole global GIMMS NDVI images monthly pixel values of Sundarbans were selected in this study for the period 1985-2006 to analyze the long-term changes of the NDVI. The solid boxes 1-36 in Fig. 2.3 represent the locations for the NDVI analyses.

3.2.2 MODIS NDVI Data

The MODIS NDVI complements NOAA's Advanced Very High Resolution Radiometer (AVHRR) NDVI products and provides continuity for time series historical applications. For this study, the study used MOD13Q1 16-day composite, 250 m spatial resolution NDVI and NDVI Quality assurance products from Terra's Moderate Resolution Imaging Spectroradiometer (MODIS). The MOD13Q1 NDVI product is computed from atmospherically corrected bi-directional surface reflectances that have been masked for water, clouds, heavy aerosols, and cloud shadows. A new compositing scheme that reduces angular, sun-target-sensor variations is also utilized. Huete et al., 1999 described the detail about the MOD13Q1 NDVI product.

This study collects MOD13Q1 NDVI data from the ORNL DAAC archive. The data set covered whole Globe MOD13Q1 data at 250-meter spatial resolution as a gridded level-3

product in the sinusoidal projection from 2000 to the present. The ORNL DACC offer subsets of MOD13Q1 NDVI products for user-selected areas from one pixel up to 201 by 201 pixels. Output files contain pixel values of NDVI products in text format and in GeoTIFF format. In addition, data visualizations (time series plots and grids showing single composite periods) are available.

In this study, subsets have been created based on the central latitude and longitude of the GIMMS NDVI data and its spatial resolution of 8-km. NDVI data averaged over 32 by 32 pixels were collected, and the monthly variation analyzed.

3.2.3 NDVI Data Smoothing

There is some noise in the NDVI time series due to variations in the sensors of the satellites, in the overpass time, and in atmospheric conditions as well as to inadequate pre-calibration (Fensholt et al., 2009), in digital quantization, orbital and sensor degradation (Viovy et al., 1992 and Kaufmann et al., 2000). NDVI data sets are generally well-documented, quality-controlled data sources that have been pre-processed to reduce many of these problems (Gutman, 1999).

However, some noise is still present in the downloadable data sets and, therefore, such noisy NDVI data should be omitted in long-term NDVI data analysis (Pettorelli et al., 2005). Such noise is mainly due to remnant cloud cover, water, snow, or shadow, sources of errors that tend to decrease the NDVI values. False highs, although much less frequent, can also occur at high solar or scan angles (in which case the numerator and denominator in the NDVI ratio are both near zero) or because of transmission errors, such as line drop-out (Viovy et al., 1992). Vegetation phenology follows a repetitive seasonal cycle (Moulin et al., 1997), so NDVI time series should reflect a smoothly progressing pattern of vegetation growth (Sellers et al., 1996). Consequently, a realistic adjustment must account for missing

data and discount negative and anomalously low NDVI values, or outliers.

In this study, manual inspection was carried out to remove the upper mentioned two types of suspicious data from both the AVHRR and MODIS NDVI data sequences: very low or negative NDVI values (less than 0.05) and less frequent sudden transitions (spikes or dips) in the NDVI data sequence. Slayback et al. (2003) used a threshold of 0.05 in an analysis of NDVI trends.

Several approaches have been developed to further smoothing the values in the NDVI time series. The literature contains reference to a broad variety of techniques designed to reduce the impacts from these noise (e.g., Beck et al., 2006, Jonsson and Eklundh, 2002, 2004; Ma and Veroustraete, 2006, and Sellers et al., 1996), but every techniques have its own advantage and disadvantage. The most common approaches to smoothing NDVI time-series are presented in Table A2. These techniques are based on temporal approaches that provide an estimate for NDVI noise reduction through temporal interpolation (Julien and Sobrino, 2010). The study chose a Fourier-based adjustment to smooth NDVI time series in our study in the post processing steps. The Fourier series can be stated as a summation of sine and cosine functions given by

$$Y_i = \sum_{j=1}^{m} a_j \cos((j-1)\varphi_i + b_j \sin((j-1)\varphi_i) \quad (3.1)$$

Where a_j and b_j are Fourier coefficients;

$$\varphi_i = 2\pi(i-1)/n \quad (3.2)$$

φ_i is the phage, m is the number of harmonics, and i varies from 1 to n, where n the number of data points in the sequence. As for monthly NDVI time-series, here n=12, and m is set to 2 in this study. The second-order Fourier series are able to represent the seasonal variability of vegetation phenology with a smooth analytical function. This technique was applied successfully to produce the FASIR-NDVI (Fourier Adjustment, Solar zenith angle, correction, Interpolation and Reconstruction) published in the ISLSCP dataset collection (Meeson et al.,

1995) at a monthly temporal and 1° spatial scale. Seller et al. (1996) has described the details of Fourier adjustment of NDVI time series and evaluated the performance.

Before performing the Fourier adjustment, linear interpolation was carried out to replace the suspiciously low values and sudden transitions. Figure 3.1(a) gives an example of data replacement of NDVI values less than 0.05 and of sudden transitions in the data sequence by linear interpolation. In Figure 3.1(a), the NDVI value for August is considered to be too low, and the value for June, a spurious spike. Linearly interpolated values using the values for the previous month and subsequent month are substituted for the suspicious data.

Finally, Fourier adjustment (with 1.0 and 0.5 year harmonics) was performed to smooth the linearly interpolated data assuming that the NDVI values at each location should have a smooth sequential variation (Fig. 3.1(b)).

3.2.4 NDVI Variables

In the following, this study compares the variation of the NDVI for 36 areas (Fig. 2.3) to understand the variation of the NDVI over the Sundarbans. Analysis was performed

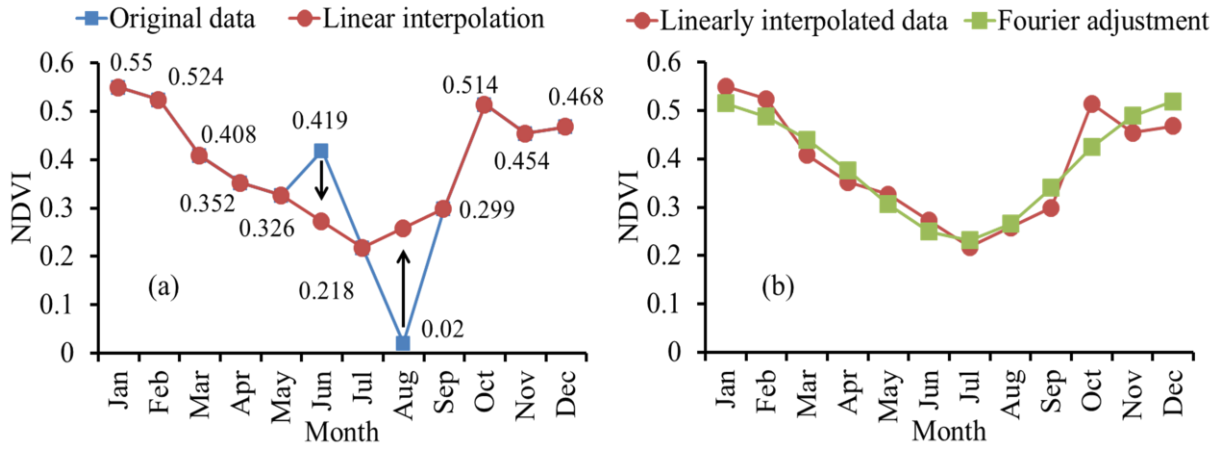

Figure 3.1 (a) Original AVHRR GIMMS NDVI data for 1999 for Area-1 and data corrected by manual inspection and linear interpolation, (b) Fourier adjustment of linearly interpolated data.

separately for each area (8 km by 8 km), and then an average over the 36 areas was processed to represent a composite NDVI value for the Sundarbans. In addition, analyses of three statistics, or variables, of the NDVI, the annual minimum, annual average, and annual maximum, for the composite of the 36 areas and each individual area were performed to identify possible long-term changes. Baldi et al. (2008) used similar types of NDVI variables in a temporal analysis of the NDVI to characterize possible functional changes in the amount and seasonality of vegetation phenology.

3.3 Shoreline Detection

The shoreline can be defined as the position of the land-water interface at one instant in time (Gens, 2010) is a highly dynamic feature and is an indicator for coastal erosion and accretion. Rapid shoreline changes can create catastrophic social, environmental and economic problems along populated strands. Multi-year shoreline extraction is considered to be a primary assessment to monitor temporal-spatial changes of shoreline that can help to understand among others, the spatial distribution of erosion hazards, predicting their development trend and supporting the mechanism research on coastal erosion and its counter measures.

Different approaches for coastline mapping are based on conventional field surveys or on the interpretation of aerial photographs. Usually, the rectified aerial photographs are manually interpreted using analytical stereo-plotting equipment. Periodic over-flights and aerial photograph analyses imply a high cost for updating coastlines. In such a context, image processing on multispectral remote sensing satellites data can provide a suitable tool for updating coastal maps over large areas at relatively low costs. Moreover, the high repetition rate of images acquired from space can provide the appropriate temporal sampling for studying the highly dynamic phenomena that determine the coastline shape.

In recent years, from 1972 the LANDSAT TM (Thematic Mapper) and ETM+ (Enhance Thematic Mapper) and other remote sensing satellites like ASTER provide digital imagery in infrared spectral bands where the land-water interface is well defined. This study relies on the LANDSAT data to monitor the shoreline dynamics along the Sundarbans coast.

3.3.1 LANDSAT Images

The LANDSAT Program is the longest running exercise in the collection of multispectral, digital data of the earth's surface from space. The temporal extent of the collection, the characteristics and quality of LANDSAT data, and the ability to collect new data directly comparable to that in the archive, make LANDSAT data a unique resource, one used extensively to address a broad range of issues to monitor and assess land and coastal zone resources. The spectral resolution and spatial resolution of different LANDSAT sensors has been tabulated in the Table A3.

To delineate the coastline positions images needed to be totally cloud free at least along the coastlines of interest. That restricted the number of images that could be used in this study. In this study, 14 images (from 1989-2010) from the LANDSAT USGS archive were analyzed to detect the variation of shoreline positions (Table A4). Most of the images were acquired in the dry season from November through December and in a cloud free day. The exception was two images from October 2009 and January 1989. The 1989, 1993 and 1995 images were from LANDSAT Thematic Mapper (TM, 4 and 5) and rests of the images were from Enhance TM (ETM+). The path and row for the images are 137 and 45 respectively.

Hourly tide-level data were collected from BIWTA (Bangladesh Inland Water Transport Authority) for the nearby tide station Hiron Point (Fig. 2.3). Details of the images used in this study are given in Table A4. Tide levels differences at the image acquisition times are also shown in Table A4 and indicate that the change in tide level was approximately 2 m.

3.3.2 Images Processing

Various methods for coastline extraction from LANDSAT imagery have been developed. Coastline can even be extracted from a single band image, since the mid- and near-infrared spectral bands of satellite images exhibit strong reflectance by soil and vegetation and absorbance by water, making it possible to separate the land from water and delineate the shoreline position (Kuleli, 2010). This can be achieved, for example, by histogram thresholding on one of the infrared bands of TM or ETM+ imagery. Table A5 shows techniques that have been used in different studies to detect the shoreline position along different location of the world using LANDSAT images. This reveals that a large number of methods are available for mapping coastline from LANDSAT sensor.

This study focuses on the shoreline detection from a single band. Experience has shown that the mid-infrared band 5 of LANDSAT TM and ETM+ is suitable for extracting the land-water interface (Alesheikh, et al., 2007). Band 5 exhibits a strong contrast between land and water features due to the high degree of absorption of mid-infrared energy by water (even turbid water) and strong reflectance of mid-infrared by vegetation and natural features in this range. Of the three TM infrared bands, band 5 consistently comprises the best spectral balance of land to water. Though there is other opinion as like Kevin and El Asmar (1999) found the use of TM band 7 is more suitable for monitoring changes in coastline position. Figure 3.2 shows example of the LANDSAT band 5 images for 1989, 1999 and 2010 of the study area. The separation of land surface from water bodies can be easily identified from the visual inspection.

In the first step of image processing, nearest-neighbor resampling methods was used to maintain the integrity of the image. For consistence, all images were resampled to a spatial resolution of 30m. Resampling of the 60 m pixels images to 30 m pixels images have been performed. Rahman et al. (2011) showed that resampling of 60 m images to 30 m neither

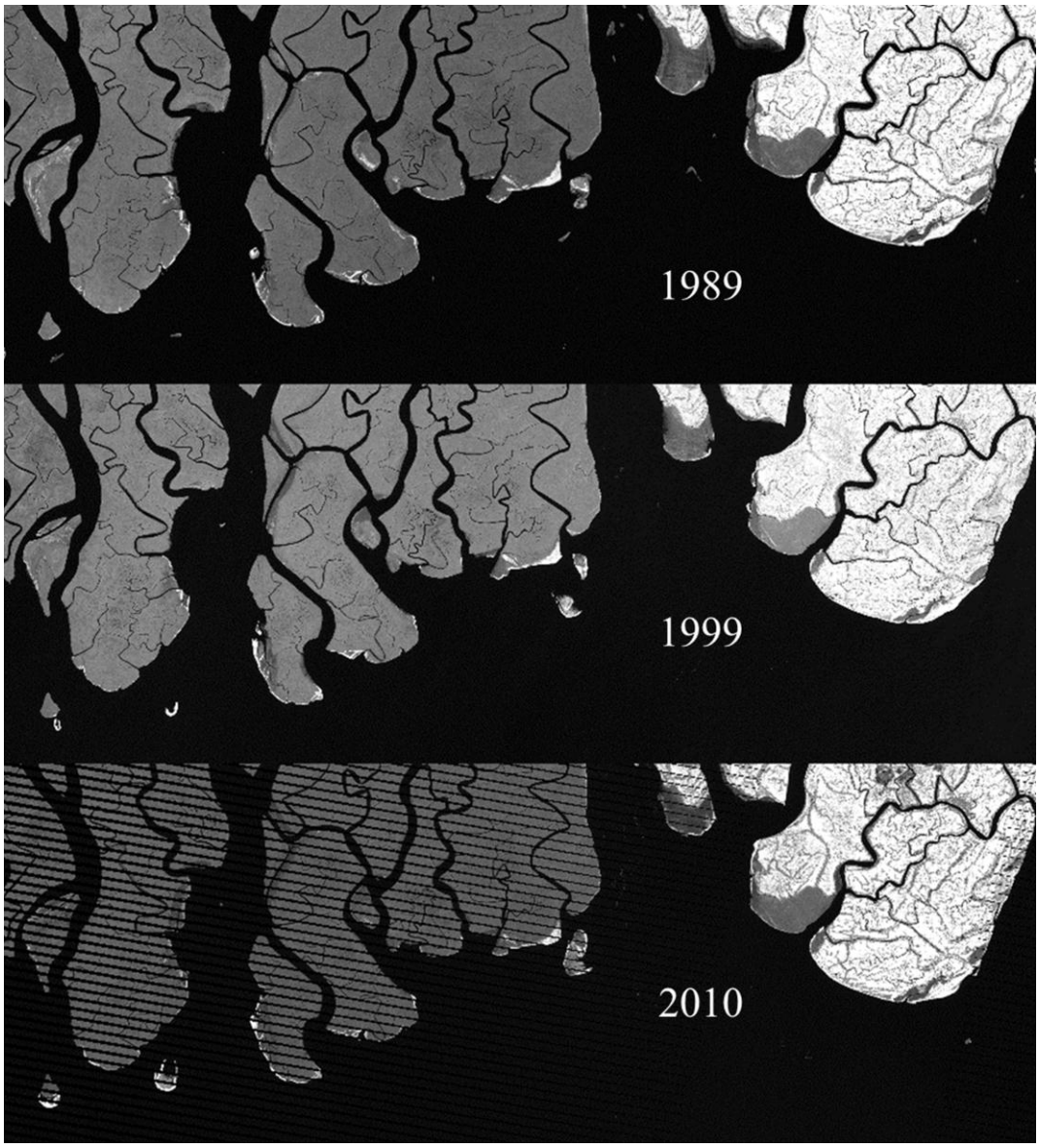

Figure 3.2 LANDSAT band 5 images for 1989, 1999 and 2010. Dark most portions represent water body, gray portion represents mangrove forest and bright portion represents bared land or agriculture land. The dashed lines in the bottom image are due to LANDSAT malfunction of the LANDSAT imaging sensor.

degrade nor improve the spatial resolution of images but reverse resampling would have degrade the spatial resolution of the images. Geo-registration was done to adjust the geographic position of the images. The 1989 image was used as the reference for rectifying all

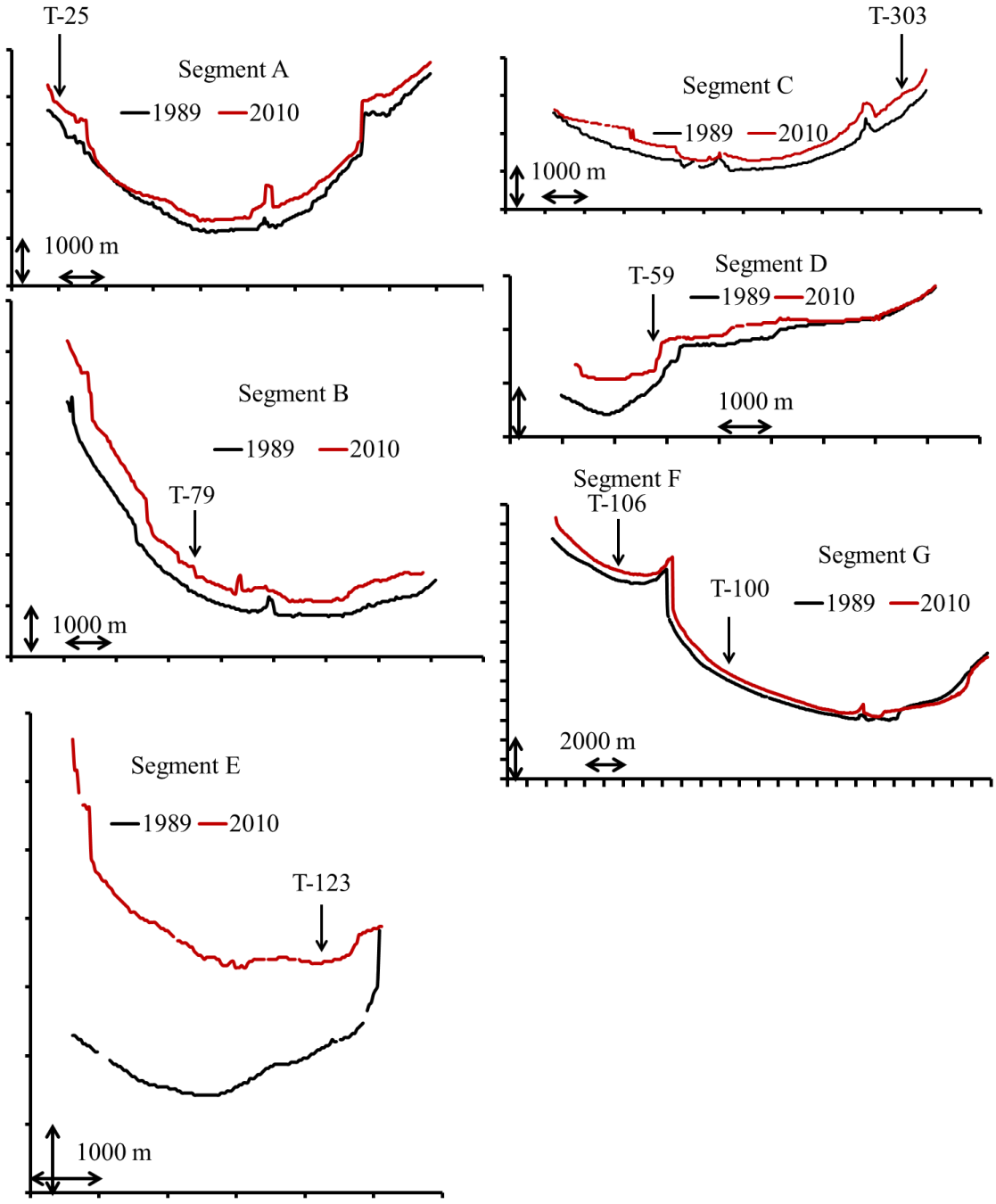

Figure 3.3 Detected shorelines position of segment A to G in the observation years 1989 and 2010. T denotes the transection line number.

other images. Then edge detection was applied to the distribution of pixel intensities of the band 5 images to locate the shoreline position. In each segment, southerly-facing shorelines were delineated at a spacing of 30 m alongshore from west to east (Fig. 3.3). Furthermore, in

each segment, west and east facing shorelines were also outlined along the river channels from north- south.

Finally, to refine the result, manual inspection was carried out to rectify erroneous data that might be due to mixed pixels (water and land) along the coastline. We were not able to verify the effect of tidal range on shoreline variations as the changes were large and we are assuming that the shoreline changes were not affected by the tidal variations.

3.4 Hydrological and Meteorological Data

River discharge and river-salinity data were collected from the Division of Hydrology, Processing and Flood Forecasting Circle, Bangladesh Water Development Board (BWDB). Monthly mean river discharge data for the Gorai River at the Gorai Railway Bridge (Station ID: SW99) for 1983-2010 were acquired to discuss the variation of freshwater supply into the Sundarbans over the years. The data contains one to five observations data records in a month. The study averaged the monthly observation records to produce a mean monthly river discharge data set. Total observational month is 324; among them 11% months in the dry season (January to May) and 3.7% months in wet season (June-September) have no data records. This study processed mean data sets for dry season (January -May) and wet season (June to September) discharge of every year.

River-salinity data for the Rupsha-Pasur River at the Khulna station (Station Id: SW421) were also collected for 1985-2010 to explain the change of water-salinity in the Sundarbans. The data set contains daily record for each month, with some missing data records. The data includes data records for 300 months; among them 7.6% months have no data in dry season and 82% month have no data in wet season. Similar to the river discharge data we produced the mean monthly dry season data of every year. The reason to choose these two stations are as follows; i) Gorai River is one of the major rivers connecting the

Ganges, Sibsha, and Pasur and variation of flows through Gorai River is an indication of variation of received amount of fresh water by Sundarbans, and ii) Khulna Station is situated on the Rupsha-Pasur River just before the Sundarbans and collects salinity data with which one can predict the long-term variation of salinity of the Sundarbans. There are some gaps in the river discharge and salinity data sets. In particular, there is very little salinity data for the wet season. Missing data could not be estimated because no nearby station has similar data. The dry season salinity data has been taken into consideration as in dry season the salinity variations are influenced by the upstream river flow, whereas in the wet season, rainfall is influential in the lower Ganges basin. Moreover very few salinity data in wet season restrict us to make analysis on wet season.

The rainfall data at Khulna stations contains daily data records from 1948 to 2009 for every year. The study picked up the data from 1985-2009 from the total data records for the study analysis, which contains only 4% missing values in the data sets. Mean monthly data for every year has been produced for further analysis.

Hindcast wave data (significant wave height, wave period, and wave direction) were acquired from the ECMWF ERA-Interim archive, which provides data for 00h, 06h, 12h, and 18h UTC each day on a 1.5° by 1.5° longitude-latitude grid covering the whole globe. ECMWF ERA-Interim wave data are freely available to the research community for the period of 1979 to presents. Dee et al. (2011) describes the forecast model, data assimilation method, and input datasets used to produce ERA-Interim, and discusses the performance of the system. Hemer et al. (2011) described and showed the use of the ECMWF ERA- Interim significant wave height, wave direction and wave period data for assessing variability in the mean wave climate in Pacific Ocean basin.

3.5 Statistical Analysis

Three types of statistical analyses were performed in this study to detect trends in the data sequences and to identify cross-correlations among the NDVI, shoreline change rates, and hydrological and meteorological factors.

First, a sequential Mann-Kendall (MK) test was applied to the time series of NDVI variables to detect the potential turning points of trends. Sneyers (1990) described the detailed procedure of the sequential MK test for the time series data. This test implicitly assumes an equidistance time series. At first, in the series of annual minimum of the NDVI x_i (i=1, 2…n, and n= number of data) of 36 areas composite from 1985 to 2006 (AVHRR data set), the original values have been replaced by their ranks y_i (order number). The only aim of this replacement is to simplify the calculation procedure. For each element x_i or, what amounts to the same thing, for each element y_i, the number n_i of elements y_j preceding it (i>j i.e. i=1, 2…n, and j=1, 2…i-1) is calculated such that $y_i > y_j$. The test statistic t_i is then given by equation

$$t_i = \sum_1^i n_i \tag{3.3}$$

and its distribution function, under the null hypothesis, is asymptotically normal with mean and variance

$$E(i) = i\,(i-1)/4 \tag{3.4}$$

$$Var(i) = i\,(i-1)\,(2i+5)/72 \tag{3.5}$$

The progressive sequential values of the statistic u(i) for each of the test statistic variables t_i are then calculated as

$$u(i) = [t_i - E(i)] / \sqrt{var(i)} \tag{3.6}$$

The values of u'(i) are then computed backwards, similarly as the progressive series but starting from the end of the original time series of annual minimum NDVI. Thus, the test calculates the backward series u'(i) using same equations (3.3)-(3.6) but with reversed data.

The graphical representation of u(i) and u'(i) in terms of i generally gives two curves. The test suggested that points where the two curves cross each other are regarded as approximate potential turning points of trends in the time series. In the absence of any trend in the series, the curves generally overlap several times (Sneyers, 1990). When either the progressive or backward series exceed certain confidence limits before or after the crossing point, the trend turning point is considered significant at the corresponding level, i.e., 1.96 for 95%. Similar test has been performed for the time series of annual average and annual maximum NDVI. Sequential MK test was separately applied for the time series of NDVI variables which was getting from the MODIS data set (2001-2010).

Second, to determine the years for potential turning points in the NDVI trends estimated from the sequential MK test, the NDVI time series were divided into different time periods. Linear regression was used to estimate rates of change in the NDVI time series and shoreline changes.

Third, a correlation coefficient (Pearson correlation) against different lag times (in years) was calculated between the seasonal components of the NDVI and the discharges and salinity to better understand the relationships among these properties.

3.6 Field Survey

A two days long field survey was conducted in 8-9, March, 2013 to understand the present conditions of water- and soil- salinity, soil characteristics and forest of Sundarban. The study covered the survey around the Kochikhali coast (Segment D; Fig. 3.4)

During the survey, five soil samples from different location (Fig. 3.4) were collected from Mongla to Kochikhali from a depth 15-20 cm in polythene bags and brought to the laboratory. Samples were tested at Bangladesh Council of Scientific and Industrial Research (BCSIR) for the four parameters as Soil Texture Classification, Exchangeable Sodium Percentage (ESP), Electrical Conductivity (EC) and P^H. River water- salinity of Supoti Khal and Kotka River (see Fig. 3.4) were measured with electrical conductivity meter during high and low tide. Some images were taken during the survey to explain present coast conditions. Some images of Sundarbans, which were taken during the survey, has been shown at the end of this thesis.

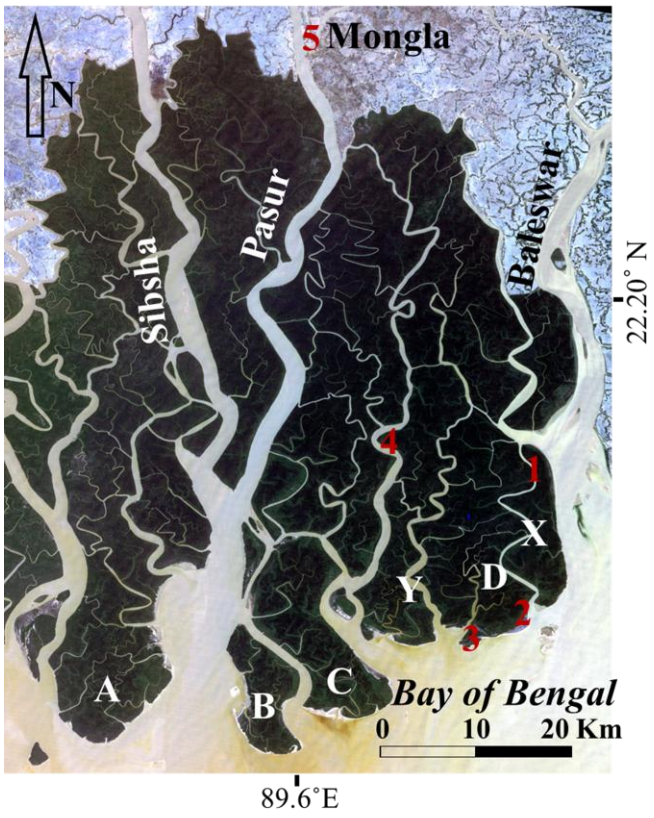

Figure 3.4 Survey locations. Point 1-5: soil sample locations. X and Y are the Supoti Khal and Kotka River respectively.

CAPTER FOUR

RESULTS

4. 1 General

Satellite remote sensing data was employed to observe the phenological and morphological changes of Sundarbans mangrove forest. This chapter describes the seasonal and spatial distribution of Sundarbans NDVI. The linear trend estimates of NDVI variables during different time periods are presented to demonstrate the potential changes of mangrove phenology over the time period of 1985-2010. Assessments of morphological changes in terms of shore erosion and accretion along Sundarbans, over different time periods are also presented in this chapter. Changes in seasonal and long term river discharge in upstream are documented during the satellite observation to understand the possible role of river discharge on the phenology and morphology of Sundarbans. The end of this chapter shows cross-correlation between river discharge and NDVI variables.

4.2 NDVI Variation and Trends

Figure 4.1 shows the seasonal variation and time series of the NDVI, corrected with the procedures described in chapter 3, at three locations Areas-1, 15 & 8 in (Fig. 2.3). The NDVI has an annual cyclic variation and achieves a maximum in November or December and a minimum in June or July. Hoq et al. (2006) also reported that major peak of density occurred in the Sundarbans mangroves species from November through February. The annual variation of the NDVI can be attributed to the annual variation of the greenness of the dominant mangrove species in the observation area. Different annual variation of NDVI observed at Area-1, 15 and 8 (Fig 4.1, upper panel), suggesting that these three areas are dominated by different mangrove species. In this context, the study attempted to categorize the observed 36 areas based on the pattern of annual variation of NDVI, and found three

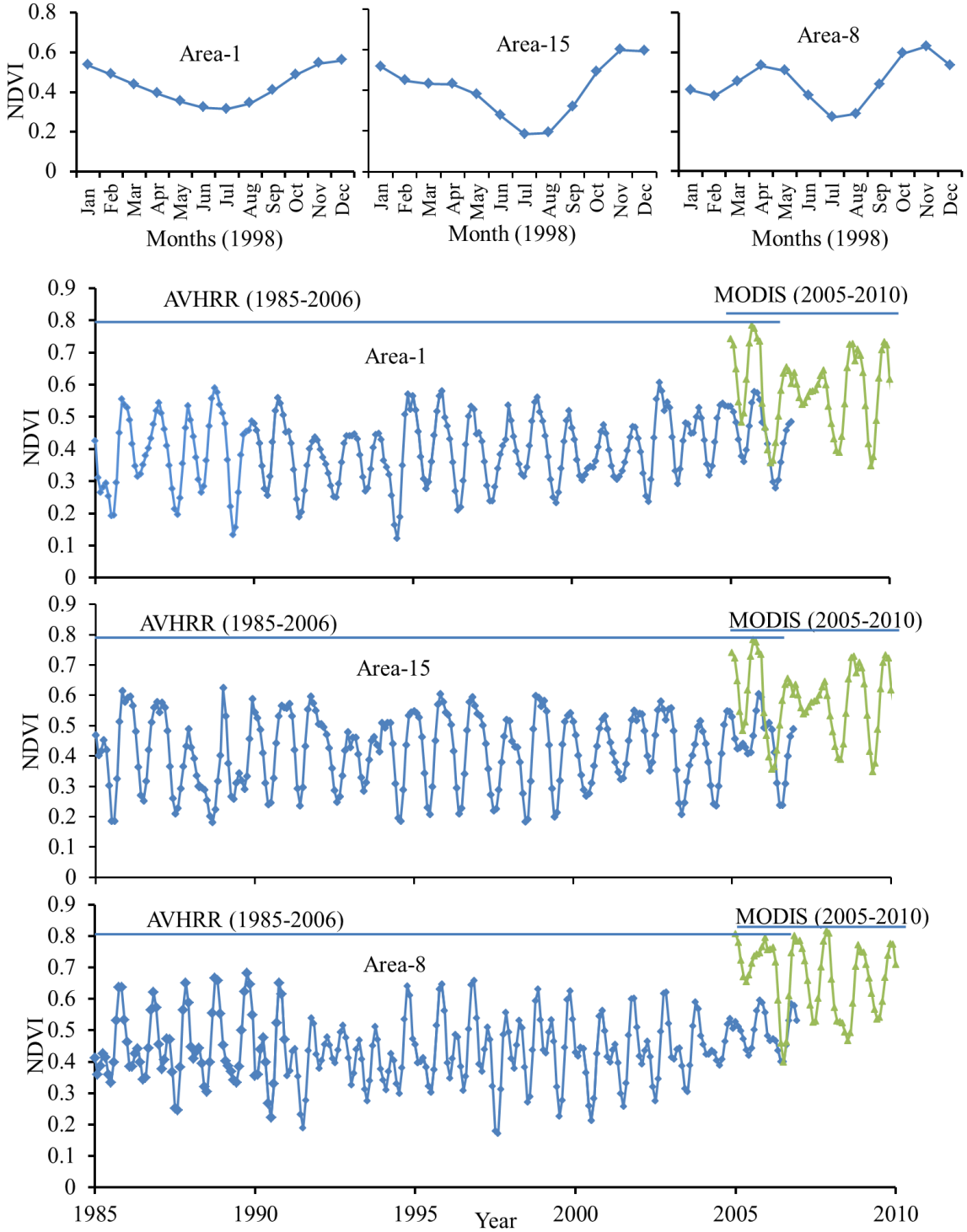

Figure 4.1 Annual variation (upper panel) and time series of NDVI at Area-1, 15 and 8 (bottom two panels).

types of annual variation of NDVI as like Area-1, 15 and 8. The Area-8 has one intermediate peak in the annual NDVI variation, whereas Area-1 doesn't show such type of intermediate peak. Further, annual NDVI variation of Area-15 is in between the annual variation of NDVI

of Area-1 and 8.

Figure 4.2 shows the spatial distribution of different types of annual NDVI variation at the 36 areas of Sundarbans categorized from the annual NDVI variation described above. The southwest corner is dominated by Type-1 (high saline zone), while in the central part (moderately saline zone) by Type-2 and in the north to east part (relative fresh water zone) byType-3. Based on the discussion at section 2.3, the study is guessing that the intermediate peak in the NDVI variation of Type-3 during the year may be due to the relative abundance of the Sundari species at this location with a mixture of Gewa. Type-1 is found on the southwest side of the Sundarbans, where Goran is the dominant mangrove species, and doesn't generate intermediate peaks in the annual variation of the NDVI as area of Type-3 does. Type-2 is found at the central part (moderately saline zones), where Gewa with irregular spreading of Sundari are the dominating species and shows reasonably similar seasonal variation of NDVI as areas of Type-3.

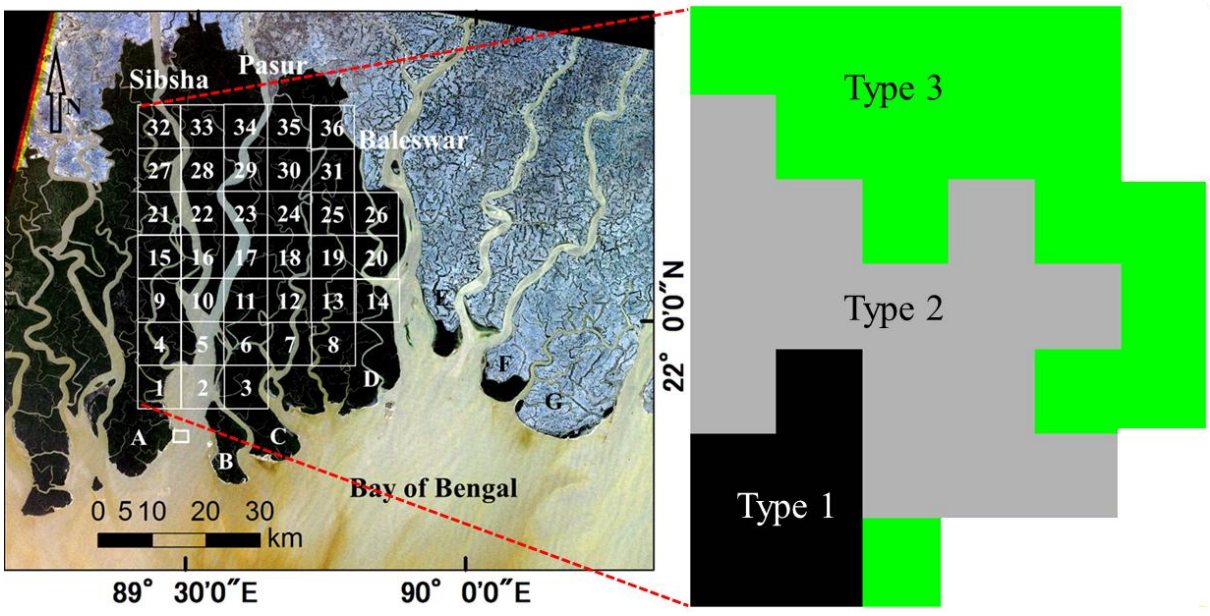

Figure 4.2 Spatial distributions of different types of seasonal variation of NDVI around the Sundarbans based on 1998 NDVI data.

Figure 4.3 (a) shows time series of NDVI for 36-area composite for 1985-2006 (AVHRR) and for 2005-2010 (MODIS). The time series of annual minimum, average and maximum for 36 areas composite, extracted from Fig. 4.3 (a) has been shown in Fig. 4.3 (b). Differences between the AVHRR and MODIS data may be due to differences in the absolute calibration, bands, and resolutions of the different satellite sensors (Ye, et al., 1999). For example, AVHRR provided NDVI values with 8-km resolution containing NDVI data dominated by bodies of water as well as by mangroves, whereas MODIS provided 8-km subsets of NDVI data with a 250-m resolution and NDVI values associated to areas of water

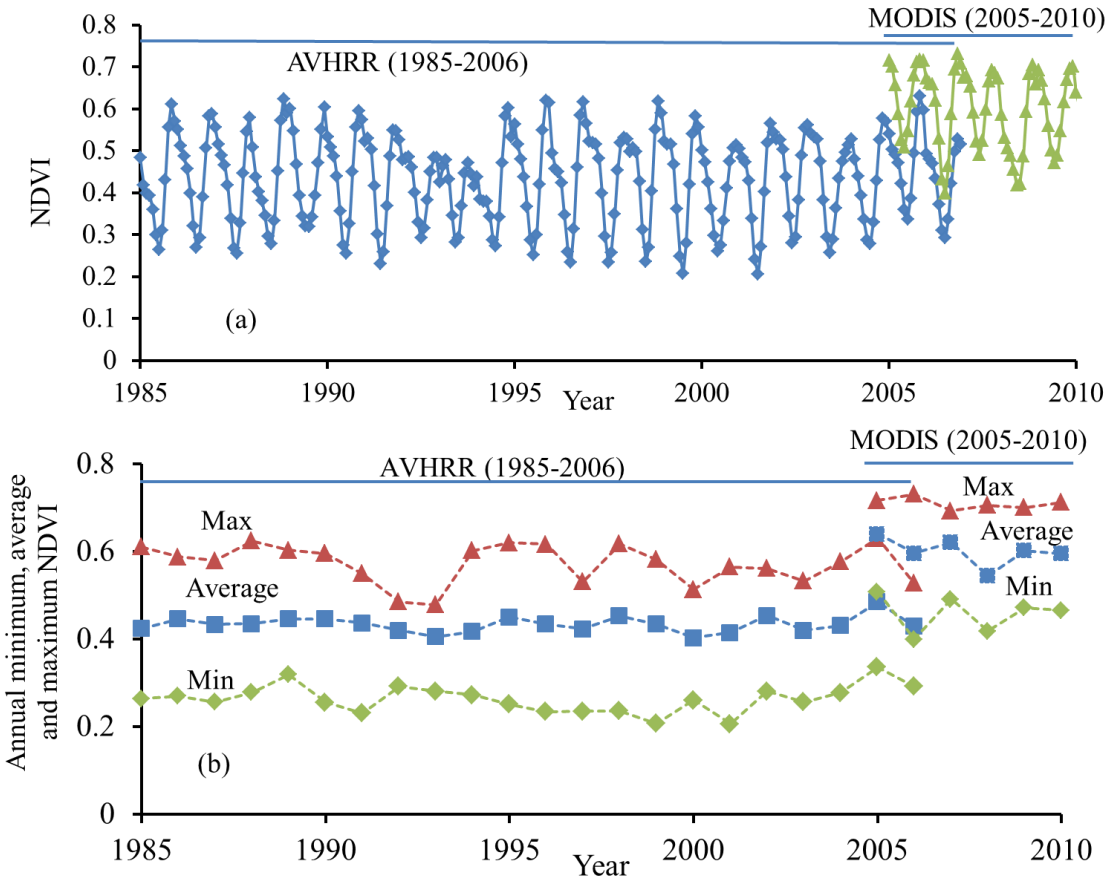

Figure 4.3 (a) Time series of NDVI for 36 areas composite. (b) Time series of annual minimum, average, and maximum NDVI for 36 areas composite.

excluded. The overall lower NDVI values of the AVHRR data may be due to this.

From visual inspection, it is hard to divide the time series into different periods to determine possible trends in the NDVI time series, so the study used a sequential MK test to estimate turning points of trends in the series of NDVI statistics. The results of the sequential MK test are presented in Fig. 4.4 for time series of the annual minimum, average, and maximum NDVI values. The progressive and backward curves intersect each other in 1999. This intersection point is a potential trend turning-point for the time series of AVHRR NDVI data. The two curves are very close to intersecting each other in 1991, so the study also

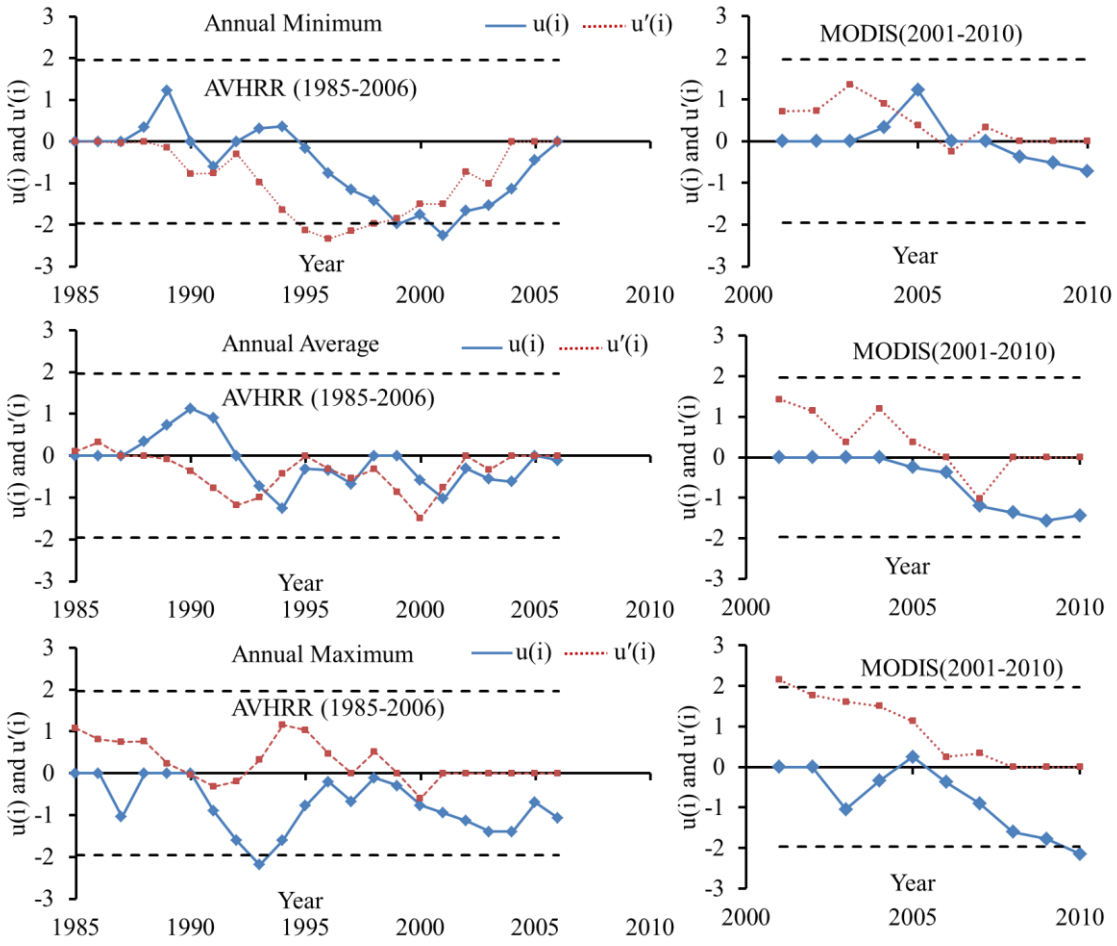

Figure 4.4 Potential turning points of trends in the NDVI variables, derived from the sequential MK test. u(i) and u′(i) are progressive and retrograde curves, respectively. The dashed lines represent the significance boundaries (t=1.96; Alpha=0.05).

Table 4.1 Percentage of area having positive or negative NDVI trends, among 36 areas. A positive (negative) percentage represents the percentage of areas that have increasing (decreasing) trends. Notable percentages are in bold.

NDVI Variables	1985-1990 (AVHRR)		1990-2000 (AVHRR)		2000-2006 (AVHRR)		2005-2010 (MODIS)	
	(+) trend (area %)	(-) trend (area %)	(+) trend (area %)	(-) trend (area %)	(+) trend (area %)	(-) trend (area %)	(+) trend (area %)	(-) trend (area %)
Min	41	59	30	**70**	**95**	5	35	**70**
Average	53	47	50	50	**95**	5	0	**100**
Max	44	66	67	33	**84**	16	18	**82**

regards this point as a potential trend turning-point. Another potential turning-point is in 2005 for the time series for the annual minimum of recent NDVI data (MODIS). There were no such potential turning points for the annual average and maximum NDVI.

Based on these results, the time series for the annual minimum, average, and maximum of the NDVI for the AVHRR and MODIS data sets were divided into the four periods 1985-1990, 1990-2000, 2000-2006 (AVHRR), and 2005-2010 (MODIS), and linear regression was applied to delineate trends in the NDVI time series.

Table 4.1 shows the statistics for the 36 areas for the annual minimum, annual average, and annual maximum NDVI trend analysis. For the period 1985-1990, there is no notable percentage of areas that have a decreasing or increasing trend in the time series of the three variables. But decreasing trends was dominating in all three NDVI variables. In the period 1990-2000, 70% of the areas have a decreasing trend in the annual minimum NDVI (Table 4.1). In the period 2000-2006, 90 % of areas have significantly positive trends in all three NDVI variables. In the latest period 2005-2010 (MODIS), the trends are negative for more than 80% of the areas.

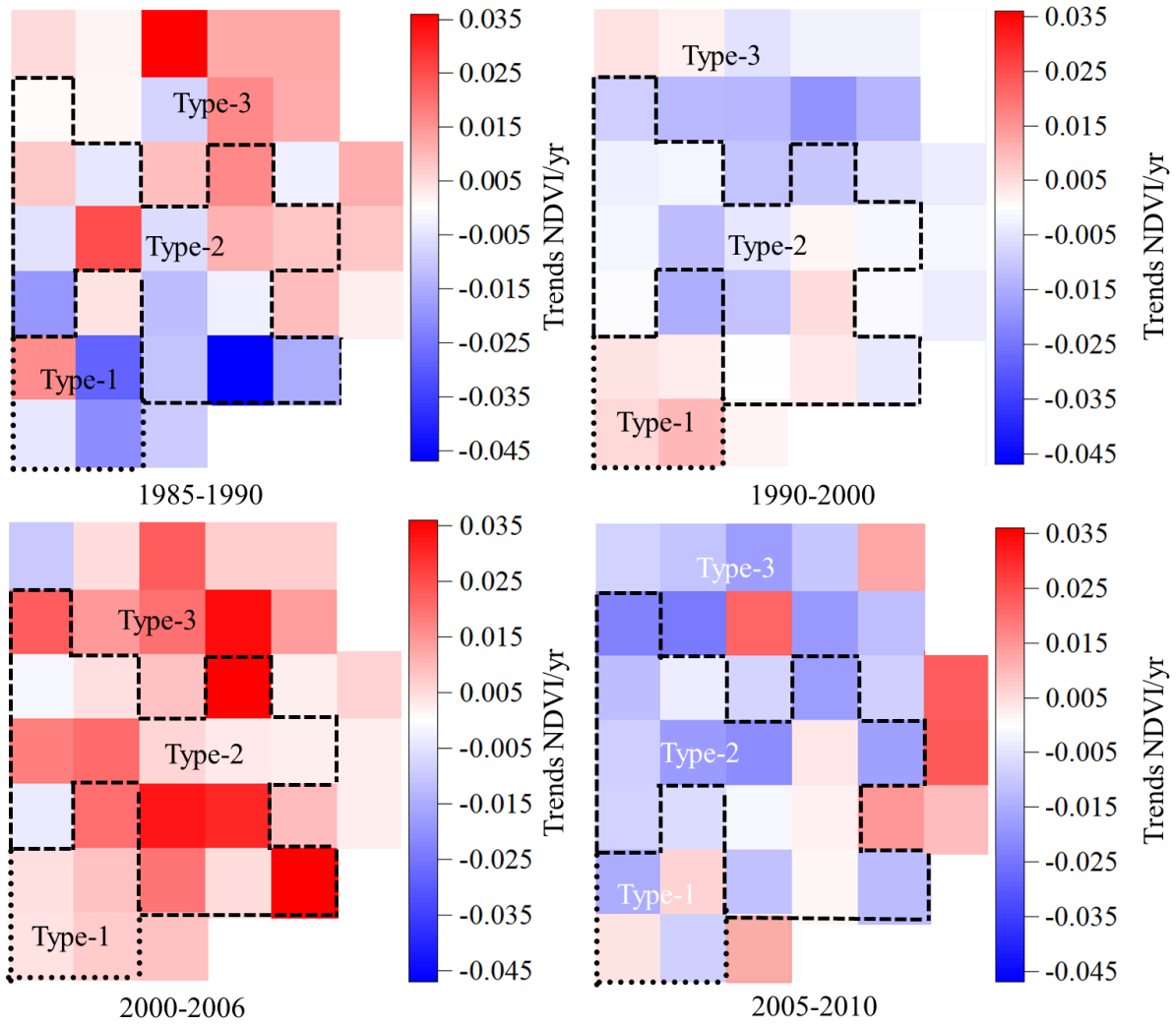

Figure 4.5 Spatial distributions of trends in annual minimum NDVI at 36 areas of Sundarbans. Red- reddish represents areas having increasing trend, blue-bluish represents areas having decreasing trend. Type-1, 2 and 3 represent the zones having different annual variation of NDVI (Fig 4.2).

Figure 4.5 shows the spatial distribution of trends of annual minimum NDVI of Sundarbans over different time period. The red to reddish color represents the areas having increasing trends and blue to bluish color represents the areas having decreasing trends. The areas, having annual NDVI variation Type-2 and Type-3 (Fig 4.2), which is found at relatively fresh and moderately saline zone, started to degrade (blue to bluish color) in the period of 1990-2000. But the mangroves of high saline zones (Type-1) still had increasing trends in the annual minimum NDVI. In the next period 2000-2006, the Fig. 4.5 shows red to

reddish color is dominating which is an indication of increasing trends in annual minimum NDVI around the Sundarbans. Some positive trends (red-reddish) are found at the southwest and east corner of Sundarbans in the present period of 2005-2010, whereas most of area is facing decreasing trends in minimum NDVI (blue- bluish). The results from Table 4.1 and Fig. 4.5 indicate that the mangrove phenology around the Sundarbans was improving in the middle period 2000-2006. The cause of this improvement is discussed latter.

4.3 Reliability of NDVI Analysis

The annual variation of NDVI depends on the type of vegetation cover of individual regions and the long term variation of NDVI is correlated with local factors i.e. climate, human influences etc. for individual regions, and their relation with the variation of local factors is also well reported (Gurge et al., 2003). Using this concept, a comparison between the processed NDVI data for the Sundarbans and that for other locations, the Simlipal forest and the Rajasthan desert, located in India, is done, to assess its reliability, whether the processed NDVI of Sundarbans is merely artifacts or not? It was found that the annual variation of the NDVI for the Simlipal forest has a different seasonal cycle compared to that of the Sundarbans, whereas the NDVI for the Rajasthan desert has a negligible seasonal variation (Fig. A1). In addition, a sequential MK test for the Simlipal forest (Fig. A2) data produced turning points in potential trends different from those of the Sundarbans.

Further, the study processed the NDVI data for the Sundarbans with other adjustment method, Saviztzky-Golay filter and then applied sequential MK test. The result was similar with negligible difference in potential trends turning points compared to the result we got with Fourier adjustment. These dissimilar variations for different locations and similar variation for different methods smoothen imply that detected trends are not merely artifacts of the specific data set or analysis procedures.

4.4 Shoreline Changes

Figure 4.6 (a) shows southerly facing shoreline positions for 1989 and 2010 of segments A to D. The shorelines of these segments, covered with mangrove, were pushed back by erosion from their earlier positions. The shorelines of zones $Ac\text{-}_A$, $Ac\text{-}_C$ and $Ac\text{-}_D$ experienced no significant changes over the period 1989-2010. One island (Is2) appeared just southeast of segment A in 2010. The land areas of island Is1, southwest of segment A, and island Is3, southeast of segment D, increased by approximately 30% over the period

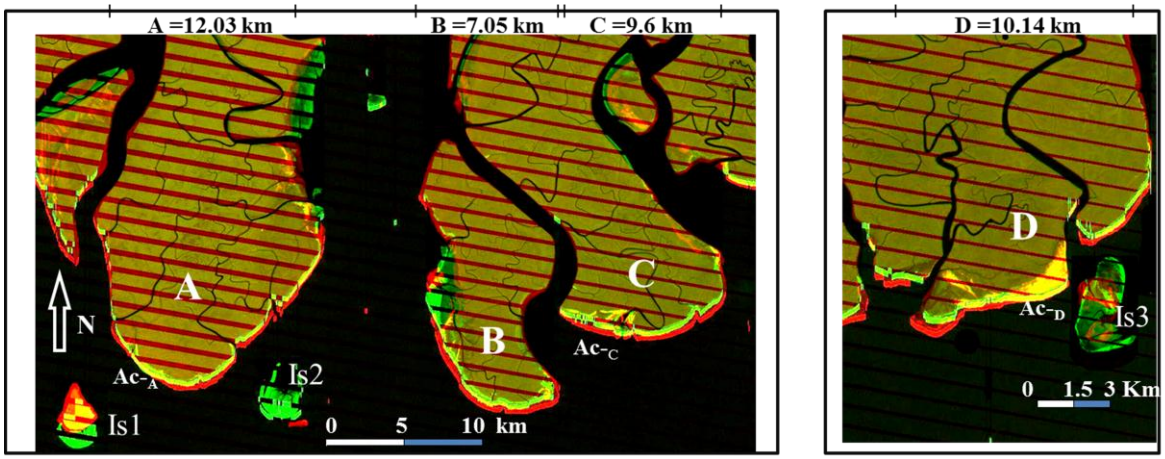

Figure 4.6 (a) Southerly facing shoreline positions in 1989 (red) and 2010 (green) for segments A-D. Oblique strips in the images are due to a malfunction of LANDSAT 7.

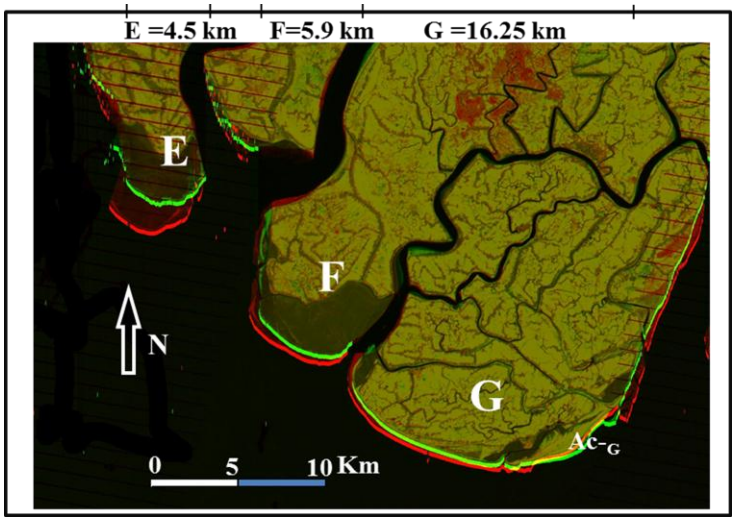

Figure 4.6 (b) Southerly facing shoreline positions in 1989 and 2010 for segments E-G. Red line shows the shoreline position in 1989 and green shows the shoreline position in 2010.

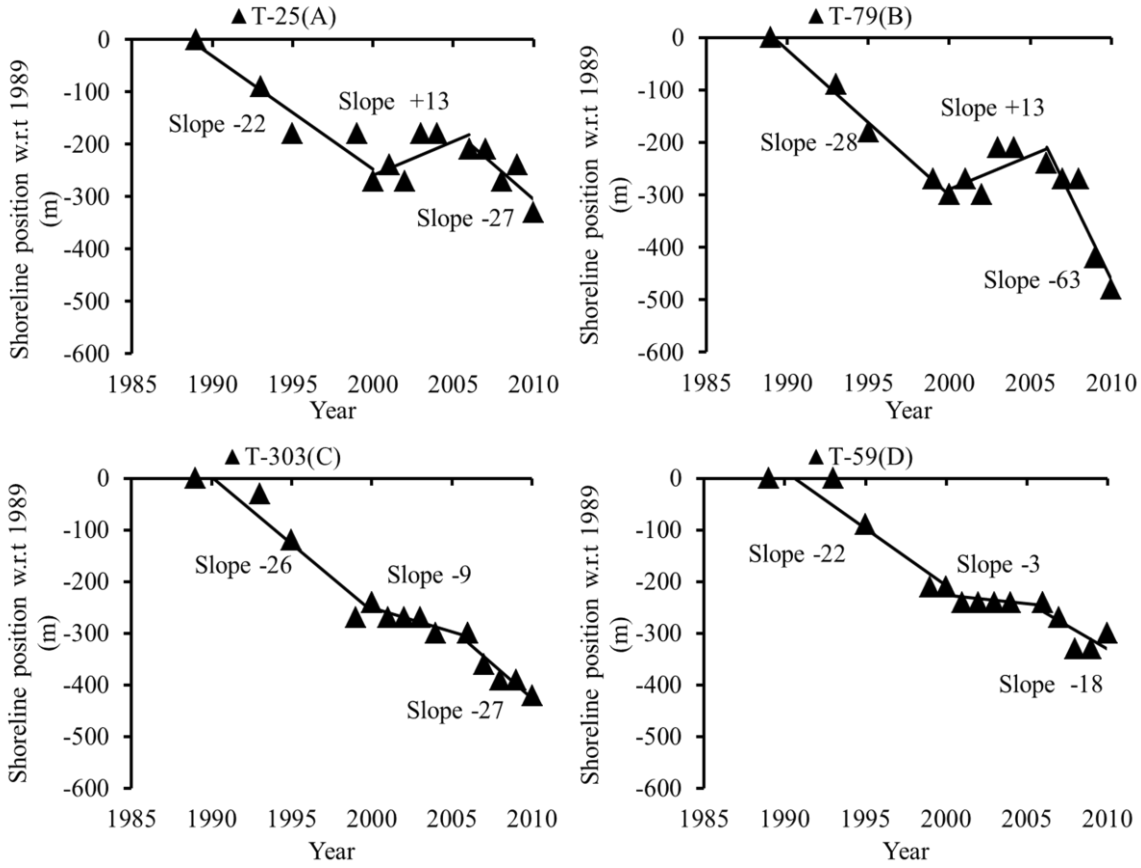

Figure 4.7 (a) Variation of southerly facing shoreline position at T-25, segment A; T-79, segment B; T-303, segment C and T-59, segment D (Fig. 3.3). Vertical axis gives the position of the shoreline with relative to the shoreline position in 1989.

NB: Negative position indicates a landwards position relative to the shoreline position in 1989. Solid lines are trend lines. T denotes a transection line.

1989-2010.

Figure 4.6 (b) shows the southerly facing shoreline positions for 1989 and 2010 for segments E to G. Most of the shorelines were farther seaward in 1989 than in 2010. Only for the portion Ac-$_G$ on the east side of segment G was the shoreline farther seaward in 2010 than in 1989 (Fig. 4.6(b)).

Figure 4.7 (a) displays an example of the variations of shoreline positions along two transects of segments A -D in N-S direction. The shoreline variations along one transection line for segment E-G have been shown in the Fig. 4.7 (b). In most locations, shoreline was moving landward during the periods 1989-2000 and 2006-2010, whereas in the period

2000-2006, it moved seaward or rate of retreat slowed down. Observing this nature of shoreline variation and to correlate changes in the shoreline position with the NDVI trends, the rate of change in shoreline position was estimated over three time periods, 1989-2000, 2000-2006, and 2006-2010, by linear regression of shoreline positions along transection lines in the N-S direction. In addition, similar rate of shoreline positions were also estimated in the W-E and E-W direction to observe the changes along the river channel. The results of average rate of shoreline changes for segment A-G over different time period in three directions are shown in Figures 4.8-4.14:

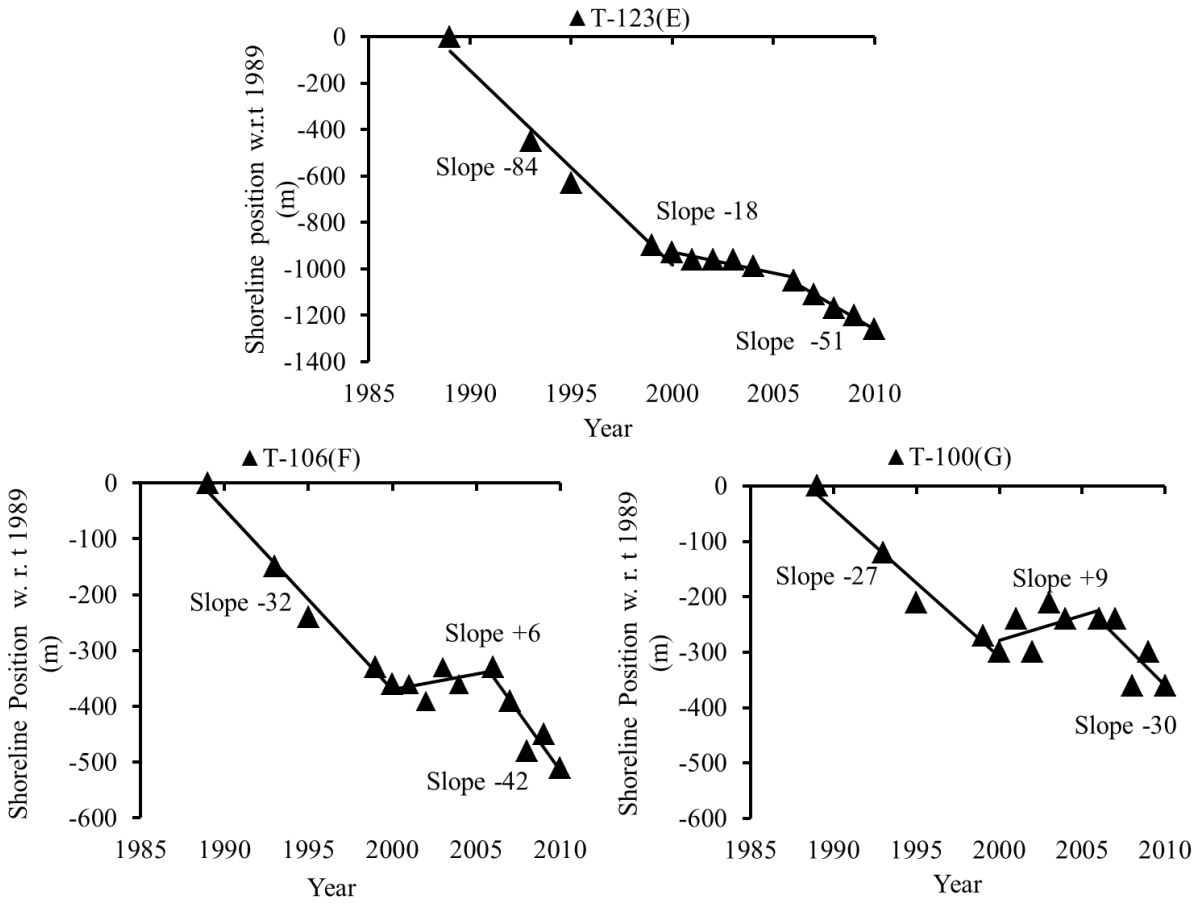

Figure 4.7 (b) Variation of southerly facing shoreline position at T-123, segment E; T-106, segment F and T-100, segment G (Fig. 3.3). Vertical axis gives the position of the shoreline with relative to the shoreline position in 1989.

NB: Negative position indicates a landwards position relative to the shoreline position in 1989. Solid lines are trend lines. T denotes a transection line.

Segment A: Covered with mangrove forest and locally known as Hiron Point. Hiron Point is close to the mouth of the river and its south face meets with the Bay of Bengal. The combined flow of two major rivers of Sundarbans, i.e. Sibsha and Pasur River (main stream of Ganges-Gorai) empties into the Bay of Bengal through the east side of this segments and west side river of this segment is a branch river, away from main stream (Ganges- Gorai).

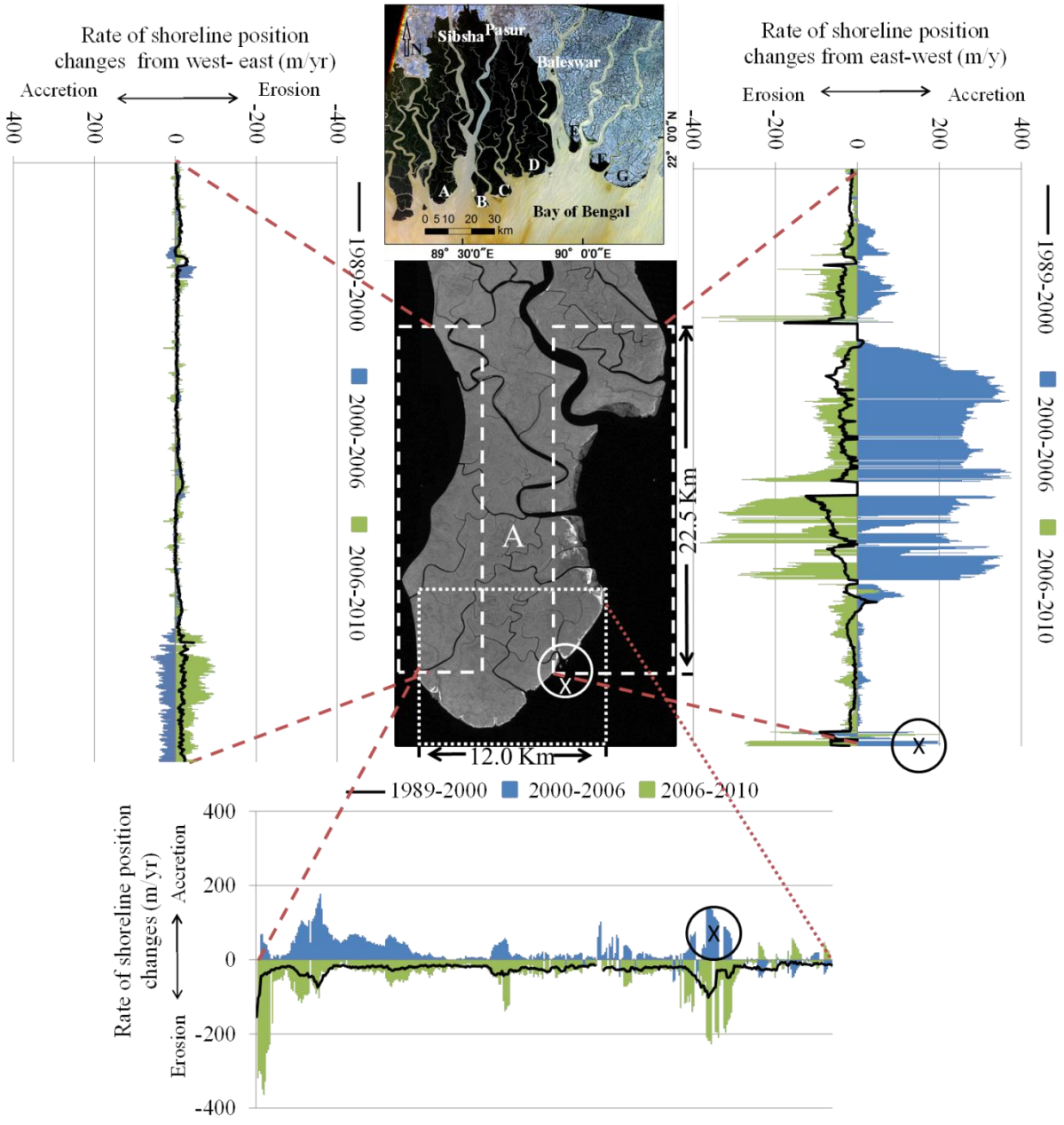

Figure 4.8 Distribution of shoreline change rates in N-S (bottom panel), W-E (left panel) and E-W (right panel) directions for the three periods 1989-2000, 2000-2006 and 2006-2010 for segment A. Negative rate corresponds to erosion.

Perhaps the rivers empties into sea is not quite the right word as the river is tidal, flowing both ways. This study estimated the rate of shoreline position changes along 12 km long coastline in the south face and 22.5 km in the west and east faces of segment A.

Figure 4.8 shows the average distribution of the shoreline change rates for the three periods of segments A in the N-S, W-E and E-W directions. There were high erosion rates for the shoreline for 1989-2000 and 2006-2010 in all three directions, whereas accretion occurred during the period 2000-2006. The west facing shoreline was almost stable compared to east facing and southerly facing shoreline. However, some changes observed in the south-west corner of this segment. Maximum accretion and erosion rate occurred in the bend portion towards the east side river channel. At the mouth of channel and creeks the changes rates are larger (shown with X in Fig. 4.8). The overlapping portion of south and east face shoreline represented quite similar nature in rate of changes over different time periods.

Segment B: Locally known as Dubla Char, is a low laying island which forms the outermost area of Sundarbans and covered with mangrove forest. The west side of this segment is situated to the east of the outer estuary of Sibsha-Pasur River, one of the main stream of Ganges-Gorai River. A narrow branch of Pasur River is passing through the east of the segment which meets Bay of Bangle to the south. This study estimates the rate of shoreline position changes of segment B along 7.0 km long coastline in the south face and 13.8 km in the west and east faces.

Figure 4.9 shows the average distribution of the shoreline change rates over three time periods for segments B in the N-S, W-E and E-W directions. Similar to the segment A, erosion was dominating during the periods of 1989-2000 and 2006-2010 in all directions, whereas accretion was dominating during the period of 2000-2006. Larger changes happed in the bend portions of west and east face, compared to other portions. Decelerating rate of

changes observed from sea to far north end. Shoreline of southerly facing shows higher rate of changes at south-west end compared to south-east end.

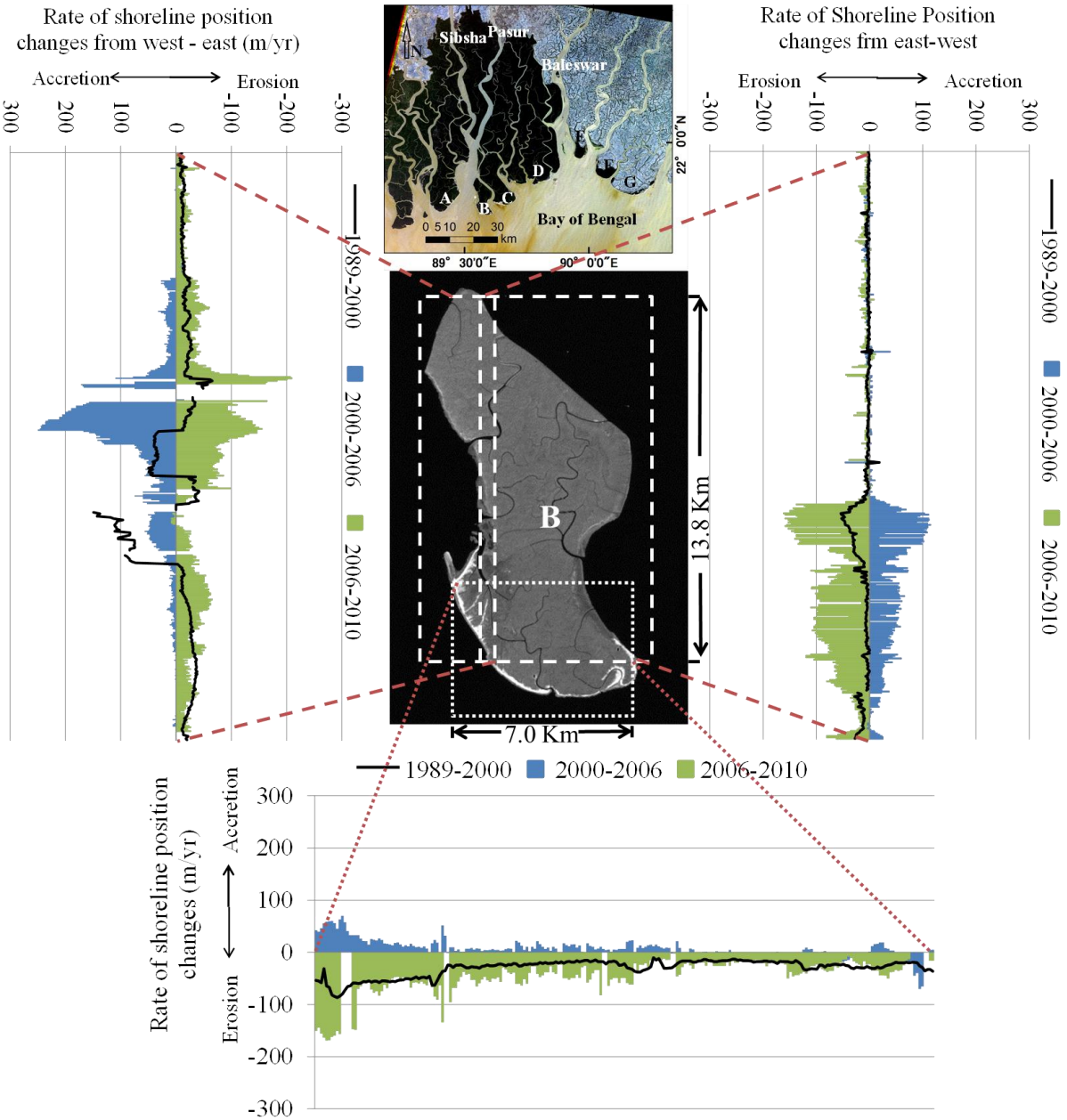

Figure 4.9 Distribution of shoreline change rates in N-S (bottom panel), W-E (left panel) and E-W (right panel) directions for the three periods 1989-2000, 2000-2006 and 2006-2010 for segment B. Negative rate corresponds to erosion.

Segment C: Same narrow branch of Pasur River is flowing between the east side of segment B and west side of segment C whereas the segment C is bound on the east side by Kotka River (Fig. 3.4), which is also a branch of Pasur River. For segment C the study estimated the rate of shoreline change along 9.6 km, 20.1 km and 17.2 km coastline in south, west and east face respectively.

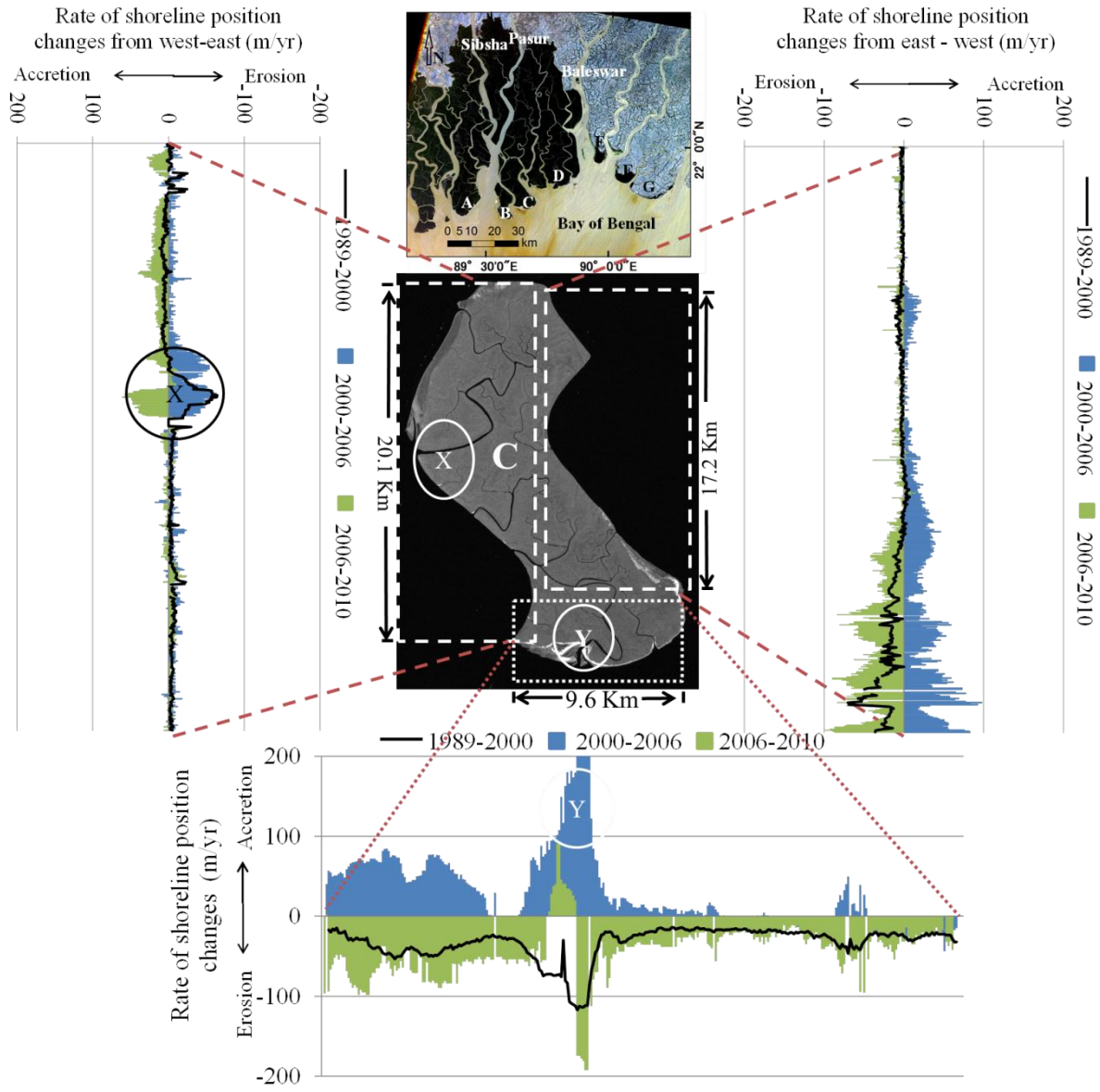

Figure 4.10 Distribution of shoreline change rates in N-S (bottom panel), W-E (left panel) and E-W (right panel) directions for the three periods 1989-2000, 2000-2006 and 2006-2010 for segment C. Negative rate corresponds to erosion**.**

Figure 4.10 shows the distribution of shoreline change rates in N-S, W-E and E-W directions for the three periods 1989-2000, 2000-2006 and 2006-2010 for segment C. Same nature of rate of shoreline changes observed compared to previous two segments over different time periods. Very small or no changes observed in the west facing shoreline, though some erosion and accretion observed at the river mouth (shows with Y and X- in Fig. 4.10). Higher rate of changes occurred at south-east end of east facing shoreline whereas stable condition found at far north end. The southerly facing shoreline was experiencing higher rate of changes of shoreline position compared to west and east facing shoreline.

Segment D: Covered with mangrove forest (locally known as Kotka and Kochikhali) and is situated between Kotka River and Baleswar River (received water from GBM system), these two rivers are flowing towards the west and east side of the segment respectively. 10.0 km, 21.3 km and 19.3 km coastline has been considered to estimate the rate of shoreline changes along south, west and east face respectively.

Figure 4.11 shows the distribution of shoreline change rates in N-S, W-E and E-W directions for the three periods 1989-2000, 2000-2006 and 2006-2010 for segment D. Less or no changes in shoreline position observed along the east face compared to west and south face. Some erosion or accretion was observed in west face, though the rate of change is much smaller than segment A-C. The south-west corner of southerly facing shoreline was experiencing continuous erosion over three time periods conversely accretion observed at the middle portion during the period of 2000-2006.

Segment E: This segment has small area of mangrove forest at south tip. The west side is dominated by Baleswar River, whereas east side is dominated by a branch river of GBM system. The study considered 24.6 km long coastline at west and east face and 4.5 km long

coastline to estimate the rate of changes. Figure 4.12 shows the distribution of shoreline change rates in N-S, W-E and E-W direction for the three periods 1989-2000, 2000-2006 and 2006-2010 for segment E. The south facing shorelines of segments E continuously retreated landward over three time periods. In the middle period 2000-2006, some accretion occurred along the east and west facing shoreline. The south facing shoreline experienced the larger

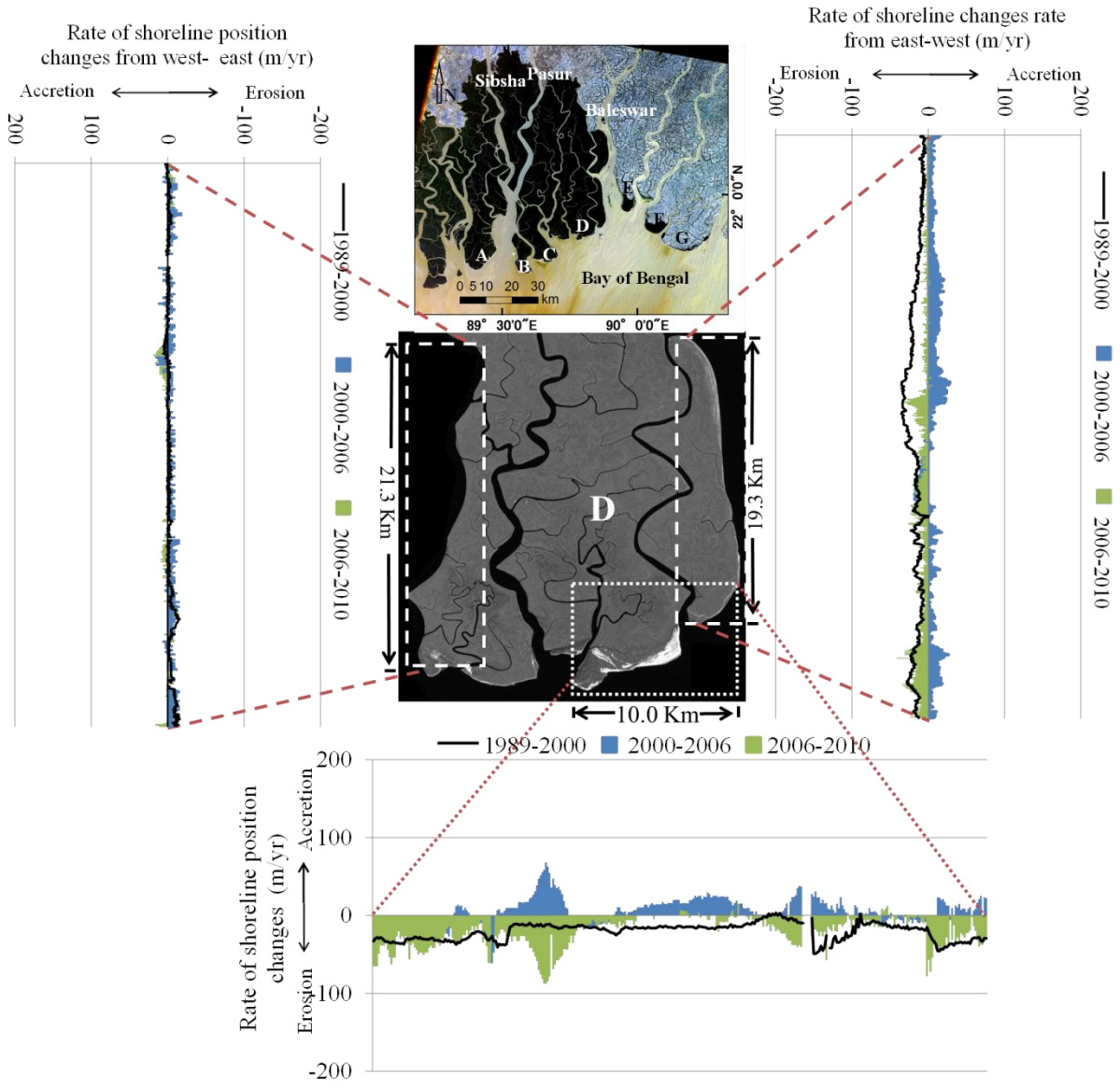

Figure 4.11 Distribution of shoreline change rates in N-S (bottom panel), W-E (left panel) and E-W (right panel) directions for the three periods 1989-2000, 2000-2006 and 2006-2010 for segment D. Negative rate corresponds to erosion.

retreat of shoreline positions. This change can also be observed from the visual inspection in the time stack image of segment E (Fig. 4.13) and which is a retreat of approximately 6.5 km during last 21 years. The mangrove portion shoreline of east and west side experienced larger changes compared to non-mangrove portion shoreline.

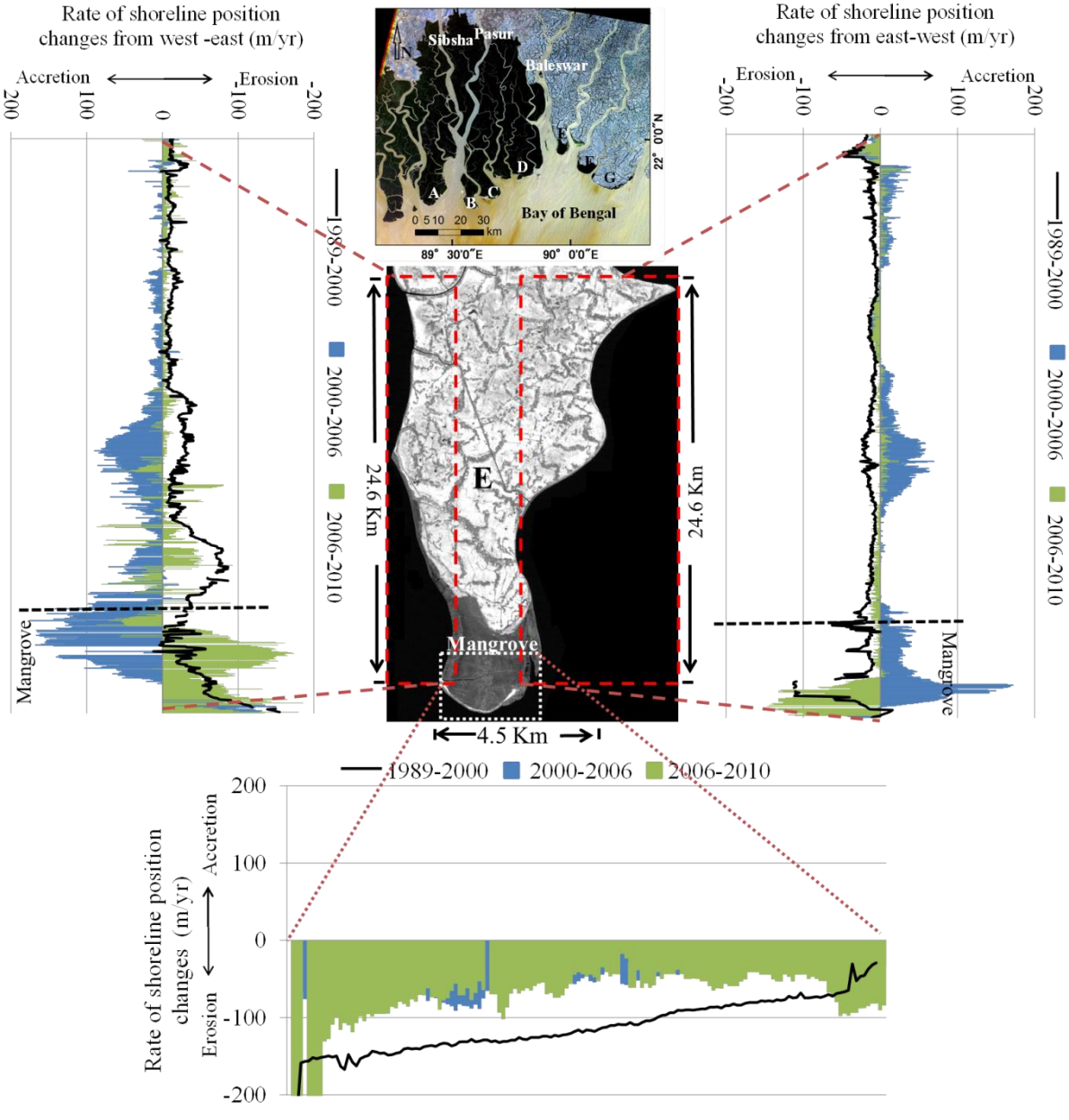

Figure 4.12 Distribution of shoreline change rates in N-S (bottom panel), W-E (left panel) and E-W (right panel) directions for the three periods 1989-2000, 2000-2006 and 2006-2010 for segment E. Negative rate corresponds to erosion.

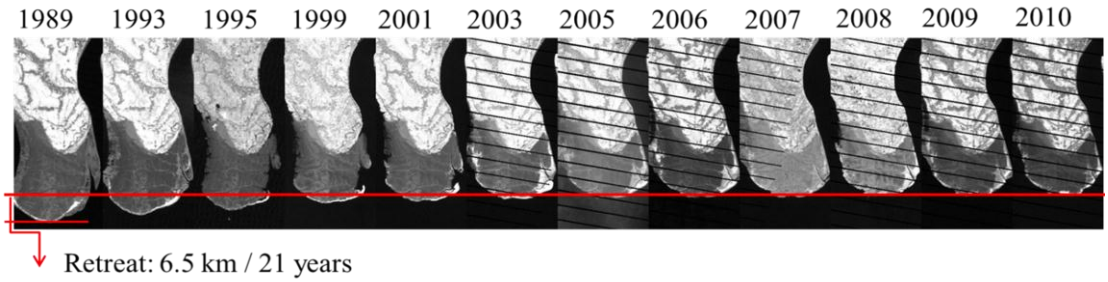

Figure 4.13 Time stack images for segment E

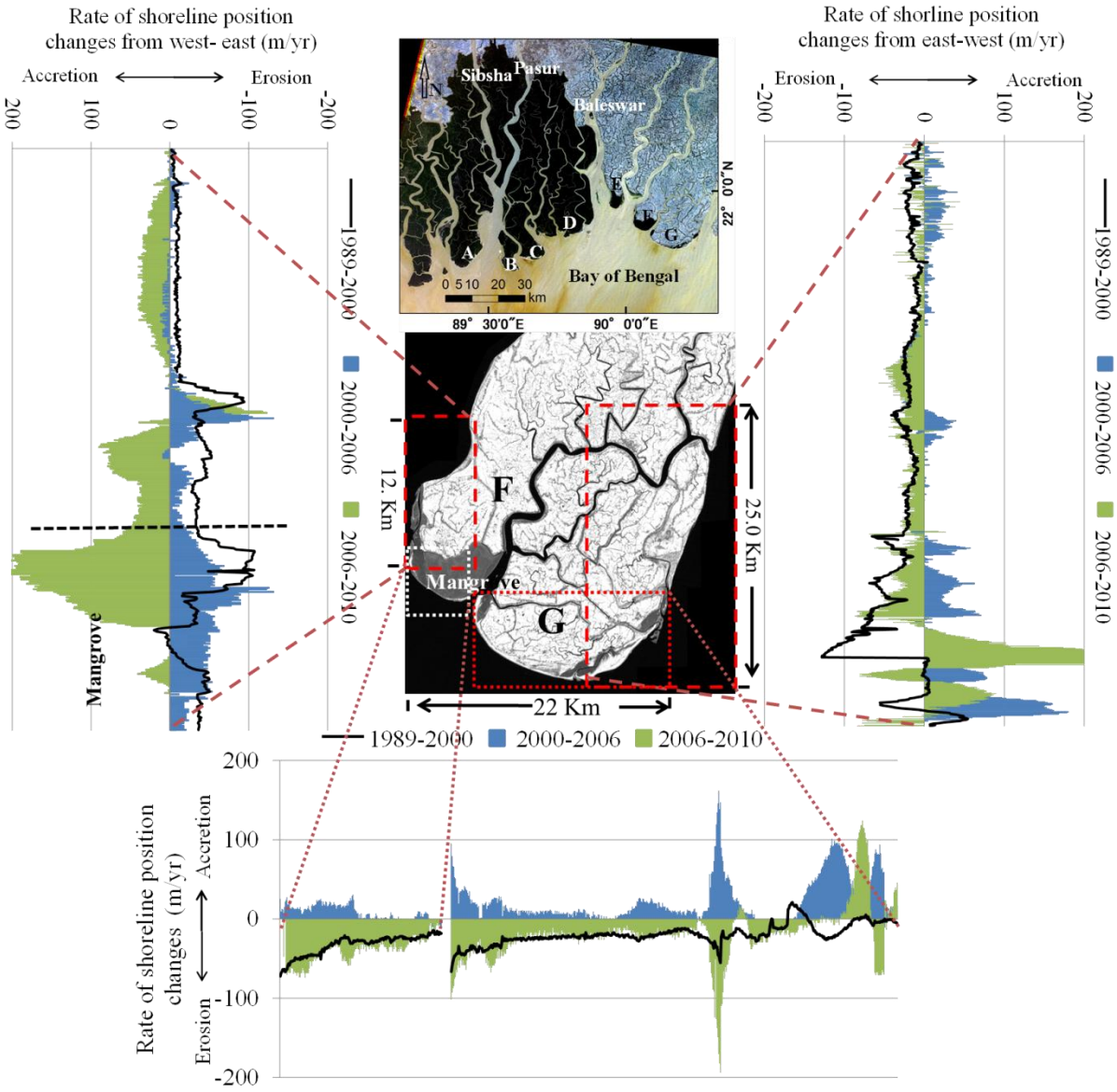

Figure 4.14 Distribution of shoreline change rates in N-S (bottom panel), W-E (left panel) and E-W (right panel) directions for the three periods 1989-2000, 2000-2006 and 2006-2010 of F and G. A negative rate corresponds to erosion.

Segment F and G: Segment F has an area of mangrove at the south tip and segment G is flat a sandy beach. The west side is dominated by a branch river of combined flow GBM system and east side is directly dominated by GBM system. Figure 4.14 shows the distribution of shoreline change rates in N-S, W-E and E-W directions for the three periods 1989-2000, 2000-2006 and 2006-2010 for segment F and G. Segments F and G also lost land in the earlier and recent periods, excepts along some transection on south-eastern side of segment G which gained land in the recent period in segment G. In the middle period, accretion occurred along most of transection of segment F and G. Larger rate of changes of shoreline position occurred at the mangrove area of segment F compared to the non-mangrove portion.

From Fig. 4.8 to 4.14, the study concludes that erosion was dominant from 1989-2000 and 2006-2010, but accretions along all the segments in the middle period 2000-2006. Exceptionally, accretion at the south-east end of segment G was observed in the recent period also (Fig. 4.14). In addition, the south-western side of southerly facing shoreline for each segment has apparently experienced more changes than the south-eastern side. The shorelines along major river channels (Sibsha, Pasur and Baleswar) showed dynamic changes, for example, east side of segment A and west side of segment B has experienced higher changes that opposite side of the same segment, where the shorelines along branch river showed less changes. Decelerating rate of changes observed from south to north along the river channel and no or very fewer changes observed at the far north end from sea.

The average rates of change of the position of the shoreline in N-S, W-E and E-W directions over the three periods are given in Table 4.2. The average rate of shoreline position changes along the southerly facing shoreline of segments A to D, covered with mangroves, was -17 m/yr, whereas for the flat sandy beach of G, it was -5 m/yr. This result is contrary to the general consensus that mangroves stabilize the beach and provide resistance to erosion. A

maximum average of -79 m/yr is observed in segment E, where the tip of the land is also covered with mangroves. The estimated erosion rate in south face of -17 m/yr for mangrove-covered segments of the Sundarbans is quite similar to that estimated by Rahman et al., (2011) and Sarwar and Woodroffe (2013). Their estimate is -20 m/yr for the period 1989-2010; however, neither of these studies provides observations for the period 2000-2006, when accumulation was dominant along the coast.

The average rate of changes along the west and east face, along the river channel was -5 m/yr which was much lesser than south face. High accumulation rate in the middle

Table 4.2 Average rates of shoreline changes for different periods for segments A-G. A negative value corresponds to erosion.

Segments	Category	Face	Shoreline change rate m/yr			
			1989-2000	2000-2006	2006-2010	Average
A	Mangrove	South	-27	24	-46	-16
		West	-9	1	-16	-8
		East	-29	113	-72	4
B	Mangrove	South	-30	7	-45	-23
		West	-6	28	-41	-7
		East	-8	16	-35	-9
C	Mangrove	South	-33	29	-43	-16
		West	-4	7	-10	-2
		East	-10	15	-24	-7
D	Mangrove	South	-21	5	-21	-12
		West	-2	-1	-4	-2
		East	-16	6	-9	-6
E	Small area of mangrove at tip	South	-112	-47	-77	-79
		West	-27	23	-19	-7
		East	-15	14	-9	-3
F	Large area of mangrove at tip	South	-33	8	-40	-22
		West	-29	38	-23	-5
G	Flat sandy beach	South	-19	23	-19	-5
		East	-21	10	-5	-5

periods and very small changes at far north end from sea reduced the average rate of changes along the river channel.

4.5 River discharge and Salinity Variation

The river discharge and salinity have an annual cyclic variation. Figure 4.15 gives the monthly variation of discharge at the Gorai Railway Bridge and of the salinity and rainfall at the Khulna station in 2006. The discharge starts to decrease in October and reaches its lowest level in the dry season (January-May), when there was little or no rainfall. It begins to increase in June. In contrast, the salinity starts to increase in January and reaches its peak in May. A decreasing trend follows from the month of June. In the dry season (January-April), there was no rainfall, so the Gorai River discharge depended solely on the upstream flows. In the wet season (June-September), rainfall plays an influential role in increasing the river

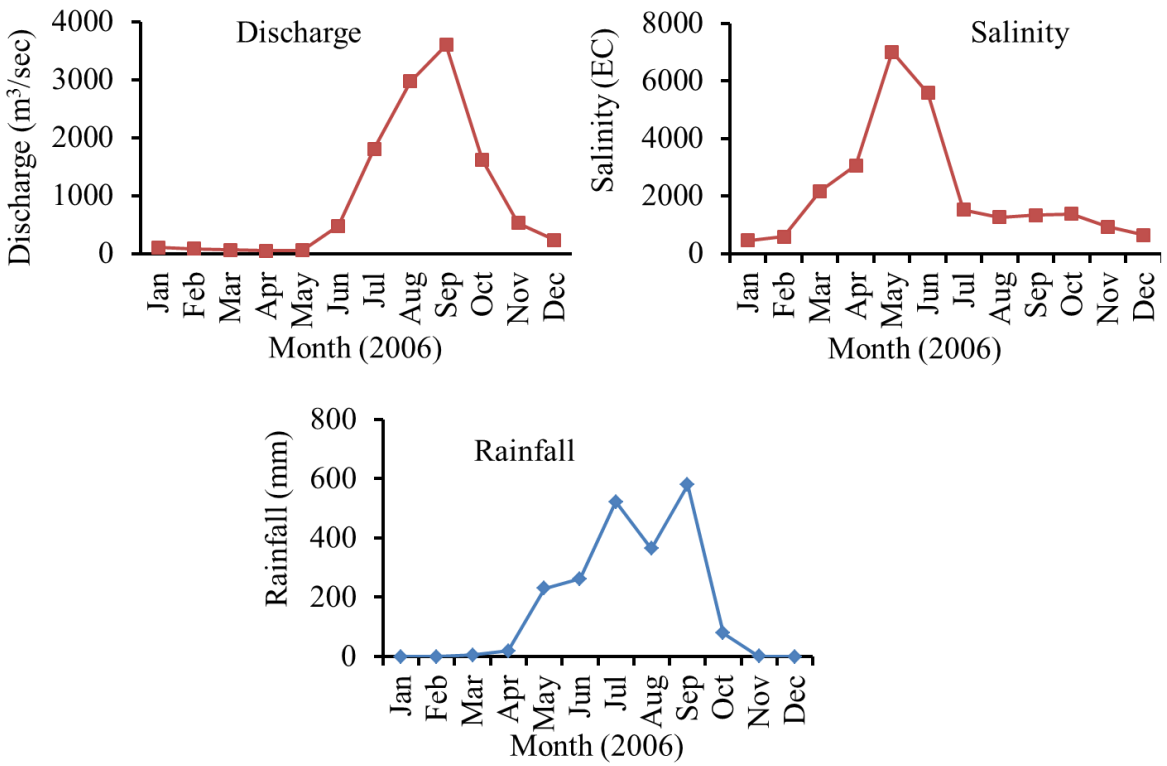

Figure 4.15 Annual variations of discharge for the Gorai Railway Bridge and salinity and rainfall at the Khulna Station in 2006.

discharge and decreasing the salinity level.

The Gorai River flow in the dry season was notably reduced for the period 1988-1996; consequently, the dry season salinity of the Rupsha-Pasur River at Khulna Station started to increase and reached its highest level in 1996 (Fig. 4.16, upper panel), leading to an increase salinity within the Sundarbans. The Gorai River discharge in the dry season later increased and salinity dropped significantly around the Sundarbans as a result of the GWSA in 1996 and the GRRP from 1998-1999 (see section 2.2), but beginning in 2004, the salinity again increased at an alarming rate because the river discharge has dramatically dropped in recent times, as in the period 1988-1996.

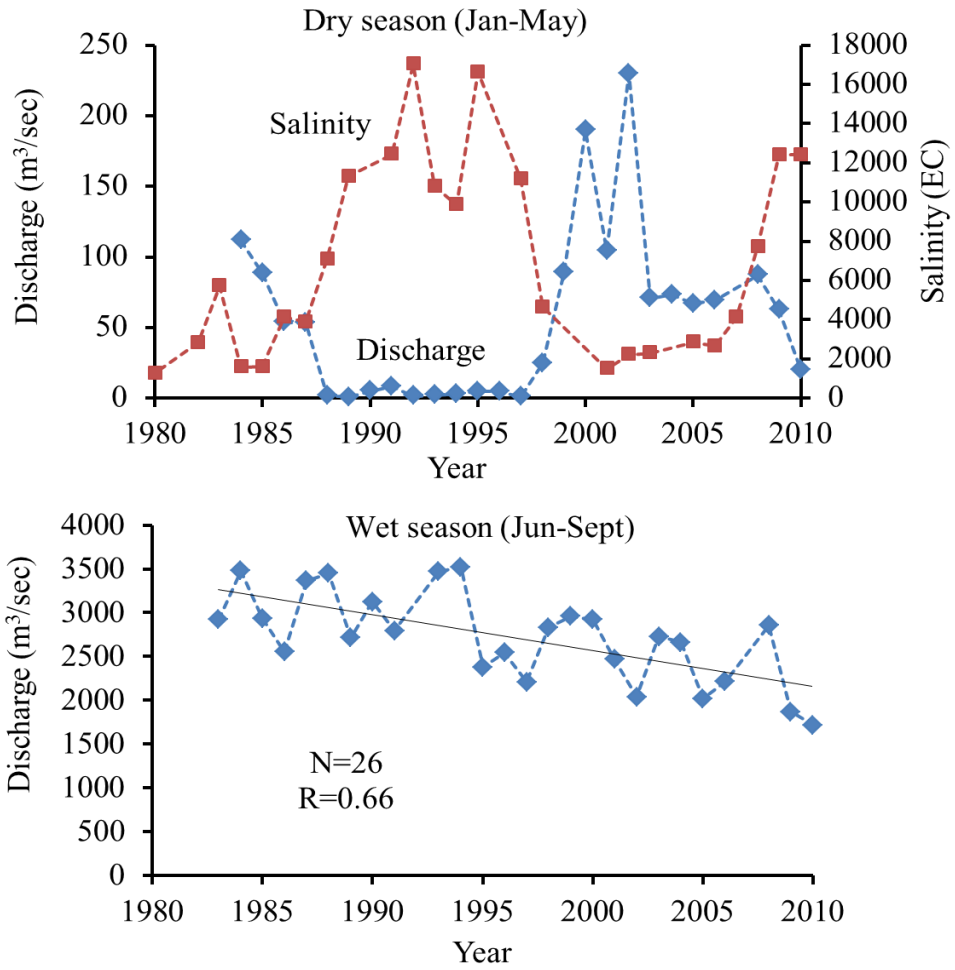

Figure 4.16 Variations of discharge of the Gorai River and salinity of the Rupsha-Pasur River in the dry season (upper panel). Variation of the Gorai River discharge in the wet season (lower panel).

This may be due to the diminishing effects of the dredging in subsequent years. There was no sharp change observed in the wet season flow for the Gorai River. Overall, the flow had a statistically significant decreasing trend during the period 1985-2010 (Fig.4.16, bottom panel). Unfortunately, little long-term data on the wet season salinity is available.

4.6 Cross -Correlation Analyses between NDVI, Discharge and Salinity

This study suspects that the scarcity of river discharge during the periods 1988-1996 and 2004-2010 affected the phenology and morphology of the Sundarbans, so the study cross-correlated the annual NDVI and the discharge. Figure 4.17(a) presents the Pearson's correlation coefficient between the annual minimum NDVI and the dry season discharge with different lags. An example of lagged scatter plots of annual minimum NDVI in year t and dry season discharge with a lag of five year (t-5) is plotted in Fig. 4.17(b). The highest correlations occur for lags in the range of 3-5 years. The minimum NDVI is highly negatively correlated to the dry season salinity for lags in the range of 2-5 years (Figs. 4.17 (c) & (d)).

This correlation analysis indicates that the minimum NDVI each year may depend on dry season discharge and salinity in the several preceding years. This implies that long-term (3-5 year) deficiency of freshwater discharge and increased salinity during the dry season can degrade the phenology of the Sundarbans mangrove forest. The other two NDVI statistics have no correlation with dry season discharge and salinity. Neither is there a significant correlation between the wet season discharge and the NDVI variables.

The annual average NDVI has a positive correlation with the annual average rainfall for the same year; i.e., the annual average NDVI responds quickly to the annual average rainfall (Fig. A3). This study didn't find any correlation between rainfall and the other NDVI variables (annual minimum and annual maximum).

The study concludes that the dry season (January-May) river discharge has a delayed impact on the long-term variation of the annual minimum NDVI. Seasonal variation of the NDVI also suggests that the NDVI reaches a minimum immediately after the dry season. Annual average rainfall also plays an important role in the variation of the annual average NDVI. So, none of these factors (river discharge, salinity, or rainfall) is solely responsible for the variation of the NDVI in the Sundarbans.

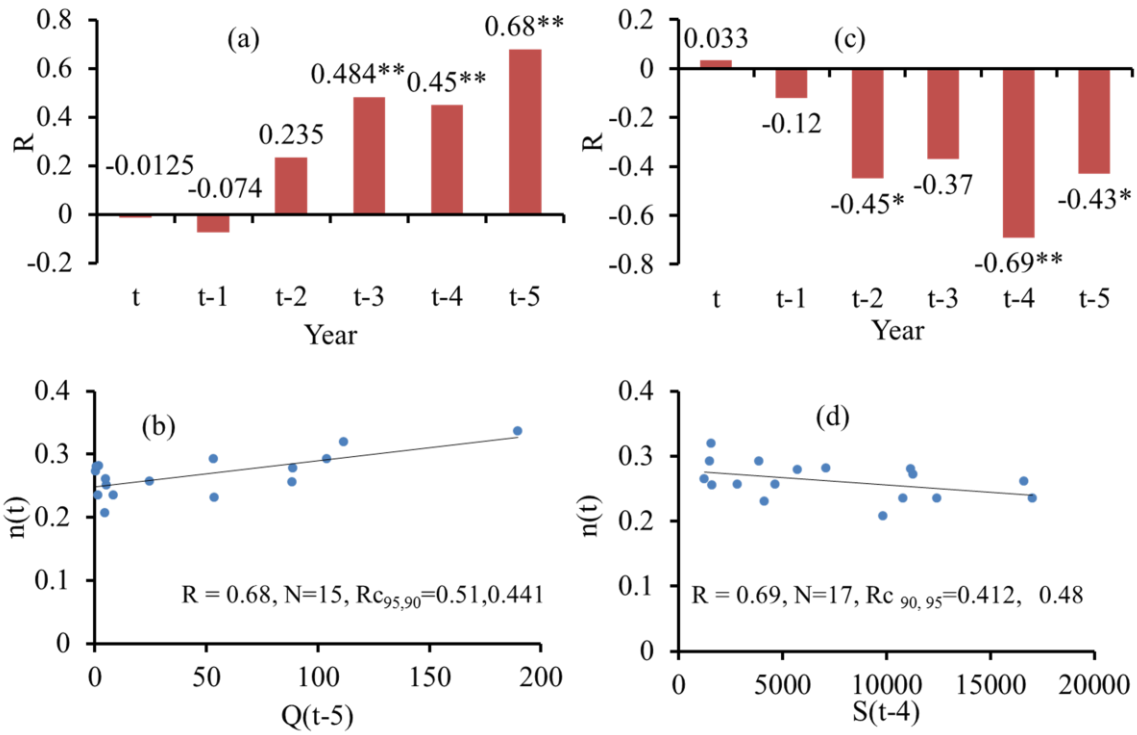

Figure 4.17 (a), (c) Pearson's correlation coefficients between annual minimum NDVI in year t and dry season discharge/salinity in years t, t-1, t-2, t-3, t-4, and t-5, (b) Annual minimum NDVI in year t plotted against dry season discharge in year t-5, and (d) annual minimum NDVI in year t plotted against dry season salinity in year t-4.

NB: R=Pearson's correlation coefficient, n(t)=annual minimum NDVI in year t, Q=dry season discharge, S=dry season salinity, * and ** mean significant with a confidence level between 90% and 95%, Rc=critical value of Pearson's coefficient.

4.7 Soil Test Results and Present Beach Condition of Segment D

Sodium salts, such as sodium chloride (NaCl), are leached from the soil by saline water. Some sodium remains in the soil, bound to clay particles, displacing other cations, such as calcium (Millar and Donuhue, 1995). Sodic soil is characterized by a high concentration of sodium ions relative to other cations (in exchangeable and/or soluble form). An excess of exchangeable sodium attached to clay in sodic soils leads to a deterioration of the soil structure through the process of slaking (mechanical breakdown of soil aggregates upon wetting), swelling, dispersion (micro-aggregates collapse and release clay), and slumping of clay particles, thus the bonds between soil particles weaken when the soil is wet and strengthen when it is dry. The role of the slaking and dispersion mechanism in soil disintegration has been widely studied (Shainberg and Letey, 1984; Qadir and Schubert, 2002) and found to be controlled mainly by the exchangeable sodium percentage (ESP) of the

Table 4.3 Test results for soil parameters i.e. P^H, EC (Electrical Conductivity), ESP (Exchangeable Sodium Percentage) and soil texture.

Sample ID	Location	P^H	EC (ms/cm)	ESP (%)	Soil Texture
Sample 1	Northside of Supoti khal	7.79	67.13	32.76	Silty Clay Loam (Sand-6.23%, Silt-61.45%, Clay-32.32%)
Sample 2	Little inside from East Kochikhali coast	8.00	26.73	31.99	Clay (Sand-23.23%, Silt-30.96%, Clay-45.11%)
Sample 3	West Kochikhali Coast	8.04	11.58	33.19	Silty Loam (Sand-2.09%, Silt-52.72%, Clay-45.19%)
Sample 4	North side of Kotka River	8.05	9.79	28.4.7	Silty Clay Loam (Sand-3.81%, Silt-61.37%, Clay-34.62%)
Sample 5	Mongla Point	8.12	10.12	21.45	Silty Clay Loam (Sand-17.02%, Silt-50.9%, Clay-32.08%)

Figure 4.18 Slaking test for soil sample 3

soil and the concentration of electrolytes in the rainwater and soil solution (Levy et al., 2003). Low EC, high ESP and P^H of the soil solution induce soil clays particle to dispersion. Oppositely high EC flocculate soil clay particles (Levy et al., 2003). Sandy soil is less affected by increase of salinity and sodic conditions.

Table 4.3 shows soil sample laboratory test result for the four parameters. The soil condition of Sundarban from Mongla to Kochikhali (Segment D) is clay, silty loam or silty clay loam. P^H data shows that the soil is slightly alkaline (7.4-7.8) to moderately alkaline (7.9-8.4). Salinity (EC) varies from strong (8-16 ms/cm) to very strong saline (>16 ms/cm) range. An ESP of 15 is generally recognized as a limit above which the soils are characterized as sodic (alkali). ESP results showed the soil is sodic also. The soil characteristics from Mongla to Kochikhali are summarized as clay, high sodic as well as high saline soil.

Slaking and dispersion test of all soil samples were done to identify the stability of soil structure. Soil samples were dried in the air and then submersed in distilled water for 24 hours. All samples are found prone to slaking and 80%-90% slaking has been observed within 5 minutes after submerging. But no dispersion has been observed within 24 hours (Fig. 4.18). High sodic condition of sample soils is responsible for rapid slaking where as high EC protects the soil from clay dispersion.

Figure 4.19 shows the present images of the Kochikhali Coast (March, 2013). Clayey soil condition, steeper slope at the water front, and dying of mangroves at western

side of the coast, may be an indication of recent erosion. Oppositely, sandy beach with a gentle slope and some accumulations of silty clay mixed with sand may be a sign of stability of the eastern coast.

Figure 4.20 shows salinity variations at low tide conditions of the river-water (Kotka River and Supoti Khal, See Fig. 3.4) salinity during the field survey, passing through the

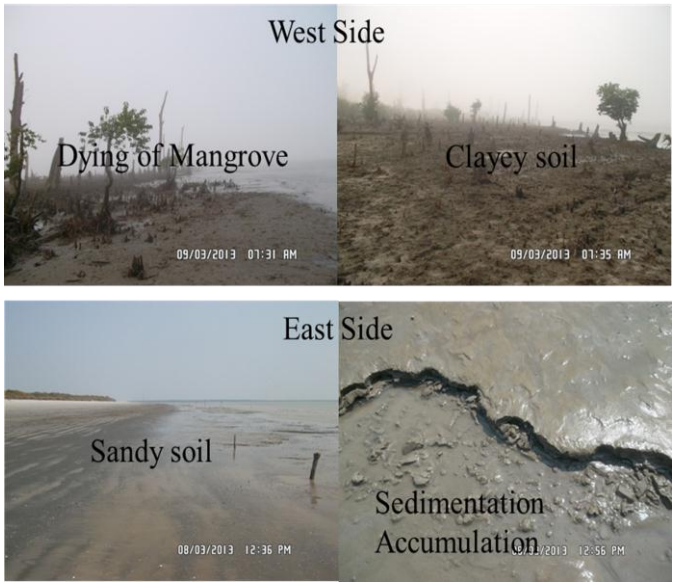

Figure 4.19 Images of west and east side of Kochikhali Coast (8 and 9 March, 2013).

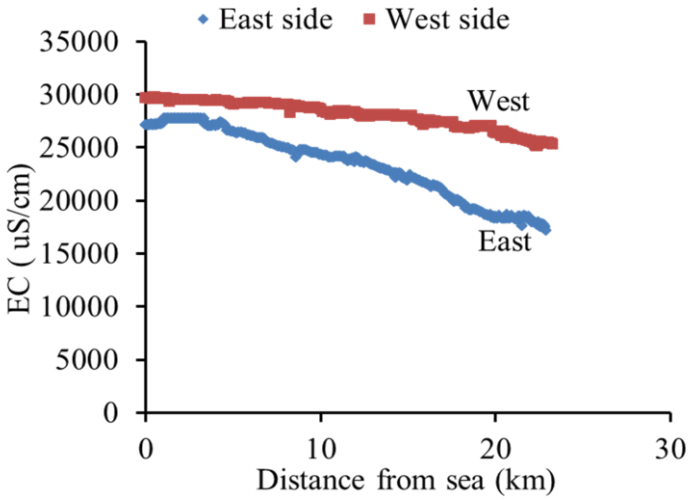

Figure 4.20 Water-salinity distributions along the rivers at west (Kotka) and east (Supoti) side of Kochikhali coast on high tide condition (8 and 9 March, 2013).

Note: 1ppt=1600 EC

western and eastern side of the coast. Higher salinity level at the western side river-water (Kotka River) may indicate the lack of fresh water discharge. The water salinity level decreases with the increase in distance from sea. The results of measured river-salinity level verified the general comment that salinity is higher nearer the coast and lowers further inland and natural west-to-east salinity gradient across the delta.

CHAPTER FIVE

DISCUSSION

5.1 General

The major changes detected from satellite observation, field data and statistical analysis are:

i) A decreasing trend in the annual minimum NDVI was observed in most of the areas of the Sundarbans for the period 1990-2000. During the period 2000-2006, the trends of the three NDVI statistics became significantly positive, indicating an improvement of the mangrove phenology. In the period of 2005-2010, a decreasing trend in all the NDVI variables was again dominant (Table 4.1and Fig. 4.5).

ii) The regional overview of shoreline changes rate analysis over the past (1989-2000) and recent (2006-2010) shows that erosion was the dominant in the whole area. In middle period (2000-2006), accretion was observed along most of shorelines (Fig. 4.8-4.14 and Table 4.2).

iii) Shoreline change rate over mangrove portions (A, B, C, and D) were larger compared to that of sandy open beach, segment G (Table 4.2).

iv) South-west corner of southerly facing shoreline of every segment is experiencing larger rate of changes compared to the south-east corner (Fig. 4.8-4.14).

v) Along the channels of major rivers, Sibsha, Pasur and Baleswar, shoreline is more dynamic than the shoreline along branch river channel (Fig. 4.8-4.14).

vi) From 1988 to 1996, the Sundarbans area was suffering for shortage of fresh water supply from upstream and affected by higher salinity level (Fig. 4.16).

vii) Statistical cross-correlation has been found between NDVI, discharge and salinity variations (Fig 4.17).

To find out the possible factors that are influencing these changes, this chapter discusses the river discharge, salinity condition of the study area, and wave hind cast data in the offshore and possible inter-connections between them.

5.2 Impact of River discharge and Salinity on Vegetation Phenology

The upstream diversion clearly resulted in low river discharge and high salinity levels in the Sundarbans forest for the period 1988-1996 and in recent times (Fig. 4.16, upper panel), posing a threat to the Sundarbans by causing the degeneration of freshwater dependent plants (Type- 2 and Type-3 in Fig. 4.5). A number of studies have indicated that the growth of several mangrove species may be affected by either the absence or excess of salinity (especially NaCl) in the substrate (Downton, 1982, Pezeshki et al., 1990, Ball and Pidsley, 1995), and the range of salinity in which the plant is able to survive varies according to the species types (Ball, 1988). Suarez and Medina (2005) concluded that levels beyond a certain range of salinity causes a decrease in the production of new leaves and in leaf longevity, a reduction in the size of leaves, and an increase in the mortality rate of mangrove plants. Sundarbans mangroves are not exception from them and Islam and Gnauck (2009) reported increased salinity in the Sundarbans may be responsible for the decay of the tops of Sundari trees, retrogression of forest types, slow forest growth, and reduced productivity of forest sites.

This study suggests the decreasing trend in the annual minimum NDVI observed during the periods 1990-2000 and 2005-2010 is due to the higher salinity levels and the scarcity of freshwater flow during the dry season. The degradation of less saline tolerance mangrove species (Type-2 and Type-3 in Fig. 4.5) and increasing trends in annual minimum NDVI of high saline tolerance species (Type-1) in the period of 1990-2000 (Fig. 4.5), may due the effect of variations of salinity and fresh water supply in the mangroves of Sundarbans.

In the recent periods 2005-2010, the increasing trends in minimum NDVI (Fig. 4.5) at the eastern side of Sundarban may due to the availability of freshwater from GBM system through Baleswar River (Fig. 4.20). In the middle period 2000-2005, the NDVI variables had a significant increasing trend which may have been due to the improved river discharge and salinity conditions during the period of 1997-2003. The delayed response of the annual minimum NDVI time series to river discharge and salinity (Fig. 4.17) implies that the impact of a decrease in the river discharge and an increase in salinity is not immediate on the mangrove phenology. The phenology of the Sundarbans mangroves started to degrade when the salinity went above the ranges in which the plants are able to grow or survive. As discussed previously (Section 2.3), salinity greater than 20 ppt (32000 EC) in surface water can degrade the growth of the Sundari species, which are the most abundant species in Sundarbans.

The annual minimum NDVI of the Sundarbans occurs at the end of the dry season (Fig. 4.1, upper panel). During the dry season when the rainfall is almost zero (Fig. 4.15), the mangrove phenology depends on the river discharge and is sensitive to the high salinity. Correlation and trend analyses corroborated the dependency of the annual minimum NDVI on the variation of dry season river discharge and salinity.

However, increases in salinity alone may not be responsible for the degradation of mangrove phenology. There may be a synergy among a number of factors, including salinity, discharge, rainfall, water logging, cyclone damage, and accumulation of toxic elements from agricultural wastes and port discharge (Mirza, 1998).

5.3 Impact of River discharge and Salinity on Shore Stability

The drastic decrease in dry season discharge and gradual decrease in wet season discharge may have reduced sediment supply to the coast as the sediment content of the

Ganges River is proportional to its discharge (Islam et al., 1999). The high erosion rate during the periods 1989-2000 and 2006-2010 may be due to an abrupt decrease in sediment supply due to the barrage and other anthropogenic disturbances upland. In the interim, an increase in the river discharge during the period of 1997-2003 helped the coast to gain land along the western coast of Bangladesh. The accretion along the major river channel (Sibsha, Pasur and Baleswar) during the high river discharge period is an evidence of how the rivers discharge plays an important role to mitigate the shoreline erosion around the Sundarbans. However, the study found some delayed response in shoreline accretion to the increase of the river discharge. Lower quantity of discharge as well as sediments is travelling through the branch rivers than major rivers (Sibsha, Pasur, Baleswar) which may be one of the reason for minor rate of shoreline changes along the branch river side of every segment.

Increases in soil and water salinity may lead to a retreat of the coast and weakening of the morphology of the Sundarbans along the shoreline through slaking and dispersion of soil aggregate, which is described in 4.5. Mamevdov et al., (2001) investigated the effects of the wetting rate on slaking and dispersion by observing the infiltration rate and runoff in cultivated soils varying in clay content and ESP in laboratory experiments with simulated rain. He concluded that an increased salinity range can increase the ESP (Exchangeable Sodium Percentage) range of soil, and a medium to high ESP (10-20%) accelerates the disintegration of clayey soil due to dispersion of clay with slow and intermediate wetting rates (Mamevdov et al., 2001). A soil with increased dispersibility becomes more susceptible to erosion by water and wind.

The field survey found that the soil is clay, silty loam, or silty clay loam around segment D and that it is sodic with a P^H of 7.79-8.12 and an ESP of 20%-30% (Table 4.3). The silty clayey soil of the Sundarbans with a high ESP may be prone to slaking and dispersion upon wetting during the rainy season. The slaking test (Fig. 4.18) also showed that

the soil sample of Sundarbans very susceptible to slaking. The silty clayey soil, steep slope of the waterfront land, and high salinity may be other reasons for the accelerated erosion in the periods 1989-2000 and 2006-2010 along the mangrove- covered segments A to D, assuming the soil was in a condition similar to that of the survey samples. However, there is no strong evidence of slaking and dispersion of the soil around the Sundarbans.

The flat sandy beach along segment G is dominated by the GBM system and was less affected by the reduction of freshwater flow of the Ganges River and the concomitant increase of salinity. Also, salinity has less impact on sandy soil in terms of slaking and dispersion. This may be one of the reasons for the low erosion rate of segment G compared to segments covered with mangroves. The continuous accretion at the southeast side of east facing shoreline of segment G (Fig.14) is also showed, this segment is not suffered in receiving sediment from GBM system.

The field observation also supports the observation that less salinity with sandy beach condition is more stable than clayey beach with high saline condition. The Baleswar River feeds the eastern side (not affected by lower Ganges flow) and Pasur River feeds the western side (Fig. 2.2) of segment D. Lower salinity level at the eastern side river-water (Fig 4.20) indicates the availability of fresh water discharge through Baleswar River, as this river received water from both Ganges and combined GBM system. Sandy beach and low salinity level may be the reason for less erosion rate at the south-eastern side of southerly facing shoreline of segment D (Fig. 4.11). Oppositely having high level salinity with clayey soil condition and steeper slope at the water front may responsible for the dynamic nature of south western side of southerly facing shoreline (Fig. 4.11).

5.4 Impact of River discharge in Expanding Island and Mangroves

Mangrove are not generally land builders but rather they can rapidly colonize newly deposited and stable intertidal sediments and in so doing they help to consolidate these recent sediments and may promote further sedimentation (Blasco et al., 1996). Based on these characteristics of mangroves, a coastal afforestation program funded by World Bank was implemented in Bangladesh, where mangroves have been used to stabilize sediments as a means of gaining land from sea. The plantation contributed both to acceleration of land accretion and to the stabilization of deposited Ganges sediments (Saenger and Siddiqi, 1993). The result of this project support that with the improvement of mangrove vegetation activity, accretion can be accelerated which also stabilized the deposited sediment.

Some sediment depositions are observed along the shoreline of segment A, C, D and G ($Ac\text{-}_A$, $Ac\text{-}_C$, $Ac\text{-}_D$ and $Ac\text{-}_G$) after 1999 (Fig. 4.6). Moreover, accretion has been dominating for the period of 2000-2005 along the coast (Fig 4.8-4.14). Further, one island Is2 newly appears and land areas of island Is1 and island Is3 gained land in front of segment A and D after 1999 (Fig. 4.6 (a)). The NDVI trend analysis showed a significant increasing trend from the period of 2000-2005, which is an indication of the improvement of the mangrove vegetation activities around the Sundarbans at that period. Furthermore, from 1997 the discharge started to increase and more sediment also transported to sea from the upstream. The accretion, improvement of vegetation and increased discharge for the period of 2000-2005, supported the afforestation project results that mangrove can accelerate accretion and stabilized sediments as a means of gaining land from sea (Blasco et al., 1996). The newly island Is2 appeared after 1999 is an indication of newly colonization of deposited land by mangroves. The result of this accretion and increasing trends of NDVI variables along the Sundarban coastline during the higher discharge period can be targeted for selective protective measure to maintain proper fresh water flow from the upstream to avoid further

loss of mangroves and land respectively.

5.5 Other Factors Affecting the Sundarbans

The diversion of upstream river discharge alone may not be responsible for the degradation of the Sundarbans (Mirza, 1998). It may be due the combined effects of a number of factors, including river discharge, salinity, wave action, relative sea level rise, cyclone damage, and human influences.

Wave Action: Waves are natural forces that easily move the unconsolidated sand and soils in the coastal area, resulting in rapid changes in the position of the shoreline. In this study, wave hindcast data for 1989-2010 were analyzed to determine the effect of wave action on erosion and accretion along the coast. Figure 5.1 shows annual variations of wave direction and significant wave height for year 1995-1999 for a grid point at 90° E and 21° N, which is the closest data point to segments E-G. Figure 5.2 displays the scatter plot of significant wave

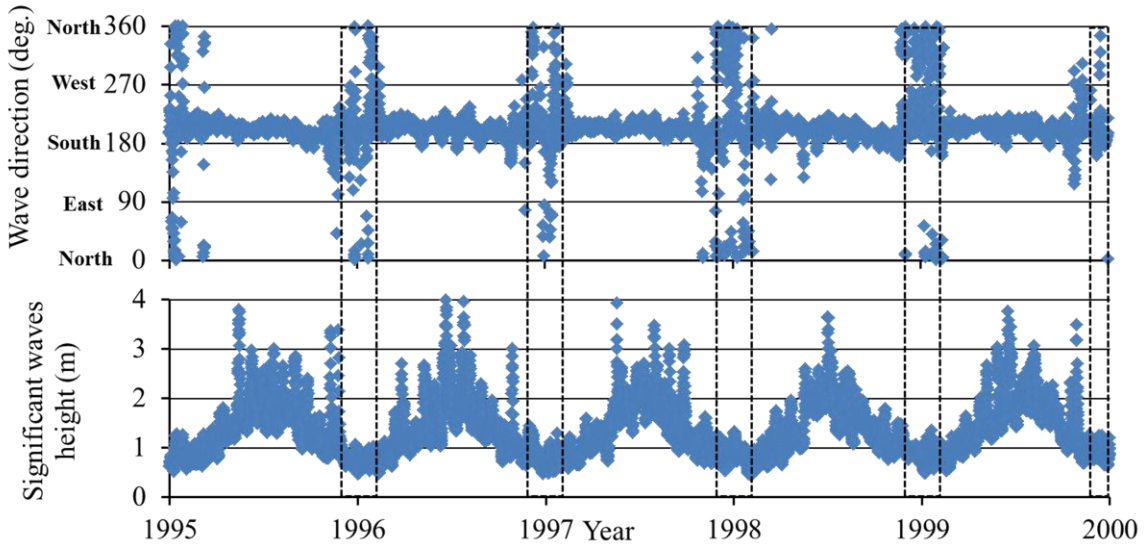

Figure 5.1 Annual variations of wave direction and significant wave height for years 1995-1999 at 90° E and 21° N retrieved from ECMWF ERA-Interim. Dashed lines indicate the months of December and January.

height and wave direction for the period 1985-2010 for the same location. The 90-degree wave direction indicates the waves were coming from the east, and 180-degrees, from the south. Waves incident from the south-southwest are dominant along the coast all over the year (Fig. 5.1) as well as all the over study period (Fig. 5.2). In months of December and January, some low waves from northwest or northeast directions are observed (waves within dashed strip in Fig. 5.1). The prevailing waves from south- southwest may yield sediment transport from west to east, consistent with observations of larger shoreline erosion rates on the southwest side of southerly facing shoreline for every segment.

Further, the accumulation zones $Ac\text{-}_A$ and $Ac\text{-}_c$ sheltered behind island Is1 and segment B, respectively, are on the south-west side of the segments A and C and are down-wave of the prevailing waves (Fig. 4.6(a)). The less erosion rate at the east face of segment B, west face and east face segment C and west face of segment D may due to the similar reason. Waves reaching the coast have more energy and become weaker when travelling along the river channel which may one reason for the decelerating rate of shoreline

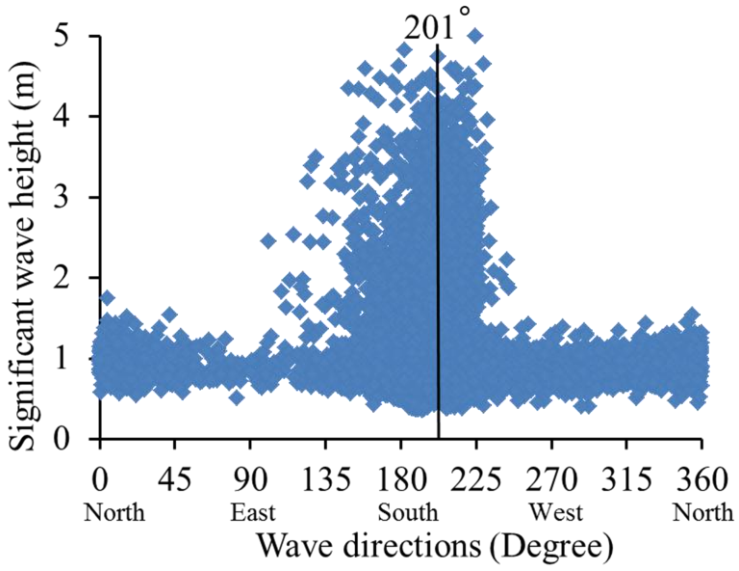

Figure 5.2 Wave height and wave direction at (90° E, 21° N) for the period of 1989-2010 retrieved from ERA- Interim. Solid line represents center of gravity of the distribution.

changes from sea to far north end.

A comparison of the wave heights for the three periods 1989-2000, 2000-2006, and 2006-2010 doesn't indicate any significant differences in that variable among the three periods, so one cannot claim that only wave action is responsible for the higher rate of erosion in the periods 1989-2000 and 2006-2010.

Cyclone Damage: Increase in the frequency of tropical cyclones and storm surges may have adversely affected the Bangladesh coast (Ali, 1999). For example, the recent two major cyclones: Sidr and Aila made landfall near the Sundarbans in November 2007 and in May 2009 respectively, resulting in destruction of the mangroves fringe, retreat of the shoreline by several meters and increase in salinity intrusion to the surrounding areas. Cyclone Reshmi (2008) and Bijli (2009) also affected weakly Bangladesh coast with few damages of some houses and crop field loss. Bijli was passing beside the Sundarbans and made landfall near the eastern coast of Bangladesh. Figure 5.3 shows the tracks for recent four cyclones (bold lines) and other historical cyclones that attacked the Bangladesh coast. The wind speed and storm surge height for recent four cyclones are shown in Table A6.

In the recent period 2005-2010, these two major cyclones, Sidr and Aila, may be another reason for the degradation of NDVI variables and higher erosion rate along the Sundarbans. Cyclones have immediate rather than long-term effects on the phenology and morphology of Sundarbans. However, we were not able to collect enough accurate and quantified data on the effects and damages by cyclones in the Sundarbans to assess the relative importance of these factors.

Relative Sea Level Rise: The retreat of Sundarbans's shoreline is expected under sea level rise and wave action as there are no dikes and other structure to protect the shore. But the

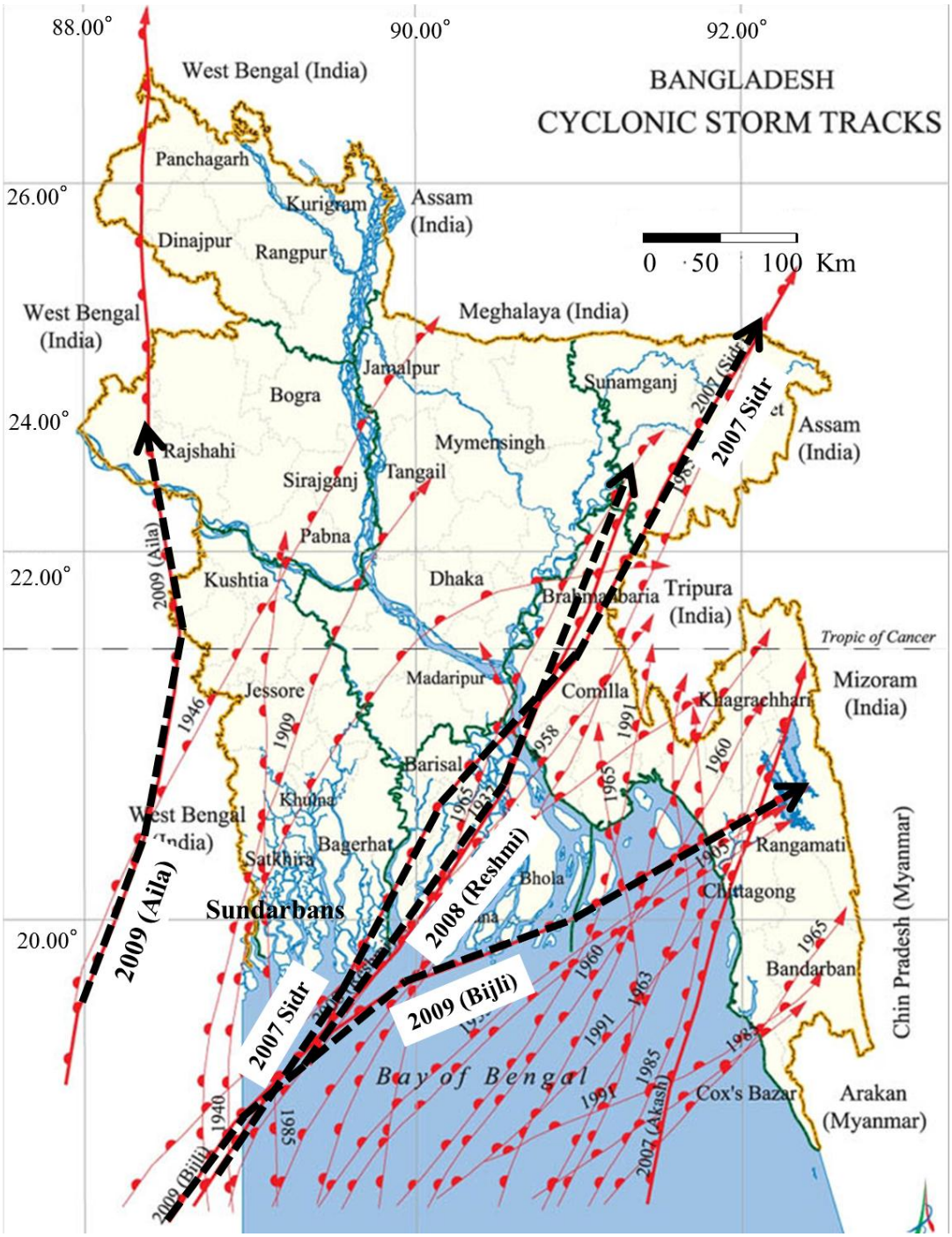

Figure 5.3 Major cyclones tracks passed through Bangladesh coast. Bold black line represents the recent cyclones (Image taken from Banglapedia web, http://www.banglapedia.org/HT/C_0469.htm, National Encyclopedia of Bangladesh).

relative sea level history of Bangladesh remains incompletely understood (Rashid et al., 2013). Lee (2013) has estimated that relative sea level rising trends at the Hiron Point (Fig.

2.3) is 4.46 mm/yr. Other study has also confirmed this trend with rate ranging 4.0 mm/yr in the western coastal zone of Bangladesh (Alam and Ahmed, 2010). On the other hand, in the global sea level rise calculation with recent altimeter-based, estimates the sea level rise along Bangladesh coast is 3.3±0.4 mm/yr which is lower than their estimation (Lee, 2013). The local factors like variation of river discharge, floods, subsidence, sediment etc. may the causes for the higher estimation rate of sea-level trends along the western coast of Bangladesh, reported by Lee (2013)**.** Current and future sea level rise is likely to exacerbate erosion that occurs in response to recurring cyclones, strong tidal currents and gradual subsidence, particularly along Bangladesh (Sarwar and Woodroffe, 2013). But there is no scientific evidence to date indicating that mangrove mass mortalities recorded on all continents are related to sea-level rise. An evaluation of the impacts of this phenomenon, if it takes place at all, requires careful assessment of possible coastal uplift or subsidence at each specific site (Hoffman, 1984).

Human Influences: The dynamics of Sundarbans changes are also influenced by direct human influences. For example, the Sundarbans is adjacent to Mongla, one of the largest ports in Bangladesh and the main port for the export of shrimp. Ships must travel through the Sundarbans via the Pasur River (Fig. 2.2 and 2.3) to get to the port. It has been reported that many small oil spills have adversely affected the mangrove ecosystem on the route to Mongla (Michael and Peterson, 2006). The consensus in the literature regarding the Sundarbans is that increasing salinity, over-harvesting of timber, and other human influences like shrimp farming, industrial pollution and oil pollution, lack of proper management, poor knowledge of mangrove ecosystem and high dependence of local population on its products and services etc. are degrading the condition of the Sundarbans mangroves (Iftekhar and Islam, 2004).

CHAPTER SIX

CONCLUSION

6.1 General

Satellite remote-sensing data were analyzed to identify the phenological and morphological changes along the western coastal zone of Bangladesh. This study relied on AVHRR GIMMS (1985-2006) and MODIS (2005-2010) satellites Normalized Difference Vegetation Index (NDVI) data sets and LANDSAT archive for the investigation. Beside the satellite data analysis hydrological data, metrological data, wave hindcast data and field data has been taken into consideration to clarify the possible role of these factors on the phonological and morphological variation along Sundarbans. A significant coherence was observed between the phonological changes and variation of upstream river discharge. This chapter summarizes the identified changes (observed from satellite data) that happened along Sundarbans during the study period with variation of hydrological regimes. This chapter also presents the limitation of the study and suggests some recommendation for future works.

6.2 Summary of the Study

Figure 6.1 summarizes the phenological, morphological, and hydrological changes of the Sundarbans for different time periods. Decreasing trends in the NDVI variables are observed for the periods 1990-2000 and 2005-2010, and increasing trends, for the period 2000-2006. Shorelines experienced erosion from 1989-2000 and in the period 2006-2010. On the other hand, in the interim, 2000-2006, accretion occurred at most of the locations.

The Ganges-Gorai River dry season flow has been notably reduced since the construction of the upstream barrage; consequently, salinity increased within the Sundarbans and may have adversely affected, with some delay, the growth of the mangrove forests and accelerated the erosion of the Sundarbans in the periods 1990-2000 and 2005-2010. In the

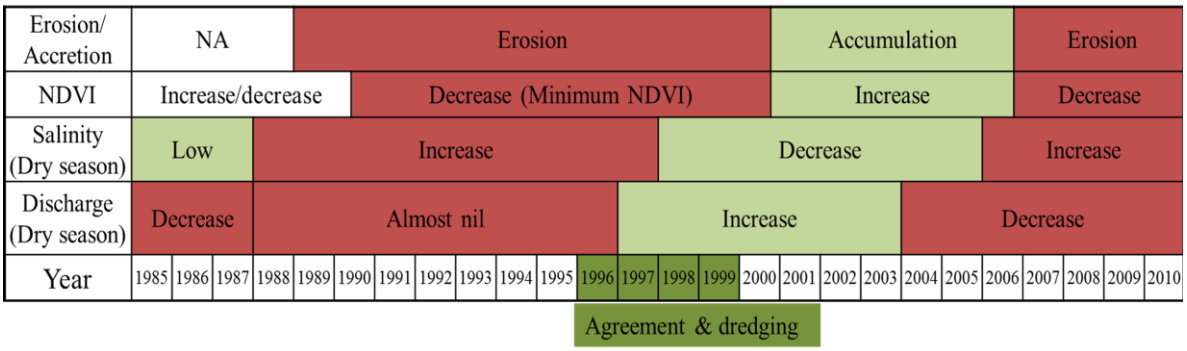

Figure 6.1 Schematic diagram for the phenological, morphological, and hydrological changes of the Sundarbans for different time periods.

interim, 2000-2006, the improved river discharge and salinity levels due to the Ganges Water Sharing Agreement (1996) and dredging of the Gorai River bed (1998-1999), enhanced the mangrove phenology and helped the coast to gain land.

Larger changes in the shoreline were observed in the mangrove portions of the coast (segments A to D) compared to the sandy open beach of segment G, contrary to the general consensus that mangroves stabilize the land. Although segment G is dominated by the GBM system and so is less affected than the mangroves by a lower Ganges discharge of freshwater and concomitant higher salinity, the sandy beach is less affected by slaking and dispersion induced by adverse saline conditions anyway in contrast to the clayey soil of the segments covered with mangroves, which may be one of possible reason for the lower erosion rate of segment G. The shoreline of the south-west side of southerly facing shorelines of every segment experienced larger changes compared to the south-east side, which may be due to the prevailing waves from the south-southwest and consequent sediment transport from west to east. Relative low discharge and low wave action through branch rivers may be the reason for the relative fewer rates of shoreline changes than the shoreline changes rate along major river channels (Sibsha, Pasur and Baleswar).

It is our hope that the results of this study will encourage research on how to optimize flow augmentation in the Ganges River to sustain the vital Sundarbans mangrove forests. For the long run of Sundarbans ecosystem, the main fundamental issue is the Ganges water or surface water, therefore the Ganges transboundary water sharing between Bangladesh and India would be a priority issue for discussion and should ensure fresh water supply into the Sundarbans. Issues should be taken into consideration as a dynamic way to mitigate the water management and to share the conflict; and reduce the high salinity intrusion in the south western region in Bangladesh. Simultaneously other alternative approaches for the solution of this environmental problem have to be searched.

6.3 Limitation of the Present Study and Recommendation for Future Study

This study can be used as a guideline and reference for the future research works, although there are several limitations. The limitation of this study with some recommendation to mitigate the following issues are describing in below:

i) This study estimates the trends of phonological changes using AVHRR-GIMMS NDVI data which have the longest data records. The AVHRR data sets contains NDVI values received from different satellite sensors and the limitations of NDVI in relation to the respective sensor characteristics and preprocessing schemes hence contribute to differences in trend analysis. This study was not able to clarify the validity of AVHRR GIMMS data with other sensor data. To validate the AVHRR GIMMS NDVI data set, it is necessary to cross check the NDVI data with the other sensor NDVI data. Though this study used MODIS NDVI data also but was not tried to inter- correlate between them.

ii) It was very difficult to collect the hydrological data e.g. tide, discharge, salinity data from different organization of Bangladesh. Moreover, the received data sets contain

lots of missing and erroneous data. Such as, the tide data was not adequate to explain the effect of tide on the variation of shoreline position. Another example is, the salinity data contains no data during the wet season and this study were failed to show the long term changes of salinity level during wet season. More reliable and valid data set require to explain their role in the phonological and morphological changes. To mitigate this problem a collaborative works require with the different organization of Bangladesh.

iii) This study detects the shoreline positions using one detection method rather than cross checking with other established methods recommended by several studies. One or two more methods should apply to detect the shoreline to reduce the inaccuracy level in detecting shoreline positions.

iv) The present study illustrates the relationships between long term variation of Ganges -Gorai River discharge and phonological or morphological changes along the Sundarbans. Future study is necessary to understand the dynamics of sediment supply along the western coast required to understand accretion and erosion processes, which is not well understood at presents.

v) In this study a short field visit in one portion of the study area was done. For better understanding of Sundarbans phenology and morphology, long term field data covering total study area is needed as in future works as a supplementary data during the remote sensing data analysis.

REFERENCES

Alam, M. J. B., and Ahmed, F. (2010). Modeling climate change: Perspective and application in the context of Bangladesh. In Y. Charabi (Ed.), Indian Ocean Tropical Cyclone and Climate Change (pp. 19).

Alesheikh, A. A., Ghorbanali, A., and Nouri, N. (2007). Coastline change detection using remote sensing, Int. *J .Environ. Sci. Tech.*, 4(1), 61-66.

Ali, A. (1999). Climate change impacts and adaptation assessment in Bangladesh. *Clim Res,* 12, 109–116.

Allison, M. A. (1998). Historical changes in the Ganges–Brahmaputra delta front. *Journal of Coastal Research*, 14(4), 1269–1275.

Alison, M. A., and Kepple E. B. (2001). Modern sediment supply to the lower delta plain of the Ganges-Brahmaputra River in Bangladesh.Geo-Mar Lett 21, 66-74.

Annibale G., Arcangela B., Angela L., Rocco S., Maria L., Trivigno, Angelo Z. and Antonio C. (2006). A multisource approach for coastline mapping and identification of shoreline changes *ANNALS OF GEOPHYSICS,* VOL. 4.7, N. 1.

Baban, S. J. (1997). Environmental monitoring of estuaries; estimating and mapping various environmental indicators in Breydon Water Estuary, U.K., using LANDSAT TM imagery, *Estuarine Coastal Shelf Sci*., 44, 589- 598.

Baldi, G., Nosetto, M. D., Aragon, R., Aversa, F., Paruelo, J. M., and Esteban, G. J. (2008)**.** Long-term satellite NDVI data sets: Evaluating their ability to detect ecosystem functional changes in South America. *Sensors,* 8, 5397-5425.

Ball, M. C. (1988). Salinity tolerance in mangroves, Aegiceras corniculatum and Avicennia marina. I. Water use in relation to growth, carbon partitioning and salt balance. *Australian Journal of Plant Physiology*. 15, 447-464

Ball, M. C., Cochrane, M. J., and Rawson, H. M. (1997). Growth and water use of the mangroves Rhizophora apiculata and R. stylosa in response to salinity and humidity under ambient and elevated concentrations of atmospheric CO_2. *Plant, Cell and Environment*, 20, 1158-1166.

Ball, M. C., and Pidsley, S. M. (1995). Growth responses to salinity in relation to distribution of two mangrove species, *Sonneratia alba* and *S. lanceolata*, in northern Australia. *Funct Ecol*, 9, 77–85.

Beck, P., Atzberer, C., Hogda, K., Johansen, B., and Skidmore, A. (2006). Improved monitoring of vegetation dynamics at very high latitudes: A new method using MODIS NDVI. *Remote Sensing of Environment*, 100, 321−334.

Brij, G., and Chauhan, M. (2006). Biodiversity and its conservation in the Sundarbans Mangrove Ecosystem. *Aquatic Science- Research across Boundaries,* 68, 338-354 (17).

Blasco, F., Aizpuru, M., and Gers, C. (2001). Depletion of the mangroves of Continental Asia. *Wetlands Ecology and Managemen*t 9, 245-256.

Blasco, F, Saenger, P. and Janodet, E. (1996). Mangroves as indicators of coastal change. *Catena*, vol. 27, 167-178.

Chen, J., Jonsson, P., Tamura, M., Gu, Z., Matsushita, B., and Eklundh, L. (2004). A simple method for reconstructing a high-quality NDVI time-series data set based on the Savitzky–Golay filter. *Remote Sensing of Environment*, 91, 332−334.

Defries, R. S., and Belward, A. S. (2000). Global and regional lands cover characterization from satellite data: An introduction to the Special Issue. I*nt. J. Remote Sens.* 21, 1083–1092.

Downton, W. J. S. (1982). Growth and osmotic relation of the mangrove *Avicennia marina* as influenced by salinity. *Aust J Plant Physiol* , 9, 519–528.

Dwivedi, R.S., Rao, B.R.M., Bhattacharya, S. (1999). Mapping wetlands of the Sundarban

delta and its environs using ERS-1 SAR data. *International Journal of Remote Sensing*, 20, 2235-2247.

Ellision, A. M., Mukherjee, B. B., and Karim, A. (2000). Testing patterns of zonation in mangroves: scale dependence and environmental correlates in the Sundarbanss of Bangladesh. *Journal of Ecology*, 88, 813-824.

Fensholt, R., Nielsen, T. T., and Stisen, S. (2006). Evaluation of AVHRR PAL and GIMMS 10-day composite NDVI time series products using SPOT-4 vegetation data for the African continent. International Journal of Remote Sensing 27: 2719–2733.

Fensholt, R., Rasmussen, K., and Mbow, C. (2009). Evaluation of earth observation based long term vegetation trends-Inter comparing NDVI time series trend analysis consistency of Sahel from AVHRR GIMMS, Terra MODIS and SPOT VGT data. *Remote Sensing of Envi.*, 113, 1886–1898.

Gens, R. (2010). Remote Sensing of Coastlines: Detection, Extraction and Monitoring. *International Journal of Remote Sensing*, 31(7), 1819-1836.

Giri, C., Pengra, B., Zhu, Z., Singh, A., and Tieszen, L. L. (2007). Monitoring mangrove forest dynamics of the Sundarbanss in Bangladesh and India using multi-temporal satellite data from 1973 to 2000. *Estuarine, Coastal and Shelf Science*, 73, 91–100.

Goodbred, Jr. S. L., and Kuehl, S. A. (2000). Enormous Ganges –Brahmaputra sediment load during strengthened early Holocene monsoon. *Geology*, 28, 1083 – 1086.

Groot, J. K., and Groen, P. (2001). The Gorai Re-Excavation Project. *Terra et Aqua*, Vol. 85, 2001, pp. 21-25.

Gutman, G. G. (1999). On the use of long-term global data of land reflectances and vegetation indices derived from the AVHRR. *J. Geophys. Res*. 104, 624.13255

Hansen, M. C., and DeFries, R. S. (2004). Detecting long-term global forest change using continuous fields of tree-cover maps from 8-km Advanced Very High Resolution

Radiometer (AVHRR) data for the years 1982-99. *Ecosystems*, 7, 695-716.

Heumann, B. W., Seaquist, J. W. Eklundh, L., and Jonsson, P. (2007). AVHRR derived phenological change in the Sahel and Soudan, Africa, 1982-2005. *Remote Sensing of Environment,* 108, 385-392.

Hoffman, J.S. (1984). Estimates of future sea-level rise. In: Greenhouse effect and sea-level rise. (Eds. Barth, M.C. and Titus, J.G.), *Van Nostrand Reinhold Company*, pp. 79-104.

Hoque, M. A., Sarkar, M. S. K. A., Khan, S. A. K. U., Moral, M. A. H., and Khurram, A. K. M. (2006). Present status of salinity rise in Sundarbanss area and its effect on Sundari (Heritiera fomes) specie**s.** *Research Journal of Agriculture and Biological Sciences,* 2(3), 115-121.

Huete, A., et al (1999). A light aircraft radiometric package for MOD Land Quick Airborne Looks (MQUALS). *Earth Observations*, 11, 22 – 25 (NASA/GSFC)

Iftekhar, M. S., and Islam, M. R. (2004): Managing mangroves in Bangladesh: A strategy analysis. *Journal of Coastal Conservation,* 10, 139-146.

Iftekhar, M. S., and Saenger, P. (2008). Vegetation dynamics in the Bangladesh Sundarbanss mangroves: A review of forest inventories. *Wetlands Ecology and Management,* 16, 291–312.

Institute of Water Modelling (IWM) (2003). Sundarbanss Biodiversity Conservation Project Surface Water Modeling. TA No. 3158-Ban (Contract COCS/00-696). Final Report, Volume 1.

Islam, M. J., Alam, M. S. and Elahi, K. M. (1997). Remote sensing for change detection in the Sundarbans, Bangladesh. *Geocarto Int.*, 12, 91–100.

Islam, M. R., Begum, S. F., Yamaguchi, Y., and Ogawa, K. (1999). The Ganges and Brahmaputra Rivers in Bangladesh: Basin denudation and sedimentation. *Hydrological processes,* 13, 2907-2923.

Islam, M. S. (2003). Perspectives of the coastal and marine fisheries of the Bay of Bengal, Bangladesh. *Ocean and Coastal Management,* 46, 763-796.

Islam, S. N., and Gnauck, A. (2008). Mangrove wetland ecosystems in Ganges-Brahmaputra delta in Bangladesh. *Front. Earth Sci.,* 2(4), 439-44.6.

Islam, S. N., and Gnauck, A. (2009). Threats to the Sundarbanss mangrove wetland ecosystems from transboundary water allocation in the Ganges basin: A preliminary problem analysis. *International Journal of Ecological Economics and Statistics (IJEES),* 13, 64-78.

Jonsson, P., and Eklundh, L. (2002). Seasonality extraction by function-fitting to time series of satellite sensor data. *IEEE Transactions on Geoscience and Remote Sensing,* 40, 1824−1832.

Julien, Y., Sobrino J. A. (2010). Comparison of cloud-reconstruction methods for time series of composite NDVI data. *Remote Sensing of Environment*, 114(3), 618-625.

Karim, M. F., and Mimura, N. (2008). Impact of climate change and sea-level rise on cyclonic storm surge floods in Bangladesh. *Glob Environ Chang*, 18, 4.70-500.

Katebi, M. N. A. (2001) 'Sundarbanss and forestry', in Haider, R. (Ed.): Cyclone '91 – An Environmental and Perceptional Study, BCAS, Dhaka, pp.79–100.

Kaufmann, R. K., Zhou, L., Yuri, K., Nikolay, V., Ranga, B., Myneni and Tucker, J.C. (2000). Effect of orbital drift and sensor changes on the time series of AVHRR vegetation index data. IEEE Trans. *Geosci. Remote Sens.* 38, 2584–2597.

Kevin, W., and EL ASMAR, H. M. (1999). Monitoring changing position of coastlines using thematic mapper imagery, an example from the Nile Delta, *Geomorfology*, **29**, 93-105.

Khan, A. T. and Vongvisessomjai S. (2002). MIKE-11 application for salinity intrusion in southwest Bangladesh, *paper presented in the 1st Asia Pacific software conference, Bangkok,* 17-18 Jun, 2002.

Kidwell, K. B. (2010). NOAA Polar Orbiter Data Users Guide :(TIROS-N, NOAA-6, NOAA-7, NOAA-8, NOAA-9, NOAA-10, NOAA-11, NOAA-12, NOAA-13, and NOAA-14); NOAA/NESDIS National Climatic Data Center: Washington, DC, USA.

Kuleli, T. (2010). Quantitative analysis of shoreline changes at the Mediterranean Coast in Turkey. *Environ Monit Assess*, 167, 387-397.

Lee, H. S. (2013). Estimation of extreme sea levels along Bnangladesh coast due to strom surge and sea level rising using EEMD and EVA. *Geophysical Research: Oceans,* 118, 1-13.

Levy, G. J., Mammedov, A., and Goldstein, D. (2003): Sodicity and water quality effects on slaking of aggregates from semi-arid soils. *Soil Science*, 168, 552-562.

Lucas, R. M., Bunting, P., Clewley, D., Proisy, C., Filho, P. W. M. S., Woodhouse, I. Ticehurst, C., Carreiras, J., Rosenqvist, A., and Accad, A. (2009). Characterisation and Monitoring of Mangroves Using ALOS PALSAR Data; The ALOS Kyoto and Carbon Initiative Science. *Team Reports Phase 1 (2006–2008); JAXA: Ibaraki, Japan*, Volume 1, 158–169.

Lunetta, R. S., Knight, J. F., Ediriwickrema, J., and Lyon, J. G., and Worthy, L. D. (2006). Land-cover change detection using multi-temporal MODIS NDVI data. *Remote Sens. Environ.*, 105, 142–154.

Ma, M., and Veroustraete, F. (2006). Reconstructing pathfinder AVHRR land NDVI time series data for the Northwest of China. *Advances in Space Research*, 37, 835−840.

Mamedov, A. I., Levy, G. J., Shainberg, I., and Letey, J. (2001). Wetting rate, sodicity, and soil texture effects on infiltration rate and runoff. *Aust. J. Soil Res.*, 2001, 39, 1293–1305.

Meeson, B. W., Corprew, F. E., Mcmanus, J. M. P., Myears, D. M., Closs, J. W., Sun, K. J., Sunday, D. J., and Sellers, P. J. (1995). ISLSCP Initiative I: Global data sets for land–atmosphere models, 1987–1988, vol. 1–5. CD ROM, NASA Goddard DAAC, USA.

Michael, E., and Peterson, M. (2006). Mangrove forest cover change in the Bangladesh

Sundarbanss from 1989-2000: A remote sensing approach. *Geocarto International*, 21, 5-12.

Miller, R. W., and Donahu, R. L. (1995). Soils in Our Environment. *Seventh Edition. Prudence Hall, Englewood, Cliffs, NJ.*, 323.

Mirza, M. M. Q. (1998). Diversion of the Ganges water at Farakka and its effects on salinity in Bangladesh. *Environmental Management*, 22(5), 711-722.

Mondal M. S., Jalal M. R. M., Khan, M. S., Kumar, U., Rahman, R., and Huq, H. (2013). Hydro-Meteorological Trends in Southwest Coastal Bangladesh: Perspectives of Climate Change and Human Interventions. *American Journal of Climate Change*, 2, 62-70.

Moulin, S., Kergoat, L., Voivy, N., and Dedieu, G., (1997). Global-scale assessment of vegetation phenology using NOAA/AVHRR satellite measurements. *Journal of Climate,* 10, 1154.970.

Nazim, U., and Anisul, H. (2010). Salinity response in southwest coastal region of Bangladesh due to Hydraulic and Hydrologic parameters. *Int. J. Sustain. Agril. Tech.*, 6(3), 01-07.

Nuruzzaman, M., Ahmed, I. U., and Banik H. (1999). The Sundarbans world heritage site: an introduction Forest Depart ment, Ministry of Environment and Forest, Government of the People's Republic of Bangladesh. 12 p..

Olsson, L., and Eklundh, L. (1994). Fourier series for analysis of temporal sequences of satellite sensor imagery. *Int. J. Remote Sens*.15, 3735–3741.

Paruelo, J. M., Epstein, H. E., Lauenroth, W. K., and Burke, I. C. (1997) ANPP estimates from NDVI for thecentral grassland region of the United States. *Ecology*, 78, 953–958.

Pettorelli, N., Vik, J. O., Mysterud, A., Gaillard, J. M., Tucker, C. J., and Stenseth, N. C. (2005). Using the satellite-derived NDVI to assess ecological responses to environmental change. *Trends in Ecology and Evolution,* 20(9), 503-510.

Pezeshki, S. R., De Laune, R. D., and Patrick, W. H. (1990). Differential response of selected mangroves to soil flooding and salinity: gas exchange and biomass partitioning. *Can J For Res*, 20:869–874.

Privette, J. L., Fowler, C., Wick, G. A., Baldwin, D., and Emery, W. J. (1995). Effects of orbital drift on advanced very high resolution radiometer products: Normalized difference vegetation index and sea surface temperature. *Remote Sens. Environ.*, 53, 164.141.

Qadir, M., and Schubert, S. (2002). Degradation processes and nutrient constraints in sodic soils. *Land Degrad develop*, 13, 275-294.

Rahman, A. F., Danilo, D., and Bassil E. (2011). Response of the Sundarbanss coastline to sea level rise and decreased sediment flow: A remote sensing assessment. *Remote Sensing of Environment*, 115, 3121–3128.

Ramachandran, S., Sundaramoorthy, S., Krishnamoorthy, R., Devasenapathy, J. and Thanikachalam, M. (1998). Application of remote sensing and GIS to coastal wetland ecology of Tamil Nadu and Andaman and Nicobar group of islands with special reference to mangroves. Curr. *Sci. India*, 75(3), 236–244.

Rashid, T., Suzuki, S., Sato, H., Monsur, M. H., Saha, S.K. (2013) Relative sea-level changes during the Holocene in Bangladesh. *J Asian Earth Sci* 64.116–150

Ryu, J. H., WON, J. S., and DUCK MIN, K. (2002). Waterline extraction from LANDSAT TM data in a tidal flat. A case study in Gomso Bay, Korea, *Remote Sensing Environ.*, 83, 442-456.

Saenger, P. and Siddiqi, N.A. (1993). Land from the sea: the mangrove afforestation program of Bangladesh. *Ocean and Coastal Managemen,t* 20:23-39.

Sarwar Md. G. M., and Woodroffe C. D. (2013). Rates of shoreline change along the coast of Bangladesh. *J Coast Conserv*, 17,515–526.

Scott J. W., Moore L. R., Harris W. M. and Reed M. D. (2003). Using the LANDSAT 7

Enhanced Thematic Mapper Tasseled Cap Transformation to Extract Shoreline. *Open-File Report OF 03-272 U.S. Geological Survey*.

Sellers, P. J., Berry, J. A., Collatz, G. J., Field, C. B., and Hall, F. G. (1992). Canopy reflectance, photosynthesis, and transpiration III. A reanalysis using improved leaf models and a new canopy integration scheme. *Remote Sensing of Environment*, 42, 187–216.

Sellers, P. J., Los S. o., Tucker, C. J., Justice C. O., Dazlich, D. A., Collatz, G. J., and Randall, D. A. (1996). A revised land surface parameterization (SiB2) for atmospheric GCMs. Part 2: The generation of global fields of terrestrial biophysical parameters from satellite data. *Journal of Climate*, 9, 706–73.

Shainberg, I., and Letey, J. (1984). Response of soils to sodic and saline conditions. *Hilgardia*, 52, 1–57.

Siddiqui, M. N. and Maajid, S. (2004). Monitoring of geomorphological changes for planning reclamation work in coastal area of Karachi, Pakistan, *Adv. Space Res.*, 33, 1200-1205.

Sinha P. C., Dube, S. K., and Roy, G. D. (1985). Influence of river on the storm surges in the Bay of Bengal. *Proceedings, International Workshop on Operational Applications of Mathematical Models (Surface Water) in Developing Countries*, 26 Feb - 1 May, 1985, New Delhi.

Slayback, D. A., Pinzon, J. E., Los, S. O., and Tucker, C. J. (2003). Northern hemisphere photosynthetic trends 1982-99. *Global Change Biology*, 9, 1-15.

Smith, B. D., Braulik, G., Mansur, R., and Ahmed, B. (2009). Habitat selection of freshwater-dependent cetaceans and the potential effects of declining freshwater flows and sea-level rise in waterways of the Sundarbanss mangrove forest, Bangladesh. *Aquatic Conserv: Mar. Freshw. Ecosyst*, 19, 209–225.

Suarez, N., and Medina, E. (2005). Salinity effect on plant growth and leaf demography of mangrove, Avicennia germinans L. *Trees*, 19, 721-727.

Sneyers, R. (1990). On the statistical analysis of series of observations, pp. 192. Tech. Note 143, WMO No. 4.13, Geneva.

Teillet, P. M., Staenz, K., and Williams, D. J. (1997). Effects of spectral, spatial, and radiometric characteristics on remote sensing vegetation indices of forested regions. *Remote Sens. Environ., 61,* 139–14.7.

Tucker, C. J., Pizon, J. E., Brown, M. E., Slayback, A., Pak, W., Mahoney, R., Vermote, E. F., and Saleous, N. E. (2005). An extended AVHRR 8-km NDVI dataset compatible with MODIS and SPOT vegetation NDVI data. *International Journal of Remote Sensing,* 26(20), 44.65-44.78.

Van Leeuwen, W. J. D., Orr, B. J., and Marsh, S. E. (2006). Herrmann, S.M. Multi-sensor NDVI data continuity: Uncertainties and implications for vegetation monitoring applications. *Remote Sens. Environ.*, 100, 67–81.

Viovy, N., Arino, O., and Velward, A. (1992). The Best Index Slope Extraction (BISE): A method for reducing noise in NDVI time-series. *International Journal of Remote Sensing,* 13, 1585−1590.

Wahid, M. S., Babel, S. M., and Bhuiyan, R. A. (2007). Hydrologic monitoring and analysis in the Sundarbanss mangrove ecosystem, Bangladesh. *Journal of Hydrology*, 332, 381-395.

Woodroffe, C.D. (1990). The impact of sea-level rise on mangrove shorelines. Progress in *Physical Geography,* 14,4.63-520.

Ye, Z. T., Gu, X. F., and Liu, X. L. (1999). Analysis of spectral characteristics among different sensors by use of simulated RS image (in Chinese). *J Wuhan Tech Univ Surv Map*, 24, 295–299.

APPENDIX

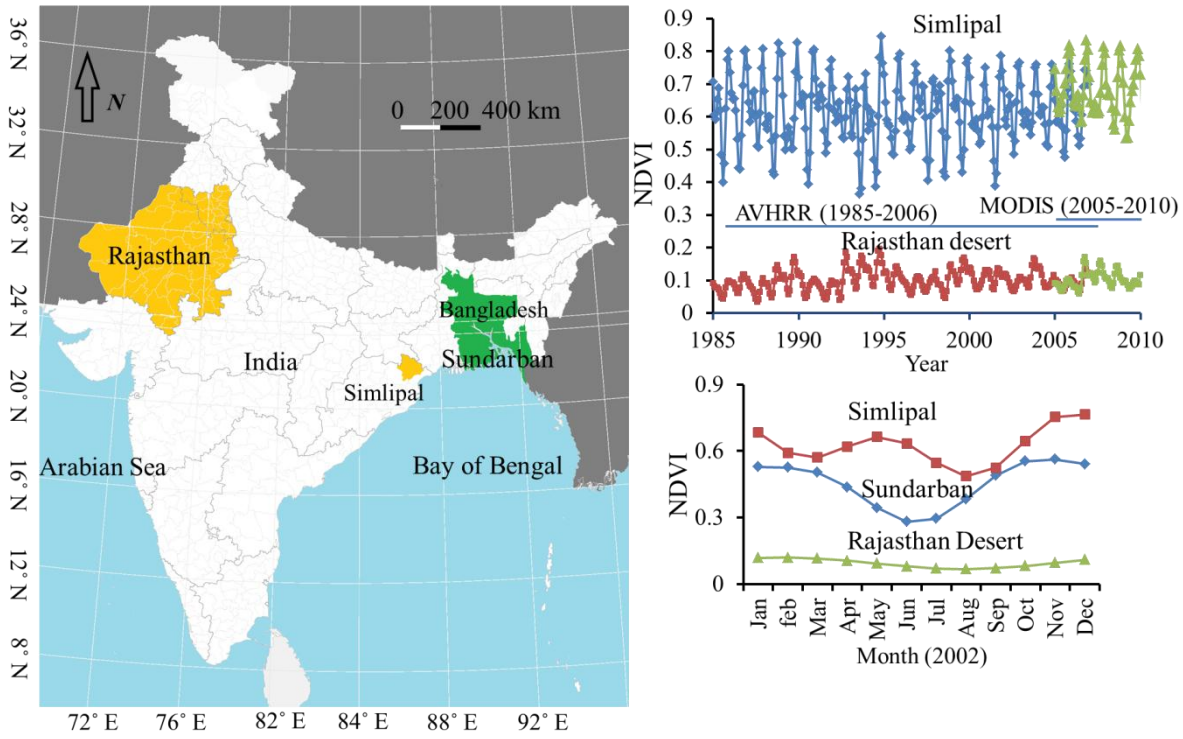

Figure A1 Geographical location of Simlipal forest, Rajasthan desert and Sundarban (left). NDVI variation of 12 areas (8✕8 km each) composite for Simlipal forest and Rajasthan desert (right side, upper panel). Inter comparison of monthly variation of NDVI for three locations; Sundarban, Simlipal forest and Rajasthan desert (right side, lower panel).

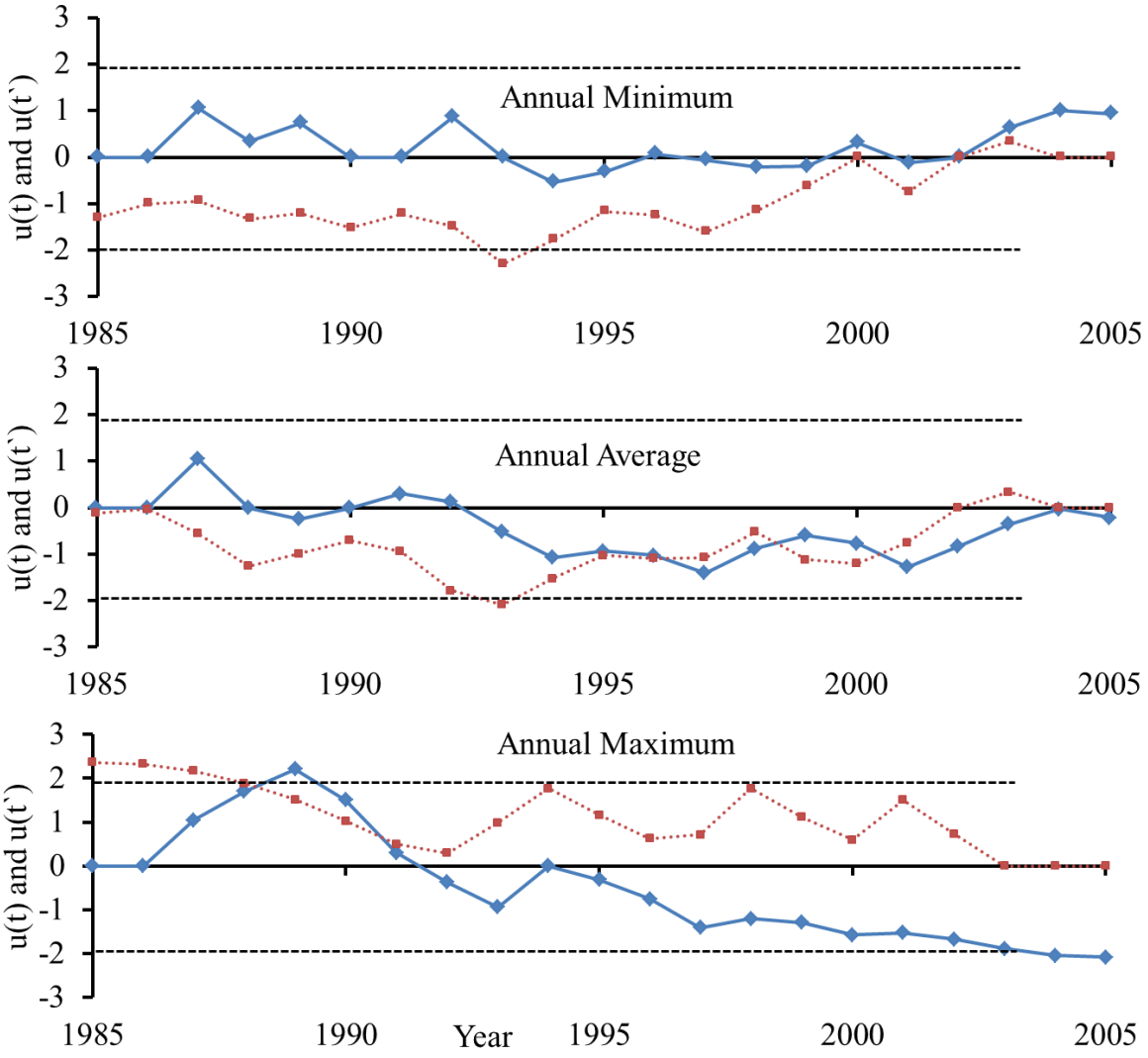

Figure A2 Potential turning points of trends in the NDVI variables for Simlipal forest, derived from the sequential MK test. u(t) and u(t′) are progressive and retrograde curves, respectively. The dashed lines represent the significance boundaries (t=1.96; Alpha=0.05).

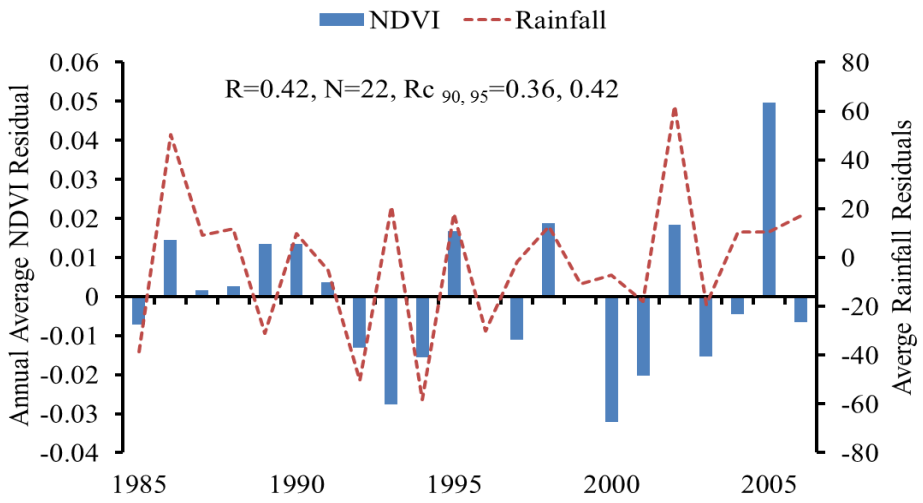

Figure A3 Variation of long term annual average rainfall residuals and annual average NDVI residuals. The residual is the deviation of annual average value of each year from the mean of all values during the observation years. A high association of this climatic variable (rainfall) with the annual average NDVI behavior was observed (R=0.42, N=22, 90-95% confidence level). Rc= Critical Pearson's correlation value at 90 and 95% confidence level. The exceptional years when the fluctuation of annual average NDVI and average annual rainfall residuals show opposite nature, the NDVI variation may be affected by other factors (river discharge, cyclone, and other climatic factors).

Table A1 Low or no-cost accessible satellite data sets for use in phenology research and applications (as of 1/4/2011).

Sensor	Satellite	Overpass/ Orbit Frequency	Data Source (terrestrial data)	Data Record (years)	Spatial Resolution	Processed Time Step	Latency
AVHRR	NOAA series	Daily	USGS/EROS[1]	1989-present	1 km	1-week, 2-week	~24 hours
AVHRR	NOAA series	Daily	Global Land Cover Facility[2]	1982-2006	8 km	Twice monthly	N/A
MSS	LANDSAT 1-5	18 days	USGS/EROS[1]	1972-1992	79 m	Distributed by scene	N/A
TM	LANDSAT 4-5	16 days	USGS/EROS[1]	1982-2011	30 m	Distributed by scene	N/A
ETM+	LANDSAT 7	16 days	USGS/EROS[1]	1999-present	30 m	Distributed by scene	~1-3 days
Vegetation	SPOT	1-2 days	VITO[3]	1999-present	1.15 km	10-day	~3 months
MODIS	Terra	1-2 days	LPDAAC[4]	2000-present	250 m, 500 m, 1 km	8-day, 16-day	~7-30 days
MODIS	Aqua	1-2 days	LPDAAC[4]	2002-present	250 m, 500 m, 1 km	8-day, 16-day	~7-30 days
eMODIS	Terra/ Aqua	1-2 days	USGS/EROS[5]	2000-present	250 m, 500 m, 1 km	7-day	~15 hours, 7 days

1. USGS Global Visualization Viewer: (http://glovis.usgs.gov/)
2. GIMMS data set: (http://glcf.umd.edu/data/gimms/)
3. Flemish Institute for Technology Research (VITO) for SPOT Vegetation S10 products: (http://www.spot-vegetation.com and http://free.vgt.vito.be)
4. Land Processes Distributed Active Archive Center: (https://lpdaac.usgs.gov/products/modis_products_table)
5. eMODIS: (http://dds.cr.usgs.gov/emodis/), Latency is approximately 15 hours for expedited data (released daily) and around 7 days for historical data.

Table A2 The most common approaches to smoothing NDVI time-series

Techniques	Description	Reference
Asymmetrical Gaussian function-fitting	Fits local, nonlinear functions at intervals around local maxima and minima, then merges these into a global function describing the full NDVI time series	Jonsson and Eklundh, 2002
Double logistic function-fitting	Uses a series of parameters (e.g. winter, maximum NDVI) to model NDVI time series with a double logistic function	Beck et al., 2006
Savitzky–Golay filter	Applies an iterative weighted moving average filter to NDVI time series, with weighting given as a polynomial of a particular degree	Chen et al., 2004
4253H, twice filter Mean-value iteration filter	Applies a series of running medians of arraying window size and a weighted average filter, with re-roughing, to the NDVI time series	Ma and Veroustraete, 2006
Best Index Slope Extraction method (BISE)	NDVI observations are judged as trustworthy or not depending on whether the rate-of-change in the NVDI is possible.	Viovy et al., 1992
Curve-fitting	Polynomial or Fourier functions are fitted to NDVI time-series	Olsson et al., 1994; Seller et al., 1996

Table A3 Spectral and spatial resolutions of LANDSAT sensors upto 2013.

Satellite	Spectral Resolution (μ)	Band	Spatial Resolution (Meters)
LANDSAT 1-3 (Multispectral Scanner)	**MSS**		
	Band 4: 0.50 - 0.60	Green	79.00
	Band 5: 0.60 - 0.70	Red	79.00
	Band 6: 0.70 - 0.80	Near IR	79.00
	Band 7: 0.80 - 1.10	Near IR	79.00
LANDSAT 4-5 (Multispectral Scanner and Thematic Mapper)	**MSS**		
	Band 4: 0.50 - 0.60	Green	82.00
	Band 5: 0.60 - 0.70	Red	82.00
	Band 6: 0.70 - 0.80	Near IR	82.00
	Band 7: 0.80 - 1.10	Near IR	82.00
	TM		
	Band 1: 0.45 - 0.52	Blue	30.00
	Band 2: 0.52 - 0.60	Green	30.00
	Band 3: 0.63 - 0.69	Red	30.00
	Band 4: 0.76 - 0.90	Near IR	30.00
	Band 5: 1.55 - 1.75	Mid IR	30.00
	Band 6: 10.4.10.5	Thermal	120.0
	Band 7: 2.08 - 2.35	Mid IR	30.00
LANDSAT 7 (Enhanced Thematic Mapper Plus)	**ETM+**		
	Band 1: 0.450 - 0.515	Blue	28.50
	Band 2: 0.525 - 0.605	Green	28.50
	Band 3: 0.630 - 0.690	Red	28.50
	Band 4: 0.760 - 0.900	Near IR	28.50
	Band 5: 1.550 - 1.750	Mid IR	28.50
	Band 6: 10.40 - 12.5	Thermal	57.00
	Band 7: 2.080 - 2.35	Far IR	28.50
	Band 8: 0.52 - 0.92	Panchromatic	14.25
LANDSAT 8 Land Imager (OLI) and Thermal Infrared Sensor (TIRS) Launched at Feb, 2013	**OLI and TIRS**		
	Band 1: 0.453 - 0.45	Coastal aerosol	30.00
	Band 2: 0.45 - 0.51	Blue	30.00
	Band 3: 0.53 - 0.59	Green	30.00
	Band 4: 0.64 - 0.67	Red	30.00
	Band 5: 0.85 - 0.88	Near IR	30.00
	Band 6: 1.57 - 1.65	SWIR1	30.00
	Band 7: 2.11 - 2.29	SWIR2	30.00
	Band 8: 0.50 - 0.682	Panchromatic	15.00
	Band 9: 1.36 - 1.38	Cirrus	30.00
	Band 10: 10.60 - 11.19	Thermal Infrared (TIRS)1	100.00
	Band 11: 11.50 - 12.51	Thermal Infrared (TIRS)2	100.00

Table A4 Satellite data and tide level at the images acquisition date measured at Hiron point station (See Fig. 2.3).

Sl. No.	Satellite Name	Acquisition Date	Tide level (mm)
1	LANDSAT 4 TM	1989/01/12	-780
2	LANDSAT 5 TM	1993/12/17	-340
3	LANDSAT 5 TM	1995/11/21	N/A
4	LANDSAT 7 ETM+	1999/11/08	1100
5	LANDSAT 7 ETM+	2000/11/26	850
6	LANDSAT 7 ETM+	2001/11/29	1080
7	LANDSAT 7 ETM+	2002/12/18	530
8	LANDSAT 7 ETM+	2003/11/19	-240
9	LANDSAT ETM+	2004.10/07	-570
10	LANDSAT 7 ETM+	2006/12/29	-1030
11	LANDSAT 7 ETM+	2007/11/30	620
12	LANDSAT 7 ETM+	2008/10/31	790
13	LANDSAT 7 ETM+	2009/12/21	-20
14	LANDSAT 7 ETM+	2010/12/24	530

Table A5 Different methods for shoreline extraction.

Techniques	References
Supervised and unsupervised classifications	Baban, 1997;
Band ratio method (Band 5 divided by band 2)	Annibale, 2006; Alesheikh et al., 2007
Principal component methods	Siddiqui and Maajid, 2004
NDVI (Normalized Difference Vegetation Index)	Ryu et al., 2002; Rahman et al., 2011
Tasseled Cap transformation	Scott et al., 2003

NB: Beside the given references more references can be found on these methods to extract the shoreline positions.

Table A6 Wind speed and storm surge of recent four cyclones attacked or passed near Sundarbans

Name	Date	Wind speed (km/hr)	Storm surge(m)
Sidr[1]	2007(15 November)	240	5
Reshmi[2]	2008 (26 October)	55	1.85
Bijli[3]	2009 (16 Arpil)	95	2.1
Aila[4]	2009 (25 May)	120	3

[1]Government of Bangladesh (GOB) (2008) Cyclone Sidr in Bangladesh: damage, loss and needs assessment for disaster recovery and reconstruction. Government of Bangladesh, Dhaka.

[2] Regional Specialised Meteorological Center New Delhi, India (November 2008). "Cyclonic Storm, 'Rashmi' a Preliminary Report". India Meteorological Department. Archived from the original on November 24.1808. Retrieved November 3, 2012.

[3] Pierce, H and Gutro R., (April 20, 2009). Hurricane Season 2009: Bijli (Northern Indian Ocean). NASA. Retrieved May 23, 2009.

[4.]Akter, S. Mallick, B. (2013). An empirical investigation of socio-economic resilience to natural disasters, UFZ Economics Working paper series 04.11

Images of the field survey (8 and 9 March, 2013)

Images were taken in and around the segment D (see Fig. 3.4)

BIBLIOGRAPHY

Anwar Md. Shibly and Satoshi Takewaka, "Morphological Changes along Bangladesh Coast Derived from Satellite Images", *Proceedings of International Sessions in Coastal Engineering, JSCE (Japan Society of Civil Engineers), Vol.3, Hiroshima, Japan, 2012.*

Anwar Md. Shibly and Satoshi Takewaka, "Morphological Changes along Bangladesh Coast Derived from Satellite Observations", *Proceedings of the International Workshop –Hue Geo- Engineering, Hue City, Vietnam, 2012.*

Anwar Md. Shibly and Satoshi Takewaka, "Morphological Changes and Vegetation Index Variation along the Western Coastal Zone of Bangladesh", *Proceedings of the 7th International Conference on Asian and Pacific Coasts (APAC), Bali, Indonesia, 2013.*

Anwar Md. Shibly and Satoshi Takewaka, "Variation of Morphology and Vegetation Index along the Kochikhali Coast, Southwestern Tip of Sundarbans, Bangladesh", *Proceedings of International Sessions in Coastal Engineering, JSCE (Japan Society of Civil Engineers), Vol.4, Fukuoka, Japan, 2013.*

Satoshi Takewaka and Anwar Md. Shibly, "Analyses on the Morphological Changes along the Western Bangladesh Coast and their Causes", *Journal of JSCE (Japan Society of Civil Engineers), Vol. 69, No. 2, p1396-1400 (in Japanese with English abstract), 2013.*

Anwar Md. Shibly and Satoshi Takewaka "Analyses on Phenological and Morphological Variations of Mangrove Forests along the Southwest Coast of Bangladesh", *Journal of Coastal Conservation, DOI 10.1007/s11852-014-0321-4 (Published online 29th May, 2014)*